Université d'Ottawa · University of Ottawa

Université d'Ottawa • University of Ottawa

FACULTÉ DES ÉTUDES SUPÉRIEURES ET POSTDOCTORALES

FACULTY OF GRADUATE AND POSTDOCTORAL STUDIES

Wenhui WANG

AUTEUR DE LA THÈSE - AUTHOR OF THESIS

M. Sc. (Chemistry)

GRADE - DEGREE

Department of Chemistry

FACULTÉ, ÉCOLE, DÉPARTEMENT - FACULTY, SCHOOL, DEPARTMENT

TITRE DE LA THÈSE - TITLE OF THE THESIS

Preparation and Characterization of Periodic Mesoporous Organosillicas

A. Sayari

DIRECTEUR DE LA THÈSE - THESIS SUPERVISOR

CO-DIRECTEUR DE LA THÈSE - THESIS CO-SUPERVISOR

EXAMINATEURS DE LA THÈSE - THESIS EXAMINERS

C. Detellier

D. Richeson

J-M. De Koninck, Ph D

LE DOYEN DE LA FACULTÉ DES ÉTUDES SUPÉRIEURES ET POSTDOCTORALES

DEAN OF THE FACULTY OF GRADUATE AND POSTODORAL STUDIES

Preparation and Characterization of Periodic Mesoporous Organosilicas

Wenhui Wang

Thesis submitted to the
Faculty of Graduate and Postdoctoral Studies
in partial fulfillment of the requirements for the
Master of Science degree in Chemistry

Department of Chemistry
Faculty of Science
University of Ottawa

Your file Votre référence
ISBN: 0-494-01633-7
Our file Notre référence
ISBN: 0-494-01633-7

Abstract

Periodic mesoporous organosilicates (PMOs) are hybrid materials whose framework is comprised of alternating organic and inorganic species. These materials are prepared via supramolecular templating assembly using bridged silsesquioxanes $(RO)_3Si\text{-}R'\text{-}Si(OR)_3$ as precursors, and surfactants as templates. This thesis is devoted to the preparation and characterization of phenyl- and ethenylene-bridged PMOs. The phenylene-containing precursor (bis(triethoxysilyl)benzene was synthesized by Barbier-Grignard reaction, whereas the ethylene derivative bis(triethoxysilyl)ethylene was prepared by self-metathesis reaction. They were characterized by ^{1}H and ^{13}C NMR, and mass spectrometry.

The corresponding mesoporous materials were prepared using these precursors in the presence of different types of surfactants including oligomeric alkyl polyethylene oxide, triblock polyalkylene oxide copolymer and alkyltrimethylammonium surfactants. To obtain highly ordered mesoporous organosilicates, different synthesis conditions were employed and optimized. All materials were characterized using XRD, TEM, SEM, nitrogen adsorption, ^{29}Si and ^{13}C solid state NMR. In addition, some post-synthesis reactions using these materials were investigated.

Dedication

This thesis is dedicated to

My mom

My hubby Ning Xu

My lovely daughter Vicky

My younger sister

Acknowledgements

Frist of all I would like to express my sincere thanks to my supervisor Prof. A. Sayari for his constant guidance, help and encouragement throughout the course of my work.

I wish to thank Prof. C. Detellier and Prof. D. Richeson for being examiners of my thesis.

I also want to say thanks to my husband for his encouragement and understanding during the time of my course.

Finally, my sincere thanks go to the staff and personnel of the department of Chemistry, University of Ottawa for their help during my research. Also I gave my thanks to all people in my group.

Table of Contents

Abstract

Acknowledgements

Table of Contents

List of Tables

List of Figures

List of Abbreviations

Chapter 1 General Introduction 1

1.1 Background of Periodic Mesoporous Organosilicates 2

1.2 Scope of this Thesis 18

Chapter 2 Synthesis of Bridged Silsesquioxane Precursors 19

2.1 Introduction 20

2.2 Synthesis of Bridged Silsesquioxane Precursors 28

2.2.1 Synthesis of Bis(triethoxysilyl) Benzene 28

2.2.1.1 Literature Review 28

2.2.1.2 Experimental 29

2.2.1.3 Discussion 30

2.2.2 Synthesis of Bis(triethoxysilyl) Ethylene 31

2.2.2.1 Literature Review 31

2.2.2.2 Experimental 32

2.2.2.3 Discussion 32

Chapter 3 Preparation of Periodic Mesoporous Organosilicates ····40

3.1 Introduction ····41

3.2 Preparation of PMOs using Bis(triethoxysilyl) benzene as Precursor ····42

3.2.1 Literature Review ····42

3.2.2 Experimental ····43

3.3 Preparation of PMOs using Bis(triethoxysilyl) ethylene as Precursor ····46

3.3.1 Literature Review ····46

3.3.2 Experimental ····48

3.3.3 Post-synthesis Reactions ····52

3.3.3.1 Literature Review ····52

3.3.3.2 Experimental ····53

Chapter 4 Results and Discussion ····55

4.1 Introduction ····56

4.2 Characterization of Bis(triethoxysilyl) benzene derived Materials ····57

4.2.1 Results and Discussion ····57

4.2.2 Summary ····67

4.3 Characterization of Bis(triethoxysilyl) ethylene derived Materials ····71

4.3.1 Ethenylenesilica prepared in the presence of Oligomeric Surfactants ····71

4.3.1.1 Results and Discussion ····71

4.3.1.2 Summary ····79

4.3.2 Ethenylenesilica prepared in the presence of Triblock Copolymer P123 ····79

4.3.2.1 Results and Discussion ····79

4.3.2.2 Summary ····88

4.3.3 Ethenylenesilica prepared in the presence of Alkyltrimethylammonium ····88

4.3.3.1 Results and Discussion ····88

4.3.3.2 Summary ····92

4.4 Evaluation of Post-synthesis Reactions····94

4.4.1 Results and Discussion ····94

4.4.2 Summary ····102

Chapter 5 Conclusion ····105

References ····108

List of Tables

Chapter 1

Table 1.1 Structure and synthesis conditions for various silica mesophases ···16

Table 1.2 Methods of pore size engineering for mesoporous silicas ·····17

Chapter 3

Table 3.1 Phenylenesilicas prepared in the presence of different amounts of acid ·····44

Table 3.2 Conditions of the second preparation stage of phenylenesilicas ·····45

Table 3.3 Phenylenesilicas prepared in the presence of different surfactants ···45

Table 3.4 Ethenylenesilicas prepared in the presence of different surfactants ··49

Table 3.5 Ethyenylenesilicas prepared in the presence of alkyl(polyethyleneoxide)oligomers using two aging steps ·····49

Table 3.6 Different preparation conditions for materials under basic pH ·····50

Chapter 4

Table 4.1 N_2 adsorption data for materials prepared in the presence of different surfactants ·····60

Table 4.2 N_2 adsorption data for samples prepared under acidic conditions with hydrothermal treatment at 50 °C for 20 h in the presence of different surfactants ·····74

Table 4.3 Pore system data for materials prepared in the presence of P123 (SW45e), P123 + butanol (SW51e) and P123 + NaI (SW52e). ·····87

Table 4.4 N_2 adsorption data for materials prepared under different conditions 89

List of Figures

Chapter 1

Figure 1.1 Structural parameters for the design of nanostructured materials ····5

Figure 1.2 Cooperative templating mechanism ····6

Figure 1.3 Neutral templating mechanism ····7

Figure 1.4 Ligand-assisted templating mechanism ····7

Figure 1.5 X-ray diffraction patterns for typical silica mesophases ····10

Figure 1.6 The five types of adsorption isotherms, I to V, in the classification of Brunauer, Deming, Deming and Teller, together with Type VI, the stepped isotherm ····13

Chapter 2

Scheme 2.1 Commercially available PMO precursors ····21

Scheme 2.2 Preparation of monomers by metalation ····22

Scheme 2.3 Preparation of monomers by hydrosilation ····23

Scheme 2.4 Preparation of bridged monomers from organotrialkoxysilanes ····23

Scheme 2.5 Miscellaneous methods of synthesizing monomers ····24

Scheme 2.6 Commercially unavailable precursors used for PMO synthesis ····26

Scheme 2.7 Reaction routes for bis(triethoxysilyl)benzene ····29

Scheme 2.8 Reaction equation for synthesis of bis(triethoxysilyl)ethylene ····32

Chapter 3

Figure 3.1 Layered arrangement of $O_{1.5}Si\text{-}C_4H_4\text{-}SiO_{1.5}$ units in the walls ····43

Chapter 4

Figure 4.1 XRD patterns for phenylene-bridged mesoporous organosilica (after extraction) prepared in the presence of (a) Brij 76, and (b) Brij 56 ····58

Figure 4.2 Nitrogen adsorption isotherms for phenylene-bridged mesoporous organosilicas prepared in the presence of Brij 76 (-○-) or Brij 56 (-●-) as structure directing agent ····59

Figure 4.3 (a) ^{29}Si NMR, and (b) ^{13}C NMR data for the phenylene-bridged mesoporous organosilica prepared in the presence of Brij 76 ····61

Figure 4.4 TEM image for phenylene-bridged mesoporous phenylenesilica viewed down the [001] zone axis ····63

Figure 4.5 (a)TEM image of the phenylene-bridged mesoporous phase viewed down the [100] zone Axis. (b) Diffraction pattern made by Fourier transform of (a). (c) TEM image created by inverse Fourier transform of (b) ····64

Figure 4.6 Pore size distribution for phenylene-bridged mesoporous organosilica prepared in the presence of Brij 58 (-♦-) or Brij 78 (-◊-) ····65

Figure 4.7 Pore size distribution for phenylene-bridged mesoporous organosilicas prepared in the presence of Brij 76 with the following HCl/BTEB ratios (-●-) 6.4, (-○-) 4.6, (-▲-) 7.7, and (-Δ-) 9.2 ····66

Figure 4.8 XRD patterns for phenylene-bridged mesoporous organosilicas

(after extraction) prepared in the presence of Brij 76 in a single step (a), or using a second hydrothermal stage for 20 h at (b) 50 °C , (c) 70 °C, and (d) 95 °C ····68

Figure 4.9 Pore size distribution for phenylene-bridged mesoporous organosilicas prepared in the presence of Brij 76 in a single step at 50 °C (-●-), or using a second hydrothermal stage for 20 h at (-♦-) 50 °C, (-○-) 70 °C, and (-◊-) 95 °C ····69

Figure 4.10 Pore size distribution for phenylene-bridged mesoporous organosilicas prepared in the presence of Brij 76 using a second hydrothermal stage at 50 °C for (-♦-) 20 h and (-◊-) 48 h····70

Figure 4.11 Pore size distribution for ethenylene-bridged mesoporous organosilicas prepared in the presence of Brij 76 in a single step (-♦-) and using a second hydrothermal stage for 20 h at 50 °C (-◊-) ····72

Figure 4.12 XRD patterns for ethenylene-bridged mesoporous organosilica (after extraction) prepared using a second hydrothermal stage for 20 h at 50 °C in the presence of (a) Brij 76, (b) Brij 56, (c) Brij 58, and (d) Brij78····73

Figure 4.13 Nitrogen adsorption-desorption isotherms for ethenylene-bridged mesoporous organosilica prepared using a second hydrothermal stage for 20 h at 50 °C in the presence of (-♦-) Brij 76, (-▲-) Brij 56, (-◊-) Brij 58, and (-△-) Brij 78 ····75

Figure 4.14 SEM image for ethenylene-bridged mesoporous organosilica prepared in the presence of Brij 76 using a second hydrothermal stage for 20 at 50 °C 76

Figure 4.15 (a) ^{29}Si NMR, and (b) ^{13}C NMR data for the ethenylene-bridged mesoporous organosilica prepared using a second hydrothermal stage for 20 h at 50 °C in the presence of Brij 76 77

Figure 4.16 TEM images for ethenylene-bridged mesoporous organosilicas prepared with hydrothermal treatment at 50 °C for 20 h in the presence of (a) Brij 76 and (b) Brij 56 78

Figure 4.17 XRD pattern for ethenylene-bridged mesoporous organosilica (after extraction) prepared in the presence of triblock copolymer P123 80

Figure 4.18 Nitrogen adsorption-desorption isotherm for ethenylene-bridged mesoporous organosilica prepared in the presence of triblock copolymer P123 81

Figure 4.19 (a) ^{29}Si NMR, and (b) ^{13}C NMR data for the ethenylene-bridged mesoporous organosilica prepared in the presence of triblock copolymer P123 82

Figure 4.20 XRD patterns for ethenylene-bridged mesoporous organosilica (after extraction) prepared in the presence of P123 only (a), P123 + butanol(b), and P123 + sodium iodide (c) 84

Figure 4.21 Pore size distribution for ethenylene-bridged mesoporous organosilicas prepared in the presence of triblock copolymer

P123 only (-♦-), P123 + butanol (-◊-), and P123 + sodium iodide (-▲-) ·····85

Figure 4.22 Nitrogen adsorption-desorption isotherms for ethenylene-bridged mesoporous organosilicas prepared in the presence of triblock copolymer P123 only (-♦-) (+600), P123 + butanol (-◊-) (+200), and P123 + sodium iodide (-▲-) (-200)·····86

Figure 4.23 TEM image of ethenylene-bridged mesoporous organosilicas prepared in the presence of triblock copolymer P123 + butanol viewed down the [001] zone axis·····87

Figure 4.24 XRD patterns for ethenylene-bridged mesoporous organosilica (after extraction) prepared in the presence of C_{16}TMACl·····90

Figure 4.25 Nitrogen adsorption-desorption isotherms for ethenylene-bridged mesoporous organosilica prepared in the presence of C_{16}TMACl····91

Figure 4.26 (a) ^{29}Si NMR, and (b) ^{13}C NMR data for the ethenylene-bridged mesoporous organosilica prepared in the presence of C_{16}TMACl····93

Figure 4.27 XRD patterns for ethenylene-bridged mesoporous organosilicas prepared in the presence of Brij 76 using a second hydrothermal stage for 20 h at 50 °C (a) before, and (b) after bromination ·····95

Figure 4.28 Nitrogen adsorption-desorption isotherms for ethenylene-bridged mesoporous organosilicas prepared in the presence of Brij 76 using a second hydrothermal stage for 20 h at 50 °C (-♦-) before, and (-■-) after bromination·····96

Figure 4.29 ^{13}C NMR for ethenylene-bridged mesoporous organosilicas

prepared in the presence of Brij 76 using a second hydrothermal stage for 20 h at 50 °C (a) before, and (b) after bromination ·····97

Figure 4.30 XRD patterns for ethenylene-bridged mesoporous organosilicas prepared in the presence of triblock copolymer P123 (a) before, and (b) after bromination ·····99

Figure 4.31 Nitrogen adsorption-desorption isotherms for ethenylene-bridged mesoporous organosilicas prepared in the presence of triblock copolymer P123 (-♦-) before, and (-■-) after bromination ·····100

Figure 4.32 ^{13}C NMR for ethenylene-bridged mesoporous organosilicas prepared in the presence of triblock copolymer P123 (a) before, and (b) after bromination ·····101

Figure 4.33 Nitrogen adsorption-desorption isotherms for vinyl and ethenylene-bridged mesoporous organosilicas prepared in the presence of CTAB (-♦-) before, and (-■-) after bromination·····103

Figure 4.34 ^{13}C NMR for vinyl and ethenylene-bridged mesoporous organosilicas prepared in the presence of CTAB (-♦-) before, and (-■-) after bromination·····104

List of abbreviations

PMMs	periodic mesoporous materials
PMOs	periodic mesoporous organosilicas
CTMAB	cetyltrimethylammoniun bromide
CTMAC	cetyltrimethylammonium chloride
ODTMAC	octadecyltrimethylammonium chloride
XRD	X-ray diffraction
TEM	transmission electron microscopy
SEM	scanning electron microscopy
NMR	nuclear magnetic resonance
IR	infrared spectroscopy
TGA	thermogravimetric analysis
BET	Brunauer-Emmett-Teller
THF	tetrahydrofuran
MS	Mass spectrometry
BTEB	bis(triethoxysilyl)benzene
BTSEY	bis(triethoxysilyl)ethylene
CTAB	cetyltrimethylammoniun bromide
TEOS	tetraethyl orthosilicate
TEVS	triethoxyvinylsilane

Chapter 1

General Introduction

1.1 Background of periodic mesoporous organosilicas

The field of periodic mesoporous materials (PMMs) has grown dramatically during the last ten years. Although periodic mesoporous silicas have been discovered in 1990 [1,2] or even earlier [3], this type of materials received a great deal of attention [4] since the discovery of the so-called M41S family of ordered mesoporous silicates by Mobil Corp. [5,6]. The ordered M41S mesoporous silicates consisted of three mesophases, MCM-41 (hexagonal, *p6mm*), MCM-48 (cubic, $Ia\bar{3}d$) and MCM-50 (lamellar). These materials have a range of framework compositions, morphologies, and pore structures. They were synthesized via supramolecular templating mechanism using alkyltrimethylammonium surfactants under basic conditions. Since then, a large variety of ordered mesoporous materials have been synthesized by templating methods, using supramolecular assembly of surfactant molecules. Over 3000 papers dealing with such materials have been published and a number of international meetings were also devoted to mesoporous materials. Figure 1.1 shows the structural parameters that have been explored in the design and synthesis of PMMs. Currently, periodic mesoporous silicas may be easily prepared under an extremely wide range of conditions. Besides cationic alkyltrimethylammonium surfactants, a variety of amphiphile molecules including cationic, anionic, neutral, zwitterionic, bolaamphiphile, Gemini and divalent surfactants as well as numerous commercially available oligomers and triblock copolymers and appropriate mixtures thereof were used for the preparation of periodic mesoporous silicas. The pH and temperature conditions ranged from

strongly acidic to highly basic conditions, and from subambient temperature to 170 °C, respectively. This rapid development led to the discovery of many new silica mesophases including SBA-1 and SBA-6 ($Pm\bar{3}n$) [7-9], SBA-2 and SBA-12 ($P6_3/mmc$) [9,10], SBA-8 (*cmm*) [11], SBA-11 ($Pm\bar{3}m$) [10], SBA-16 [10] and FDU-1 ($Im\bar{3}m$) [12], disordered HMS [13], MSU-n [14], MSU-V [15] , MSU-G [16] and others. The supramolecular templating approach was also extended to the synthesis of transition and other metal substituted silicas, and to numerous non-silica materials. In addition, several approaches were invented to control the pore size from the low end of mesopore dimensions, i.e. ≈2nm, to well in the macropore regime [17]. Mesostructured materials with unique morphologies were also synthesized [18-24].

There are three basic synthesis mechanisms for periodic mesoporous materials.

(1) Figure 1.2 shows one example of the so-called *cooperative templating mechanism* [25, 26]. In this case, the synthesis is carried out under basic conditions using cationic surfactants. The first step of this process is triggered by electrostatic interactions. It corresponds to the displacement of the surfactant counterions by polydentate and polycharged inorganic anions leading to organic-inorganic ion-pairs, which self organize into a liquid crystal-like mesophase. This is followed by cross-linking of the inorganic species, and formation of a rigid replica of the underlying liquid crystalline phase. The formation of M41S silica mesophases takes place according to this mechanism.

(2) *The neutral templating mechanism* (Figure 1.3) [27, 28] was proposed for the synthesis of PMMs in the presence of neutral (alkylamines) or non-ionic (polyethylene oxide) surfactants. Instead of the electrostatic interactions, in the

presence of neutral surfactants, hydrogen bonding becomes the predominant driving force in pairing organic and inorganic species. The neutral species formed by partial hydrolysis of tetraethyl orthosilicate interact with the surfactant amine head group via hydrogen bonding. The obtained organic-inorganic complex may be considered as an amphiphile with a very bulky head group, i.e., small packing factor, thus favoring the formation of high curvature micelles such as rod-like micelles, which exhibit a natural tendency to self-assemble into a hexagonal lyotropic mesophase. This is followed by condensation of silanol groups and formation of rigid silica walls.

(3) *The ligand-assisted templating mechanism* involves the formation of a covalent bond between organic and inorganic species [29]. The synthesis of mesoporous transition metal oxides (e.g. Nb_2O_5) in the presence of alkylamine for example, is believed to take place according to this mechanism (Fig. 1.4). The first step which takes place in the absence of water is the formation of a Nb-N covalent bond between the precursor $Nb(OEt)_5$ and the long-chain amine surfactant. This is followed by intermolecular condensation of these species in the presence of water leading to the formation of cylindrical micelles, and ultimately to a mesophase.

Functionalization of ordered inorganic mesoporous and microporous materials with organic groups has also attracted much attention. One of the main driving forces for the synthesis of such organic-inorganic mesoporous hybrid materials is the beneficial combined properties, which may correspond to enhanced or new properties, uncharacteristic of the individual components. Furthermore, the presence of organic functional groups in such ordered nanoporous materials also offers a wide range of potential applications for these materials such as host-guest inclusion [30],

nanotechnology [31], chemoselective separation and adsorption [32], chemical sensing [33], and catalysis [34].

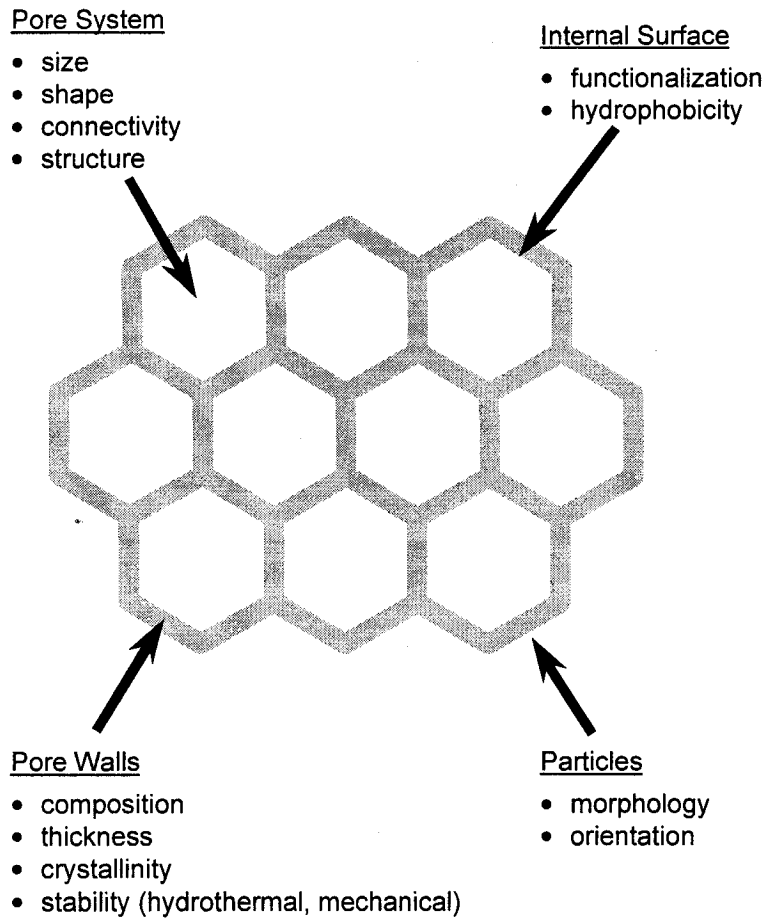

Figure 1.1. Structural parameters for the design of nanostructured materials

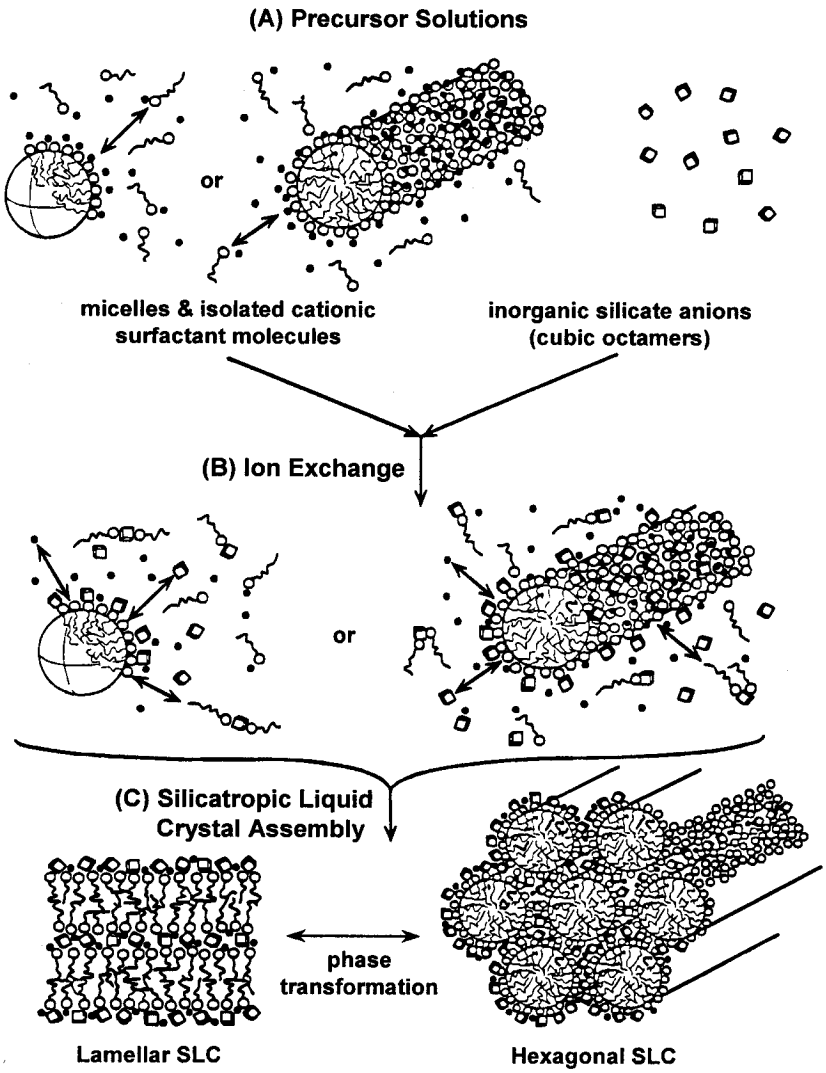

Figure 1.2 Cooperative templating mechanism [25]

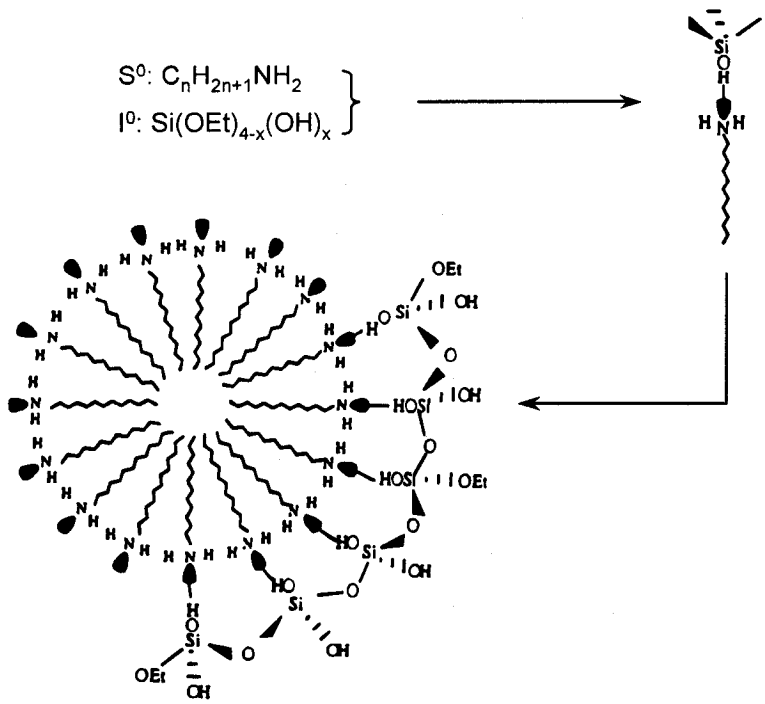

Figure 1.3 Neutral templating mechanism [28]

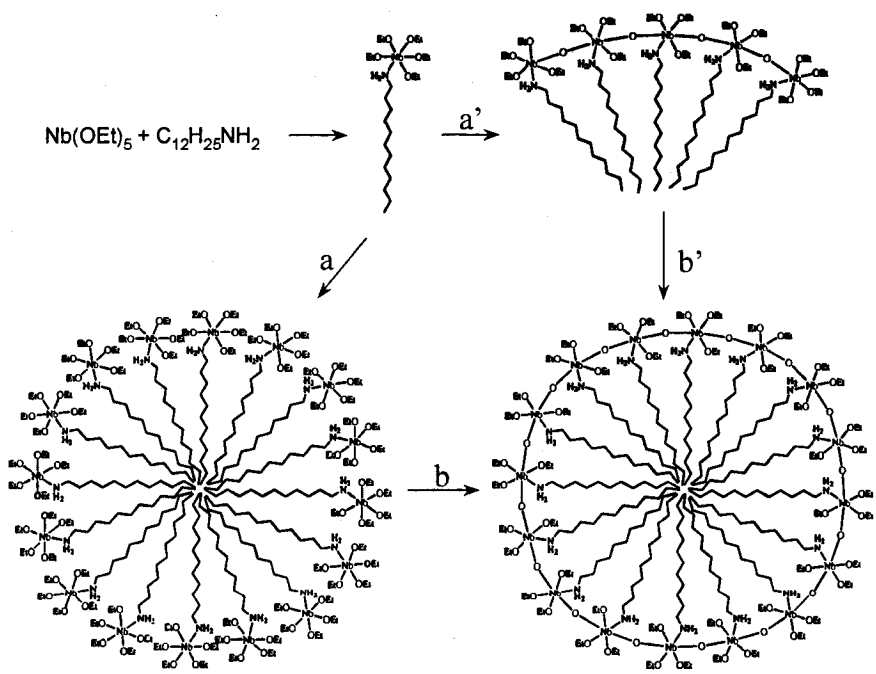

Fig. 1.4 Ligand-assisted templating mechanism [29]

Contrary to surface modified periodic mesoporous silicas, periodic mesoporous organosilicas (PMOs) are organic-inorganic hybrid nanocomposites in which the organic component is built in the walls of the channels [13, 18, 35-41] instead of protruding into them. They are synthesized, like MCM-41 materials through one-pot surfactant-templated supramolecular self-assembly procedures via the hydrolysis and condensation of poly(trialkyoxysilyl) organic precursors ($[(R'O)_3Si]_xR$, X = 2, 3). The template can be removed by solvent extraction without the collapse of the ordered composite, giving access to an ordered high surface area mesoporous structure. Changes in the nature of the organic spacer R offer a wide range of opportunities to control the surface properties, while maintaining a periodic pore system. The presence of organic functional groups in such ordered nanoporous materials offers additional advantages that make such materials potentially useful as catalytic and chromatographic supports, chemical and biochemical sensors and membranes.

Since the discovery of PMOs in 1999, a number of bridged silsesquioxanes have been successfully used as precursors. These included bis-silylated methylene [13,35,42], ethane [18,36-40,42-44], ethylene [38,40,42], acetylene [42,45], saturated alkyl chains, such as propane [43], thiophene [42,45], benzene [42-45], bithiophene [45], and ferrocene [42,45]. Most periodic mesoporous organosilicates were prepared under basic conditions. The most common surfactants used were CTMAB (cetyltrimethylammonium bromide) [13,38,40,45], CTMAC (cetyltrimethyl-ammonium chloride) [18,36] and ODTMAC octadecyltrimethylammonium chloride) [18,36,44]. But syntheses under acidic conditions were also used in the presence of

other surfactants such as oligomeric alkyl (polyethylene oxide) and triblock polyalkylene oxide copolymers. In most cases, the obtained materials exhibited two-dimensional hexagonal symmetry. However, cubic mesoporous materials have also been prepared.

PMOs were characterized by a battery of techniques including X-ray diffraction (XRD), transmission electron microscopy (TEM), scanning electron microscopy (SEM), nitrogen adsorption measurements, ^{29}Si and ^{13}C solid state nuclear magnetic resonance (NMR), infrared spectroscopy (IR), UV-visible, thermogravimetric analysis (TGA), and elemental analysis.

XRD. XRD is a powerful non-destructive technique for characterizing crystalline materials. It provides information on structures, phases, preferred crystal orientations (texture) and other structural parameters such as average grain size, crystallinity, strain and crystal defects. X-ray diffraction peaks are produced by constructive interference of monochromatic beam scattered from each set of lattice planes at specific angles. The peak intensities are determined by the atomic decoration within the lattice planes. Consequently, the X-ray diffraction pattern is the fingerprint of periodic atomic arrangements in a given material. In powder X-ray diffraction experiments, a collimated beam of nearly monochromatic X-rays is directed onto the flat surface of a relatively thin layer of finely ground material. The sample-diffracted X-rays are then collected to reveal information about the structural state of the material(s) present in the sample. The basic relationship between the diffraction angle and the distance between adjacent diffracting plans is known as Bragg's Law.

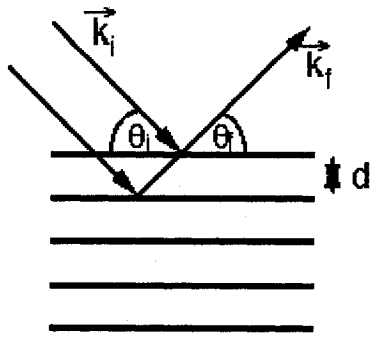

$$\theta_i = \theta_f = \theta$$

$$n\lambda = 2d \sin\theta$$

$$d = n\lambda / (2\sin\theta)$$

where the integer *n* is the order of the diffracted beam, λ is the wavelength of the incident X-ray beam, *d* is the distance between adjacent planes of atoms (the *d*-spacings), and θ is the angle of incidence of the X-ray beam.

Figure 1.5 shows some typical silica mesophases XRD patterns.

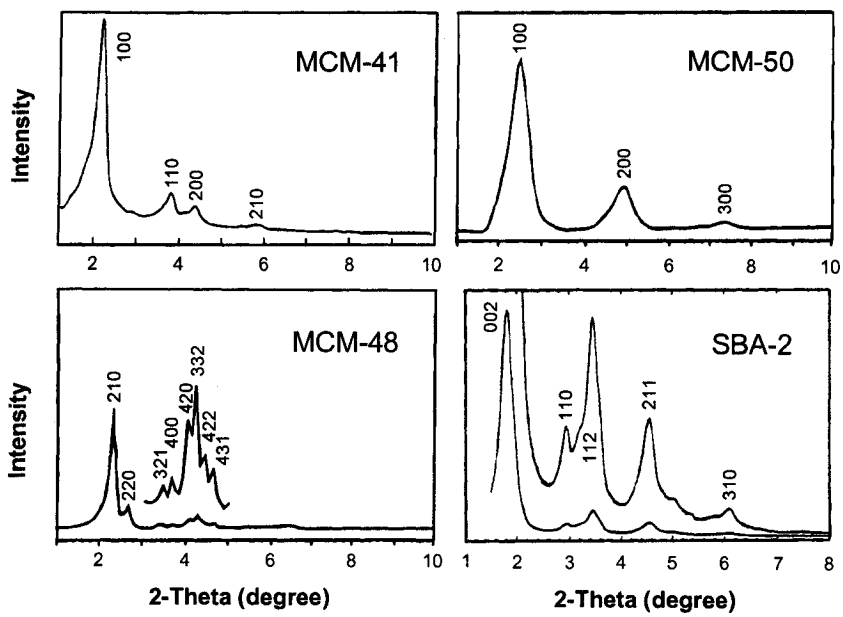

Fig. 1.5 X-ray diffraction patterns for typical silica mesophases [6,10]

TEM. In TEM, a beam of highly focused electrons are directed toward a thin layer of sample (< 200 nm). These highly energetic incident electrons interact with the atoms in the sample producing characteristic radiation and particles providing information for materials characterization. Information is obtained from both deflected and non-deflected transmitted electrons, backscattered and secondary electrons, and emitted photons. Because the electron beam goes through the sample, transmission electron microscopy reveals the interior of the specimen. It gives the following structure information: the size, shape, and the distribution of the phases that make up the material. It gives also the distribution of the elements in the sample, including segregation if present. TEM can also help determine the crystal structure of the phases and the character of the crystal defects.

SEM. In SEM, the images are formed using a very fine electron beam, which is focused on the surface of the specimen. When the beam scans an object, two types of electrons are emitted: backscattered and secondary electrons. The back scattered electrons travel in straight lines while the secondary electrons move in curved paths. The images produced by the SEM are three-dimensional. SEM is used mostly to investigate the morphological features of solid phase materials.

Nitrogen adsorption measurements. Nitrogen adsorption-desorption at 77 K is a commonly applied technique to determine various characteristics of porous materials. The amount of adsorbed nitrogen is measured as a function of the applied vapor pressure. The obtained isotherm allows us to derive the following characteristics:

- ❖ Total pore volume, also known as Gurvitch volume. This is the volume of all pores with diameter smaller than 100 nm.
- ❖ Micropore volume: This is the volume of pores with diameter smaller than 2 nm.
- ❖ Mesopore volumes: This is the volume of pores whose diameter is between 2 and 50 nm.
- ❖ Macropore volume: This is the volume of pores larger than 50 nm.
- ❖ Surface area. Nitrogen adsorption at 77 K is generally considered to be the most suitable technique for surface area determination. The most widely used procedure for the calculation of the surface area of solid materials is the Brunauer-Emmett-Teller (BET) method. The BET surface area is calculated by constructing the so-called BET plot over the relative pressure range up to 0.3. In this part of the isotherm a single layer of nitrogen molecules is formed on the surface (monolayer). Surface areas down to 1 m^2/g can be measured with the instrument available in our laboratory (Coulter Omnisorp 100).
- ❖ Pore size distribution. Nitrogen adsorption isotherms can be measured at relative pressures as low as 10^{-7} torr. This allows for the calculation of micropore size distributions between 0.4 and 2 nm, for example using the method of Horvath-Kawazoe. Furthermore, mesopore size distributions up to 50 nm are derived using the Kelvin equation.

The amount of sample mass that is needed for the experiment typically lies between 0.02 and 1.0 gram.

Figure 1.6 exhibits the five types of adsorption isotherms, I to V, in the classification of Brunauer, Deming, Deming and Teller [46] and the stepped isotherm VI. Type I represents microporous materials. Type II is for nonporous solids. Type IV represents mesoporous materials. Type III and type V are characteristic of weak gas-solid interactions, type III being given by a nonporous or macroporous solid and type V by a mesoporous or microporous solid.

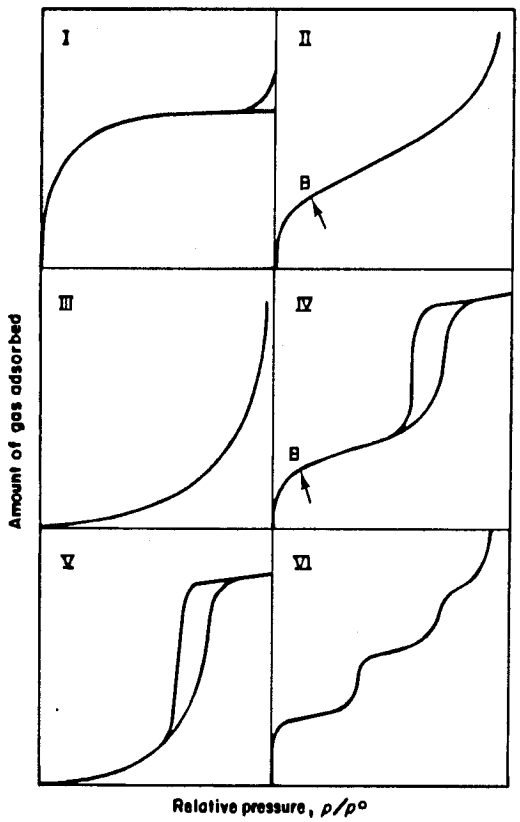

Figure 1.6 The five types of adsorption isotherms, I to V, in the claasification of Brunauer, Deming, Deming and Teller, together with Type VI, the stepped isotherm

Solid state NMR. NMR spectroscopy is a key technique for the characterization of periodic mesoporous organosilicates. It provides direct evidence that the integrity of the Si – R – Si unit is preserved during the precipitation process and the template extraction stage, thus indicating that the organic-inorganic moiety constituted the building block of the mesoporous channel walls. ^{29}Si MAS NMR is expected to show mainly T^n [C-***Si***$(OSi)_n(OH)_{3-n}$; n = 1-3] species with little or no Q^n [***Si***$(OSi)_n (OH)_{4-n}$; n = 1-4] species. ^{13}C MAS NMR on the basis of well-known chemical shifts corresponding to specific functional groups provides direct proof that the organic group is in the framework.

Other techniques such as IR and UV-visible spectroscopy can help to indicate the occurrence of the functional groups within the pore walls. TGA indicates thermostability.

Using these techniques, extensive information about materials, such as structure, pore system, pore walls and morphology, may be gained.

Structure. Table 1.1 lists the structure and synthesis conditions for the silica mesophases discovered to date. The structure of a mesophase obtained under a set of experimental conditions is determined by the dynamic interplay among organic-inorganic ion-pairs, the charge density, coordination and steric requirement of both the organic and inorganic species at the interface. This is ultimately dependent on the synthesis parameters such as the composition of the mixture, the pH and the temperature. TEM is the best and direct way to characterize the mesophase structure. XRD also provides useful information in this regard.

Pore system. The pore system of periodic mesoporous silicas may consist of a two-dimensional array of uniform channels (e.g., MCM-41, SBA-15), a three-dimensional array of connected channels (e.g. MCM-48) or cage-like pores (e.g. SBA-2, FDU-1). Since the determination of the pore system characteristics such as the surface area, the pore volume, the pore size distribution and the pore connectivity is of paramount importance, gas adsorption has quickly become a key characterization technique for mesoporous materials. As shown in Table 1.2, the pore sizes of mesoporous materials can be varied from the low end of mesopore sizes well into the macropore regime. There are two main strategies for pore size engineering. The first is through direct synthesis, for example by using surfactants with different chain lengths, adding expanders or by increasing the temperature during the hydrothermal treatment. The second approach is via post-synthesis treatment in the mother liquid, in water or in aqueous suspensions of long chain amines.

Pore walls. For mesophases with hexagonal structures (e.g. MCM-41, SBA-15), the pore wall thickness is calculated from the equation: $b = 2d_{100}/(3)^{1/2} - w_{KJS.}$, where d_{100} is the distance between successive (100) plans and w_{KJS} is the pore size. Both d and w are obtained from XRD and nitrogen adsorption, respectively [48].

Morphology. Periodic mesoporous silica may be prepared in a variety of morphologies such as thin films, spheres, fibers and large monoliths. SEM provides this information.

The synthesis and characterization of PMO materials are very recent new developments in material chemistry. So far, only a few types of organic functionalized PMOs have been reported. Also relatively little is known about how to

control their pore size and morphology. There are some detailed investigations of the structural integrity, and thermal and chemical stability of Si-C bonds for various kinds of organic groups in PMOs and their applications.

Table 1.1. Structure and synthesis conditions for various silica mesophases

Mesophase	Amphiphile template	pH	Structure
MCM-41	$C_nH_{2n+1}(CH_3)_3N^+$	basic	2D hexagonal (*p6mm*)
MCM-48	$C_nH_{2n+1}(CH_3)_3N^+$ Gemini $C_{n\text{-}s\text{-}n}$ [a]	basic	cubic ($Ia\bar{3}d$)
MCM-50	$C_nH_{2n+1}(CH_3)_3N^+$	basic	lamellar
FSM-16	$C_{16}H_{31}(CH_3)_3N^+$	basic	2D hexagonal (*p6mm*)
SBA-1	$C_{18}H_{37}N(C_2H_5)_3^+$	acidic	cubic ($Pm\bar{3}n$)
SBA-2	Divalent $C_{n\text{-}s\text{-}1}$ [b]	acidic / basic	3D hexagonal ($P6_3/mmc$)
SBA-3	$C_nH_{2n+1}N(CH_3)_3^+$	acidic	2D hexagonal (*p6mm*)
SBA-6	Divalent $18B_{4\text{-}3\text{-}1}$ [c]	basic	cubic ($Pm\bar{3}n$)
SBA-8	Bolaform [d]	basic	2D rectangular (*cmm*)
SBA-11	Brij 56; $C_{16}EO_{10}$	acidic	cubic ($Pm\bar{3}m$)
SBA-12	Brij 76; $C_{18}EO_{10}$	acidic	3D hex. ($P6_3/mmc$)
SBA-14	Brij 30; $C_{12}EO_4$	acidic	cubic
SBA-15	P123; $EO_{20}PO_{70}EO_{20}$	acidic	2D hex. (*p6mm*)
SBA-16	F127; $EO_{106}PO_{70}EO_{106}$	acidic	cubic ($Im\bar{3}m$)
FDU-1	B50-6600; $EO_{39}BO_{47}EO_{39}$	acidic	cubic ($Im\bar{3}m$)
MSU-1	Tergitol; $C_{11\text{-}15}(EO)_{12}$	neutral	disordered
MSU-2	TX-114; $C_8Ph(EO)_8$ TX-100; $C_8Ph(EO)_{10}$	neutral	disordered
MSU-3	P64L; $(EO_{13}PO_{30}EO_{13})$	neutral	disordered
MSU-4	Tween-20, 40, 60, 80	neutral	disordered
MSU-V	$H_2N(CH_2)_nNH_2$	neutral	lamellar
MSU-G	$C_nH_{2n+1}NH(CH_2)_2NH_2$	neutral	lamellar
HMS	$C_nH_{2n+1}NH_2$	neutral	disordered

(a) Gemini surfactants $C_{n\text{-}s\text{-}n}$: $C_nH_{2n+1}N^+(CH_3)_2(CH_2)_sN^+(CH_3)_2C_nH_{2n+1}$.

(b) Divalent surfactants $C_{n\text{-}s\text{-}1}$: $C_nH_{2n+1}N^+(CH_3)_2(CH_2)_sN^+(CH_3)_3$.

(c) Divalent surfactant $18B_{4\text{-}3\text{-}1}$: $C_{18}H_{37}O\text{-}C_6H_4\text{-}O(CH_2)_4N^+(CH_3)_2(CH_2)_3N^+(CH_3)_3$.

(d) Bolaform surfactants :$(CH_3)_3N^+(CH_2)_nO\text{-}C_6H_4\text{-}C_6H_4\text{-}O(CH_2)_nN^+(CH_3)_3$.

Table 1.2. Methods of pore size engineering for mesoporous silicas [17]

Pore size (nm)	Method
2-5	Use of surfactants of different chain lengths
	Charged (alkylammonium)
4-10	Neutral (alkylamine)
	Use of micelle expanders
	Aromatic hydrocarbons
	Alkanes
	Trialkylamines
4-7	Alkyldimethylamines
	Hydrothermal post-synthesis treatment
	In mother liquor
	In water
2.5-6.6	High temperature synthesis
3.5-25	Water-amine post-synthesis treatment
5-30	Use of triblock copolymer and expander
> 50	Emulsion templating
> 200	Colloidal crystal templating

1.2 Scope of this thesis

The present study is focused on the following aspects:

(1) Preparation of organosilicon precursors (bis(triethoxysilyl)benzene and bis(triethoxysilyl)ethylene)

(2) Optimization of the synthesis conditions to obtain highly ordered materials.

(3) Characterization of the obtained PMOs, and investigation of their reactivity.

This thesis is comprised of five chapters. After a general introduction (Chapter one) on the background of mesoporous organosilicas and the recent progress in this field, the synthesis of organosilicon precursors is described in Chapter two. Published methods for synthesis of organosilicons are reviewed. The details of an improved method to synthesize the precursors and identify them are also reported in Chapter two. Chapter three is dedicated to the preparation of periodic mesoporous organosilicate materials. All the details of preparation of PMOs under different conditions are provided. The experimental results and discussion are presented in Chapter four which has three sections. First, the materials involving phenylene bridged group are characterized using XRD, SEM, TEM, ^{29}Si and ^{13}C NMR and nitrogen adsorption measurements. Second, materials involving the ethenylene bridged group are characterized by the same techniques. Finally, the results of post-synthesis reactions for ethenylene bridged materials are discussed. In the final Chapter, a summary of this study and some future plans are provided.

Chapter 2

Synthesis of organic silicon precursors

2.1 Introduction

PMOs are comprised of bridge-bonded organic groups as integral components of the framework [13,18,36-38,40,45,47]. In order to prepare such materials, we used poly(trialkoxysilyl) organic precursors ($[(R'O)_3Si]_xR$, x = 2, 3). In most case "bridged silsesquioxanes" $(R'O)_3Si\text{-}R\text{-}Si(OR')_3$ were used as precursors. The obtained materials have similarity with organically surface modified mesoporous silicas which are obtained by either post-synthesis grafting of functionalized trialkoxysilane $R\text{-}Si(OR')_3$, or via cocondensation of such molecules with TEOS. Using $(R'O)_3Si\text{-}R\text{-}Si(OR')_3$ has several advantages over the use of $R\text{-}Si(OR')_3$: (i) it leaves the void space completely free, (ii) it allows the physical properties of the framework to be tailored , (iii) it permits chemical modification of the framework by further reactions of the organic group, and (iv) it affords materials with many potential applications by choosing various types of bridging organic functional groups with specific electrooptic, catalytic and hydrophilic/ hydrophobic properties. Up to now, only a few types of organic functional groups were used in PMOs, including methylene [13,35,42], ethane [18,36-40,42-44], ethylene [38,40,42], acetylene [42, 45], thiophene [42,45], benzene [42-45] and bithiophene [45]. The main problem is that many silicon-containing organic precursors are not commercially available and need to be synthesized. In addition, in some cases Si-C bonds are sensitive, indicating that there is a need to investigate the thermal and chemical stability of Si-C and find new way to stable PMOs.

Scheme 2.1 shows most of the commercially available precursors (either triethoxysilylated or trichlorosilylated) suitable for the synthesis of PMO materials.

Scheme 2.1 Commercially available PMO precursors (Si denotes – $Si(OEt)_3$ or $–SiCl_3$)

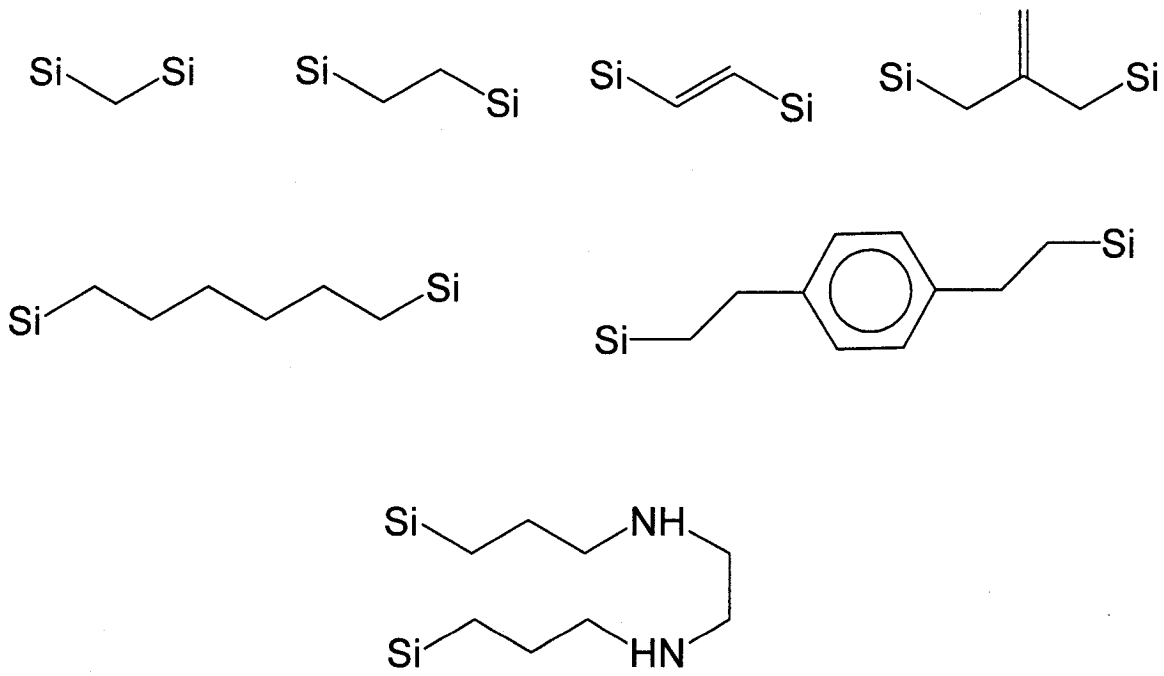

There are a number of synthetic strategies to prepare silsesquioxane monomers. The three most commonly used approaches are (1) metalation of aryl, alkyl, and alkynyl precursors followed by reaction with a tetrafunctional silane. (2) hydrosilylation of dienes (or polyenes) or, less commonly, diynes, and (3) reaction of a bifunctional organic group with an organotrialkoxysilane bearing a reactive functional group.

Metalation. Metalation (Scheme 2.2) includes Grignard reaction [48], lithium-halogen exchange [48-51] and deprotonation of acetylenes [48, 50] or treatment of bis(trialkoxysilyl)methane with a Grignard reagent, organolithium, or metal hydride [52]. In each case, the resulting organometallic reagent is then reacted with a tetraalkoxysilane or chlorotrialkoxysilane to give the final product in moderate to good yields.

Scheme 2.2 Preparation of monomers by metalation

(1) Grignard

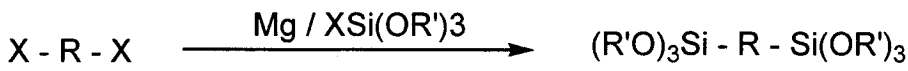

(2) Lithiation

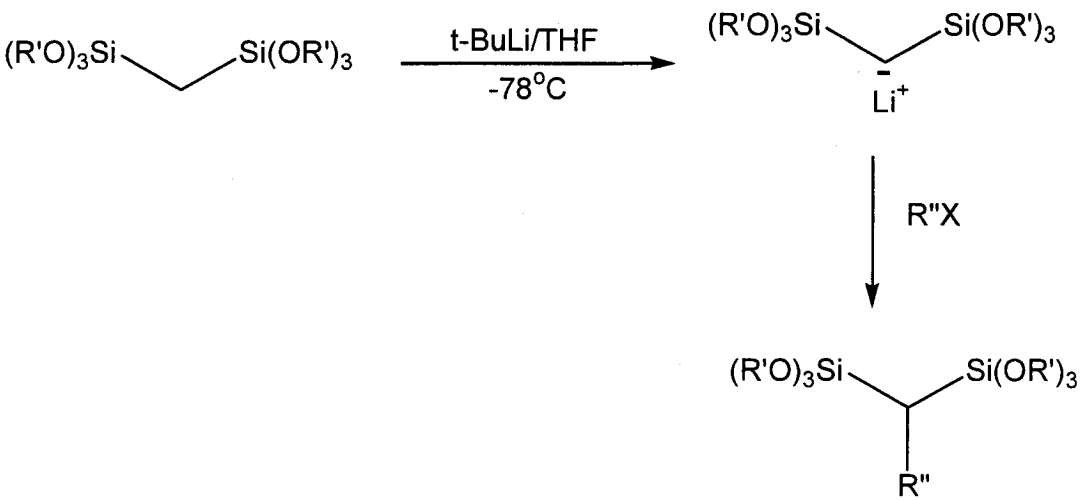

Hydrosilylation. Hydrosilylation (Scheme 2.3) is an efficient reaction for preparing silsesquioxane monomers in high yields from chemicals bearing two or more terminal olefins [53,54]. It has been used for alkylene and heteroatom-functionalized bridging groups.

Scheme 2.3 Preparation of monomers by hydrosilylation

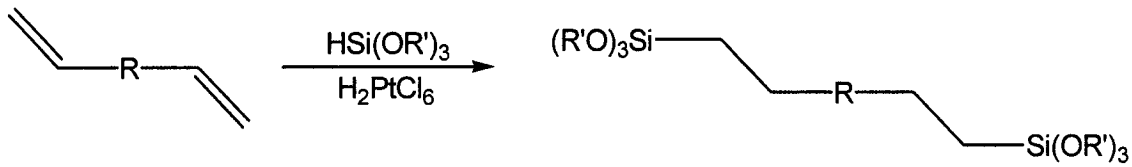

Functionalization of an organotrialkoxysilane. This synthetic route has become increasingly common because it permits a great number of bridging groups to be prepared from readily available starting materials. Scheme 2.4 lists some examples.

Scheme 2.4. Preparation of bridged monomers from organotrialkoxysilanes.

(1)

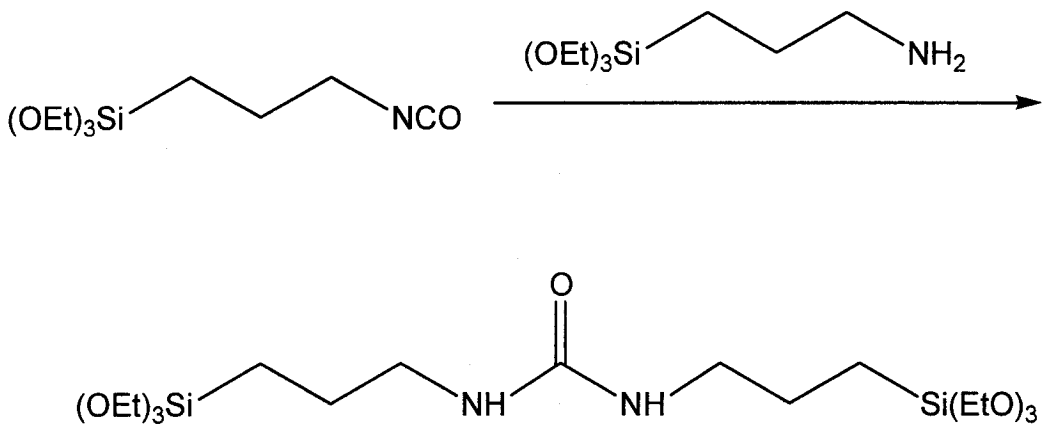

(2)

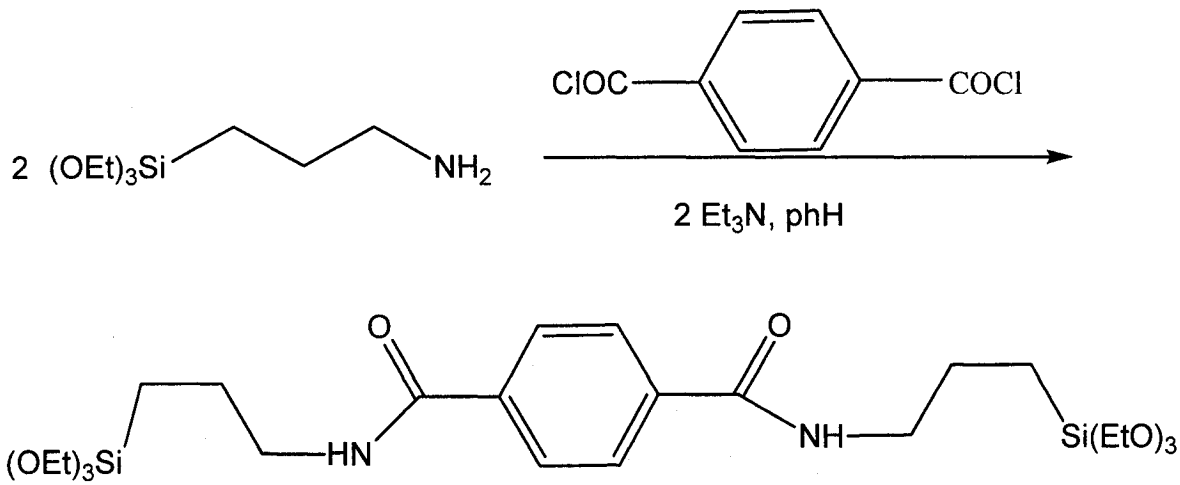

Miscellaneous Approaches. Some examples are listed in Scheme 2.5.

Scheme 2.5 Miscellaneous methods of synthesizing monomers

(1) Alcoholysis

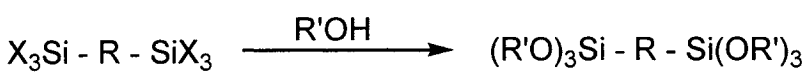

(2) Pd-coupling Heck Reaction

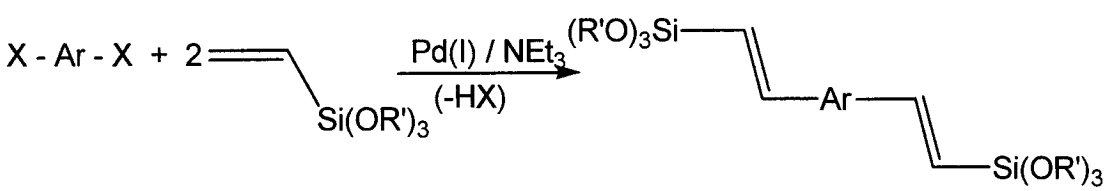

(3) Hydroboration

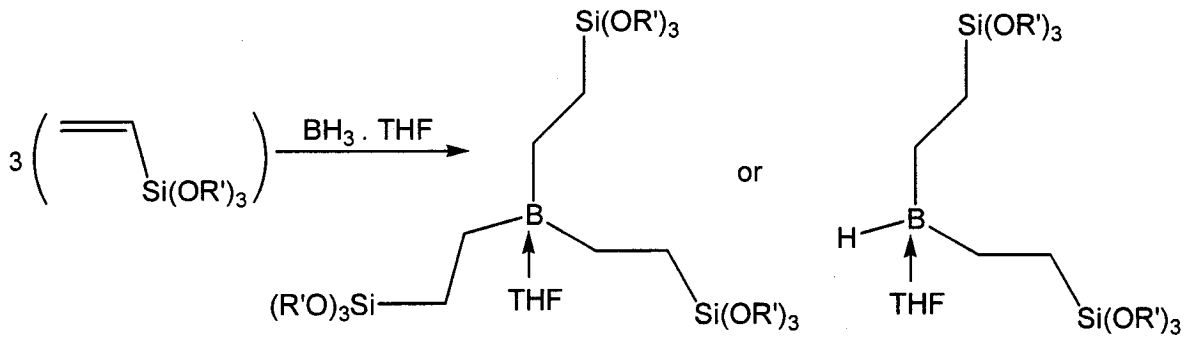

(7) Silylation of acid halides (acyl halides)

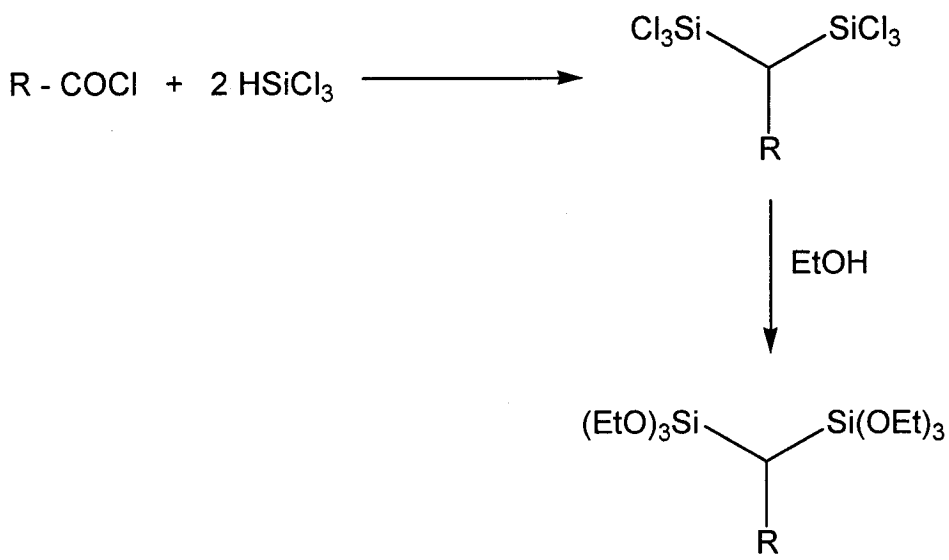

Scheme 2.6 exhibits some commercially unavailable precursors that have been prepared and used for the synthesis of PMOs.

Scheme 2.6. Commercially unavailable precursors used for PMO synthesis

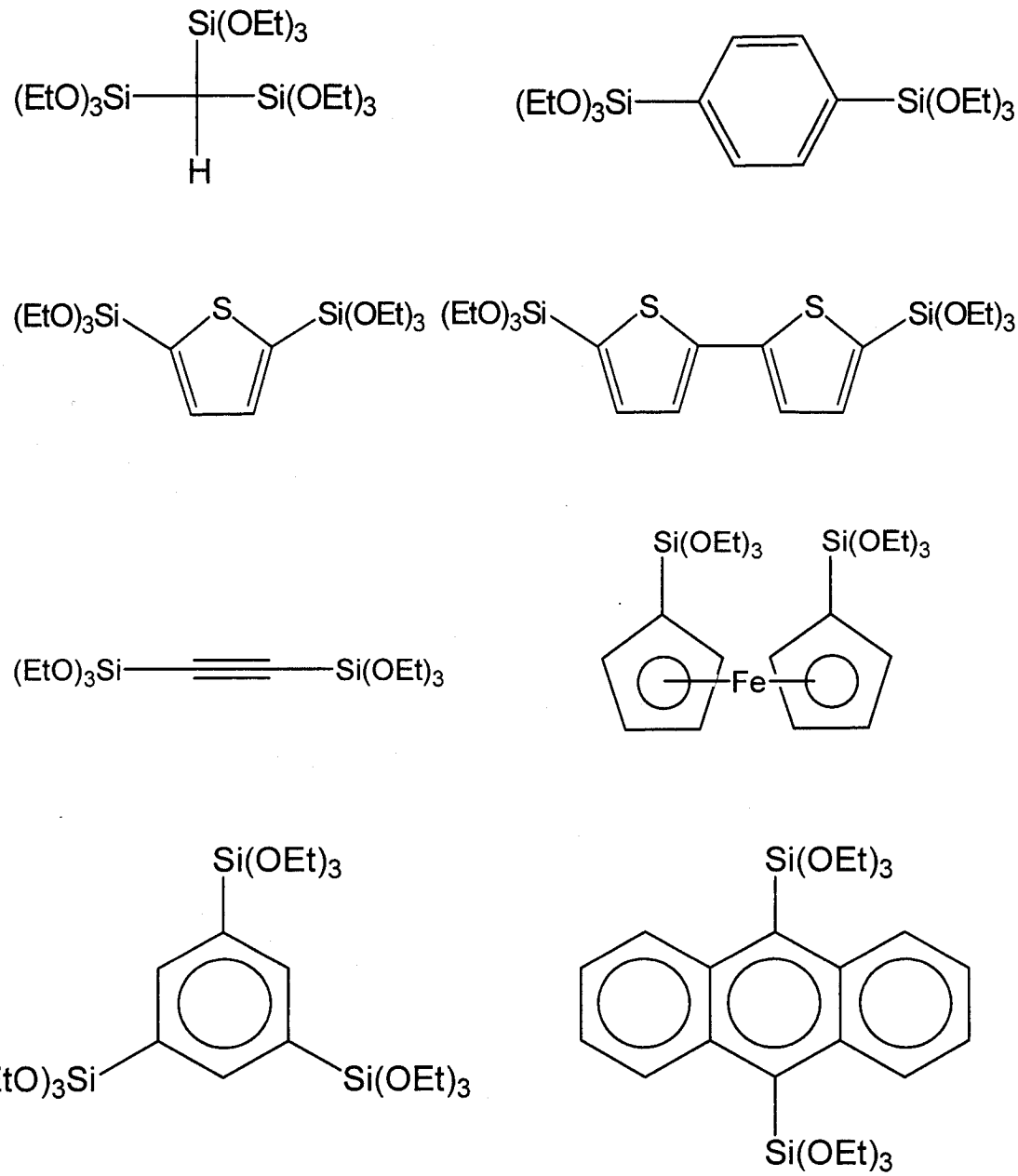

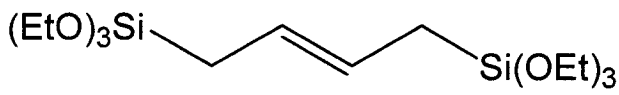
(EtO)3Si
Si(OEt)3

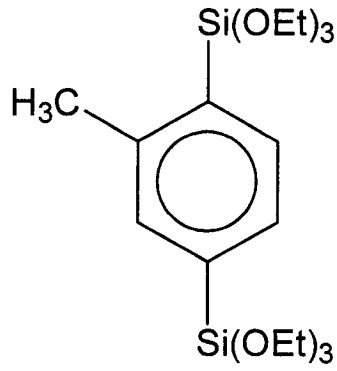
Si(OEt)3
H3C
Si(OEt)3

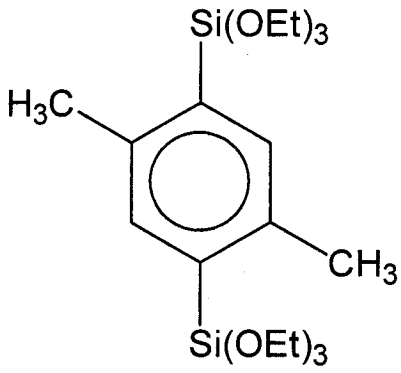
Si(OEt)3
H3C
CH3
Si(OEt)3

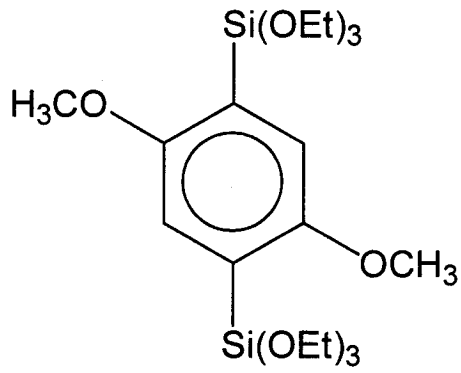
Si(OEt)3
H3CO
OCH3
Si(OEt)3

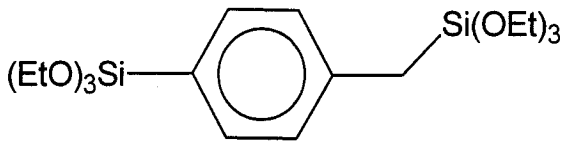
(EtO)3Si
Si(OEt)3

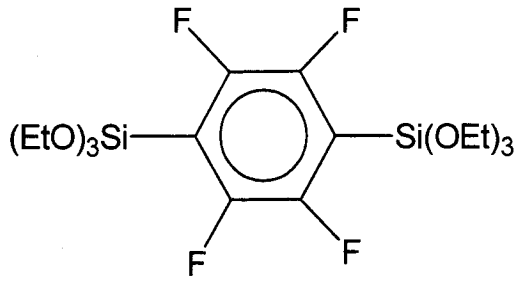
F
F
(EtO)3Si
Si(OEt)3
F
F

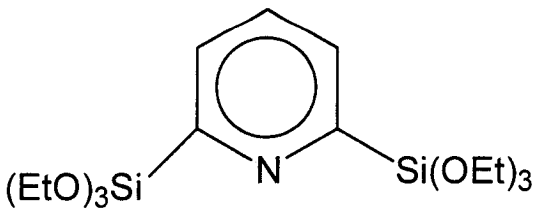
(EtO)3Si
N
Si(OEt)3

2.2 Synthesis of precursors

The precursors used in this thesis are bis(triethoxysilyl)benzene and bis(triethoxysilyl)ethylene. The first one is commercially unavailable. The second one is expensive and takes a long time to acquire. They were both synthesized in our laboratory.

2.2.1 Synthesis of bis(triethoxysilyl)benzene

This aromatic precursor is normally synthesized by Grignard reaction (Scheme 2.7).

2.2.1.1 Literature review

According to the literature, there are two ways to synthesize bis(triethoxysilyl)benzene [48,50]. Both of them are based on the Grignard reaction. The first method uses 1,4–dibromobenzene and $XSi(OCH_2CH_3)_3$, whereas the second method use 1,4–dibromobenzene and $Si(OCH_2CH_3)_4$. The reaction formula is shown in Scheme 2.7. The yield obtained was 44 and 55% for the first and second method, respectively. Considering that $Si(OCH_2CH_3)_4$ is more stable and safer than $XSi(OCH_2CH_3)_3$, the second procedure was chosen for further synthesis.

Scheme 2.7. Reaction routes for bis(triethoxysilyl)benzene

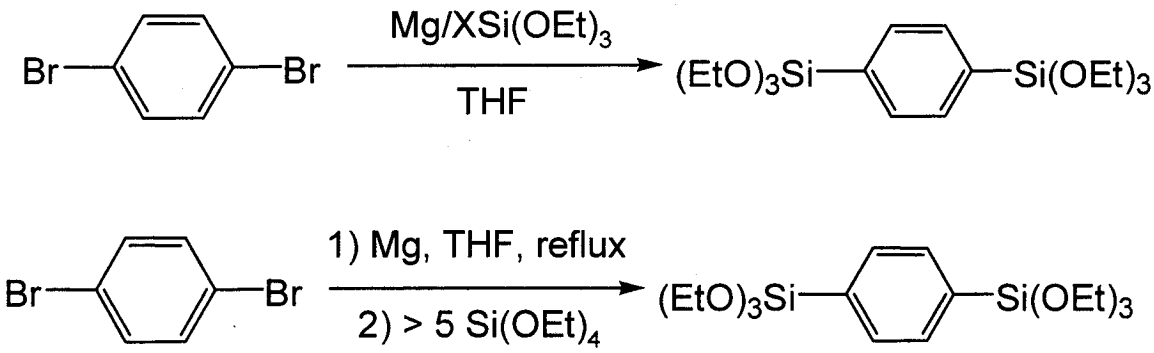

2.2.1.2 Experimental

Materials. Magnesium turning, tetraethoxysilane, iodine, THF and hexane were obtained from Aldrich. THF and hexane were distilled from Na/benzophenone before use.

Bis(triethoxysilyl)benzene. To a mixture of magnesium turnings (3.0 g, 0.125 mol) and tetraethoxysilane (90 ml, 0.4 mol) in THF (60 ml) under nitrogen, a small crystal of iodine was added, and the mixture was heated to reflux. A solution of 1,4-dibromobenzene (9.6 g, 4.08 mmol) in THF (25 ml) was added dropwise. After 1.5 h, the addition of dibromide was completed. The mixture was kept under reflux for one and half hour. A white solid appeared. When the mixture was cooled to room temperature, it was subjected to filtration. Then hexane (40 ml) was added after removing THF. The mixture was filtered again to separate the solid. Hexane was removed by vacuum distillation, and the remaining TEOS was distilled in vacuum leaving a light yellow oil which is the product (8.7 g, 57%) as identified by NMR, IR

and MS. ^{1}HNMR (500 MHz, $CDCl_3$, ppm): 7.65 (4H, s), 3.85 (12H, q, J = 7.0 Hz) and 1.27 (18H, t, J = 7.0 Hz); ^{13}C NMR ($CDCl_3$, ppm): 18.15, 58.72, 133.17, 133.98. IR (film on NaCl): 3056, 2975, 2886, 1390, 1167, 1147, 1103, 1081, 961, 780, 706 cm^{-1}. Low resolution mass spectrum (EI, 70 eV) m/z: 357, 329, 297, 285, 195, 163, 147, 119, 100, 91, 79.

2.2.1.3. Discussion

In this reaction, the iodine was used as indicator. When it was added, the mixture became brown, then as the 1,4–dibromobenzene was added, the color would disappear indicating that the reaction runs well. If upon addition of the iodine, the brown color disappears immediately, that means that the system contains residual water, and the reaction will fail. The dropwise addition of 1,4–dibromobenzene was the key step of this reaction. If 1,4–dibromobenzene is added too fast, the side-product 1-bromo-4- triethoxysilylbenzene is obtained. This is because the second triethoxysilyl group does not have enough time to react. To avoid this side-product, the reaction should be kept under reflux, tetraethoxysilane should be used in excess and the 1,4– dibromobenzene solution should be added slowly in dropwise. ^{13}C NMR: 18.15 is for δ (CH_3), 58.72 is for δ (CH_2O), 133.17 and 133.98 are for δ (C_6H_4). ^{1}H NMR: 7.65 is for the four H of benzene, 3.85 is twelve H of OCH_2, and 1.27 is eighteen H of CH_3. IR and MS matched with the literature [48]. MS spectrum did have 402 amu peak, but really small. This is because bis(triethoxysilyl)benzene loses –OEt easily to give a peak at 357 amu. The strongest peak is 163 amu which

corresponds to the elimination of $-Si(OEt)_3$. In summary, NMR, IR and MS data confirmed that the obtained product is bis(triethoxysilyl)benzene.

2.2.2. Synthesis of bis(triethoxysilyl)ethylene

Metathesis of olefins is a well-known disproportionation reaction that occurs via heterogeneous or homogeneous catalysis. It allows new internal olefins to be synthesized. Self-metathesis was used to prepare bis(triethoxysilyl)ethylene in this work.

2.2.2.1. Literature review

The literature shows that metathesis is a very common method to synthesize new internal olefins. However alkenyl-silanes, like other unsaturated organosilicon compounds, do not easily undergo olefin metathesis. Marciniec *et al.* [55,56] run the hydrosilylation of vinyltrialkoxysilanes by trialkoxysilanes in the presence of ruthenium complexes, and obtained an unsaturated product $(RO)_3SiCH=CHSi(OR)_3$. Since then, bis(triethoxysilyl)ethylene was synthesized from vinyltriethoxysilane in the presence of ruthenium catalysts [57,58]. One successful approach was to use $(Ph_3P)_3Ru(CO)H$ as catalyst and $PhCH_3$ as solvent under reflux. Another approach was to use $RuCl_2(PPh_3)_3$ as catalyst and reflux without solvent. In this work, we used the second method because it does not need a solvent and the catalyst is cheaper. Scheme 2.8 shows the reaction formula.

Scheme 2.8. Reaction formula for the synthesis of bis(triethoxysilyl)ethylene

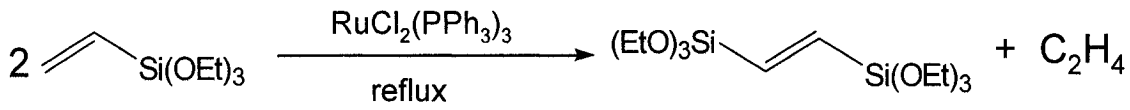

2.2.2.2 Experimental

Materials. vinyltriethoxysilane and $RuCl_2(PPh_3)_3$ were obtained from Aldrich.

Bis(triethoxysilyl)ethylene. A solution of vinyltriethoxysilane (47.859 g) and $RuCl_2(PPh_3)_3$ (0.297 g) was refluxed for 24 h. Then the remaining vinyltriethoxysilane was distilled off in vacuum and the residue was vacuum distilled to obtain the product (30.529 g, 57.28%). ^1H NMR (300 MHz, $CDCl_3$, ppm): 6.63 (2H, s), 3.80 (12H, q), 1.25 (18H, t). ^{13}C NMR ($CDCl_3$, ppm): 18.17, 58.56, 145.68. Low resolution mass spetrum (EI, 70 eV) m/z: 308, 279, 253, 235, 207, 163, 119, 107, 91, 79.

2.2.2.3 Discussion

The most important feature in this reaction is to keep the reaction refluxing all the time. As the reaction proceeds, the boiling point increases, so the temperature has to be adjusted to make sure that the reaction is kept refluxing. If not, the product is not formed. The ^1H NMR: 6.63 is for the H of double bond, 3.80 is for the H of OCH_2,

and 1.25 is for the H of CH_3. However, integration of the NMR peaks indicated that the $-CH_2$ and $-CH_3$ groups were a little higher than expected. This was attributed to the fact that the product has two isomers trans and cis. Indeed, the ^1H NMR spectrum shows a small peak (6.74 ppm) which belongs to the other isomer. The ^{13}C NMR: 18.17 is for δ (CH_3), 58.56 is for δ (CH_2O), 145.68 is for δ (CH=), The MS spectrum did not show M^+ because bis(triethoxysilyl)ethylene loses –OEt easily to give the 308 amu peak. The strongest peak was 163 amu which corresponds to the loss of $-Si(OEt)_3$. MS was consistent with the literature [57]. From NMR and MS, it is confirmed that the product is bis(triethoxysilyl)ethylene.

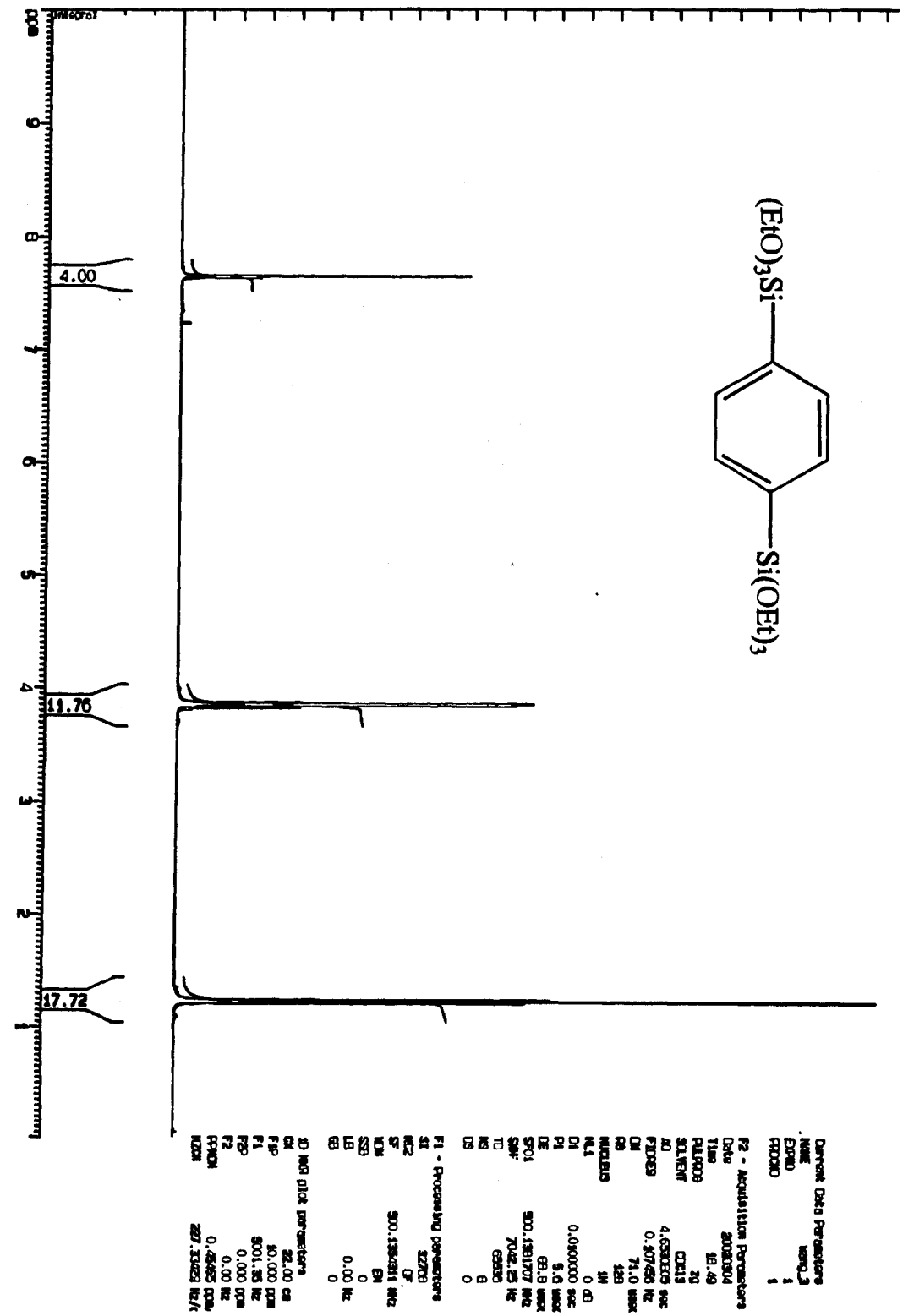
(EtO)3Si
Si(OEt)3
4.00
11.76
17.72

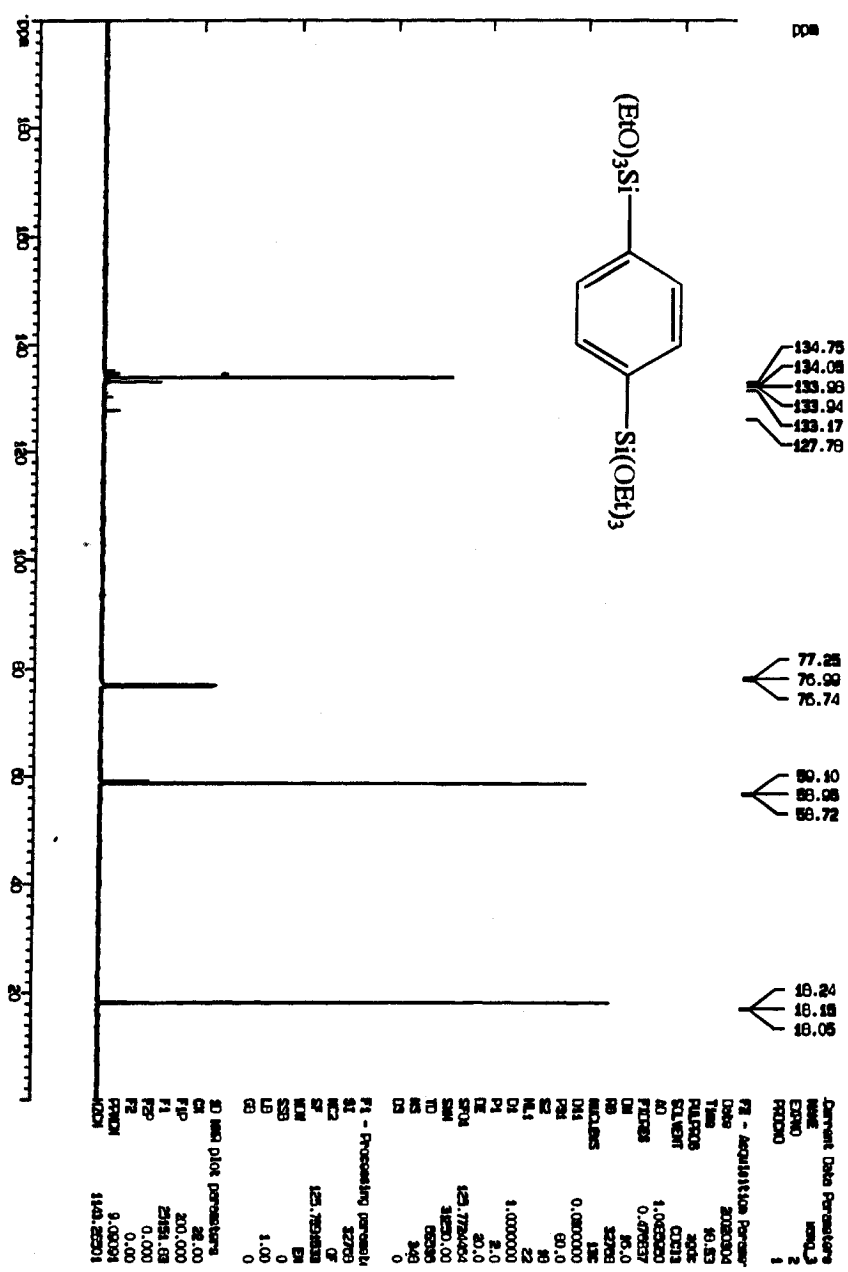
(EtO)3Si
Si(OEt)3
134.75
134.08
133.98
133.94
133.17
127.78
77.25
76.99
76.74
59.10
58.98
58.72
18.24
18.15
18.05
ppm

1g2030 Scan 33 RT=0:55 100%=160804 mv 17-Jun-2003 10:16
LRP +EI bteb

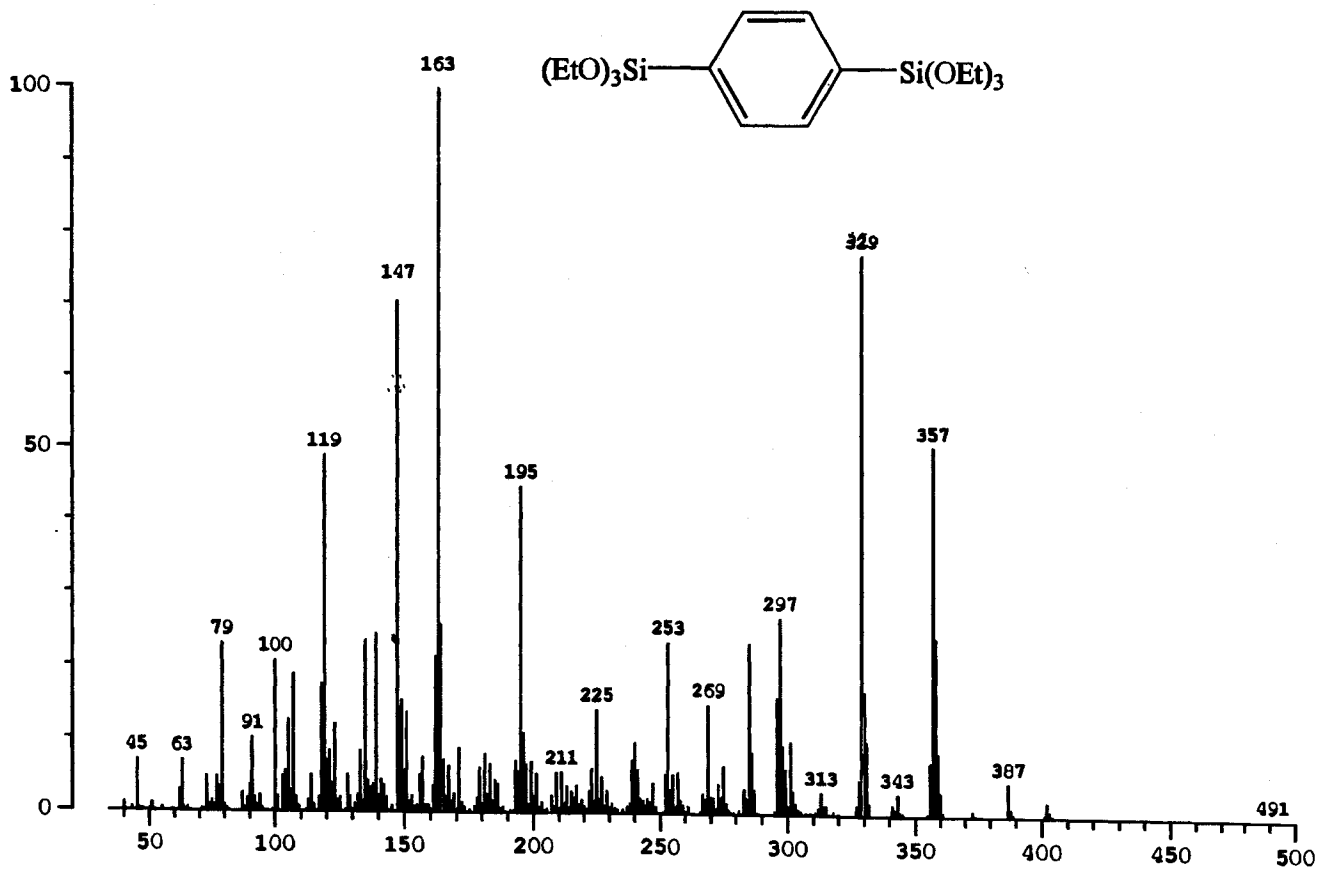

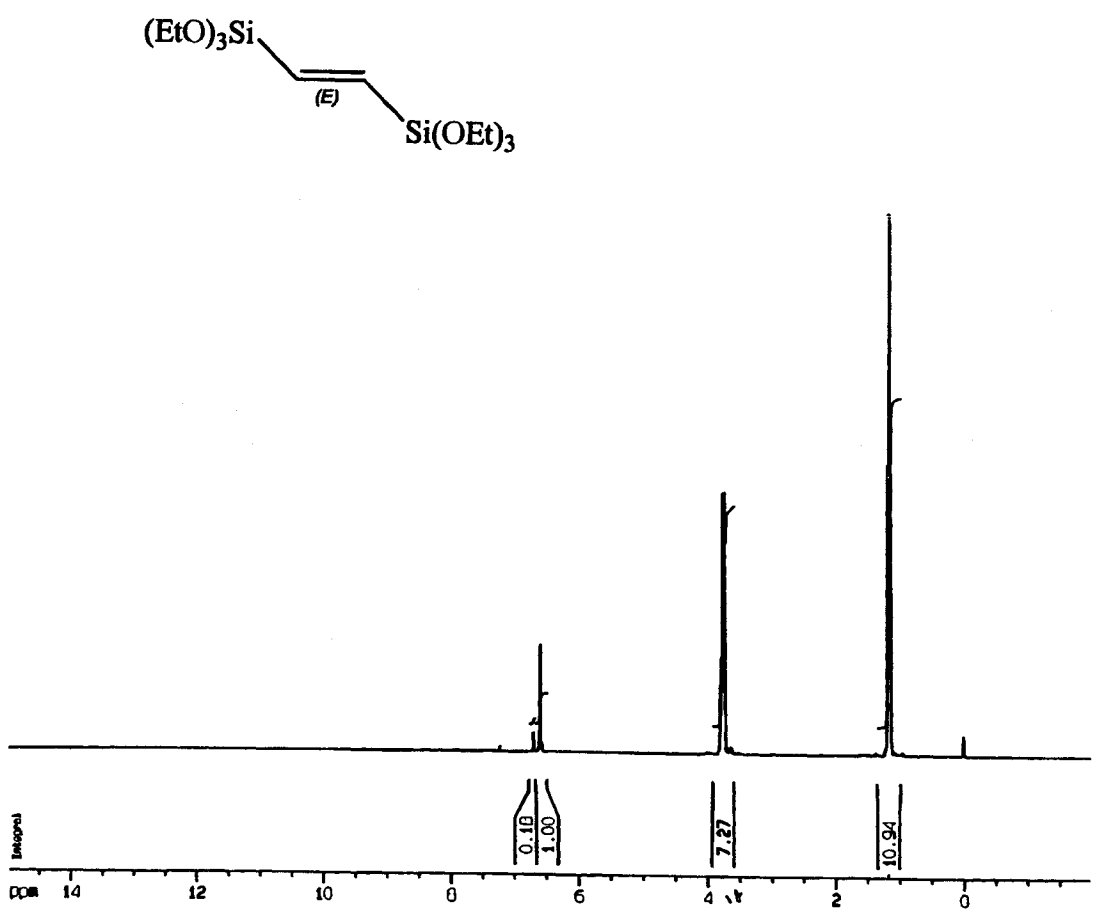


```
Current Data Parameters
NAME                  pswv6
EXPNO                     1
PROCNO                    1

F2 - Acquisition Parameters
Date_              20020912
Time                   9 32
INSTRUM                av300
PROBHD   5 mm CNP  1H/1
PULPROG                zg30
TD                    30720
SOLVENT               CDCl3
NS                        1
DS                        0
SWH               9091.301 Hz
FIDRES            0.165407 Hz
AQ                3.0220900 sec
RG                     45.3
DW                  98.400 usec
DE                   6.00 usec
TE                  300.0 K
D1                1.00000000 sec

======== CHANNEL f1 ========
NUC1                   1H
P1                   8.00 usec
PL1                 -3.00 dB
SFO1          300.1319477 MHz

F2 - Processing parameters
SI                    65536
SF          300.1300000 MHz
WDW                    EM
SSB                       0
LB                   0.10 Hz
GB                        0
PC                     1.00

1D NMR plot parameters
CX                  20.00 cm
CY                  10.00 cm
F1P                 14.988 ppm
F1                4498.35 Hz
F2P                -1.976 ppm
F2                 -592.94 Hz
PPMCM             0.84652 ppm/cm
HZCM              254.06503 Hz/cm
```

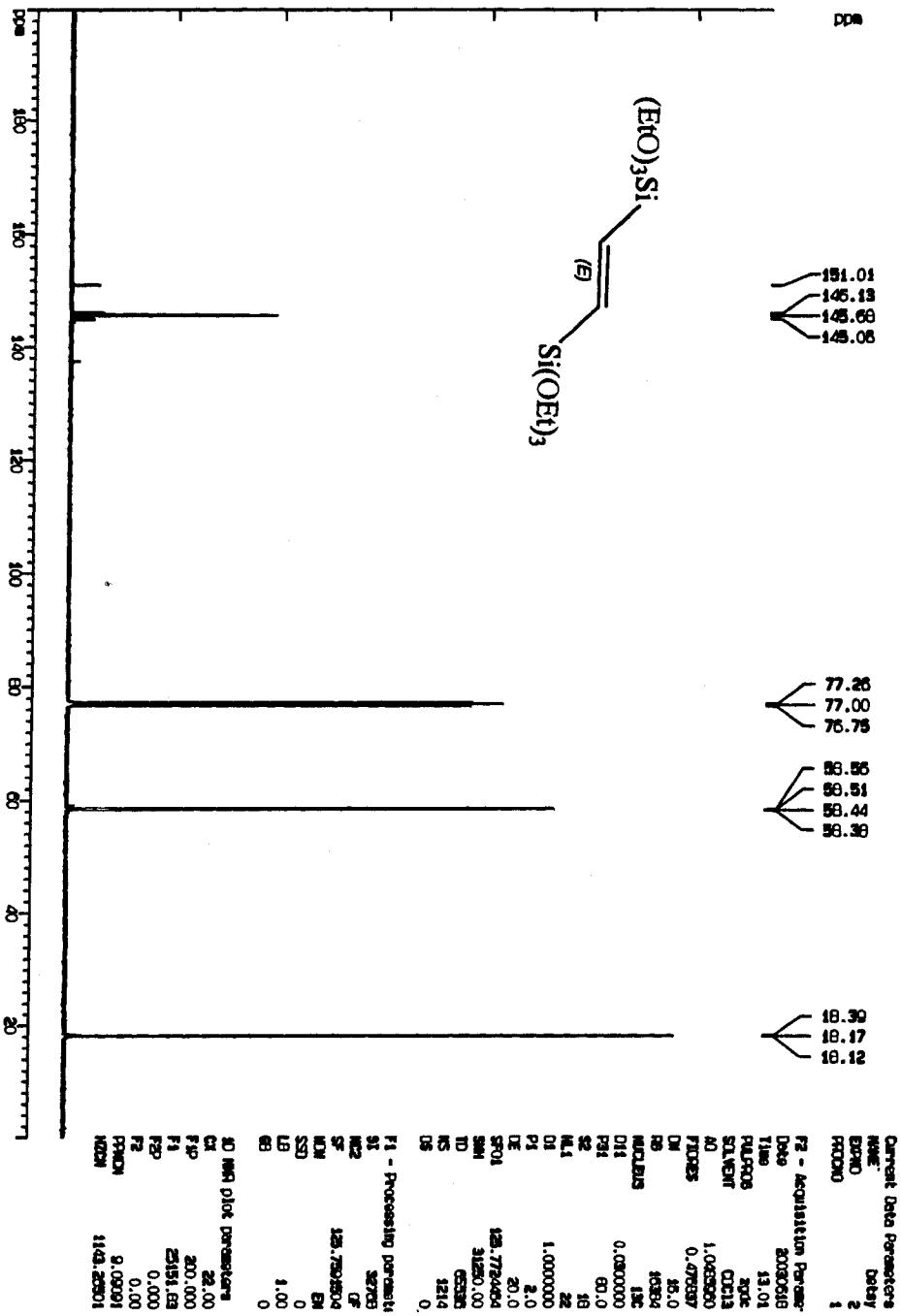
(EtO)3Si
(E)
Si(OEt)3
ppm
151.01
145.13
145.68
145.06
77.26
77.00
76.75
58.55
58.51
58.44
58.38
18.39
18.17
18.12

1g2029 Scan 24 RT=0:40 100%=23760 mv 17-Jun-2003 10:12
LRP +EI

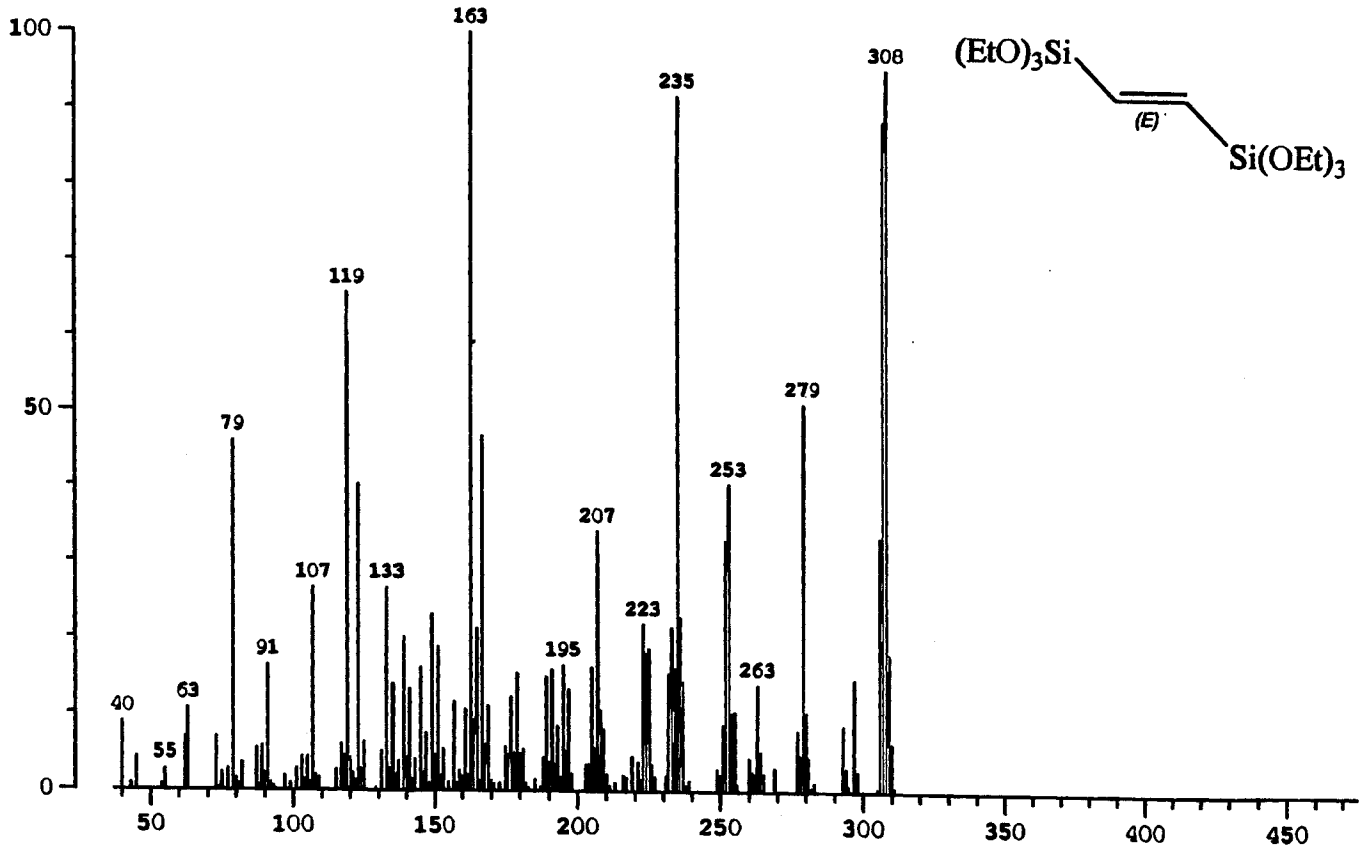

Chapter 3

Preparation of periodic mesoporous organosilicates materials

3.1 Introduction

The synthesis of high surface area, periodic mesoporous materials containing organic groups in the framework is drawing much attention. This exciting recent development is the result of combining the self-assembly approach for making ordered mesoporous silica and the use of bridged silsesquioxanes $(R'O)_3Si\text{-}R\text{-}Si(OR')_3$ as precursors. PMOs are synthesized by a one-pot surfactant-templated supramolecular self-assembly procedure, then the surfactant is removed by solvent-extraction. In this thesis, phenylene-bridged mesoporous materials were prepared using bis(triethoxysilyl)benzene as precursor in the presence of oligomeric surfactants. Likewise, ethenylene-bridged mesoporous materials were prepared by using bis(triethoxysilyl)ethylene as precursor and different types of supramolecular templates, i.e., oligomeric alkyl polyethylene oxide (Brij 56, 58, 76 and 78), Pluronic polyalkylene oxide triblock copolymer (P123) and alkyltrimethylammonium surfactants.

One advantage of introducing organic groups into the framework of mesoporous materials is that the organic linker can be further modified leading to new surface properties. In this work, post-synthesis reactions on PMOs were also investigated.

3.2 Preparation of PMOs using bis(triethoxysilyl)benzene as precursor

3.2.1 Literature review

Inagaki et al. [59] showed that using 1,4-bis(triethoxysilyl)benzene under basic conditions in the presence of octadecyltrimethylammonium chloride affords materials which exhibit both long and short-range order. In addition to the periodic system of 4.5 nm diameter hexagonally packed cylindrical pores, the pore walls also exhibited a structural periodicity with a spacing of 0.76 nm along the channel direction due to the π - π stacking of bridging phenylene groups (Figure 3.1). Similar molecular scale periodicity with 1.16 nm spacing occurred also within the pore walls of biphenylene-bridged mesoporous organosilica [60]. Prepared under acidic conditions using Pluronic P123 as structure directing agent, phenylene-bridged organosilica showed little evidence of molecular order within the pore wall [61]. Periodic mesoporous organosilicates with aryl groups such as tolyl, xylyl and dimethoxyphenyl prepared under acidic conditions in the presence of cetylpyridinium chloride also showed some arylsilica ordering in the channel walls [62].

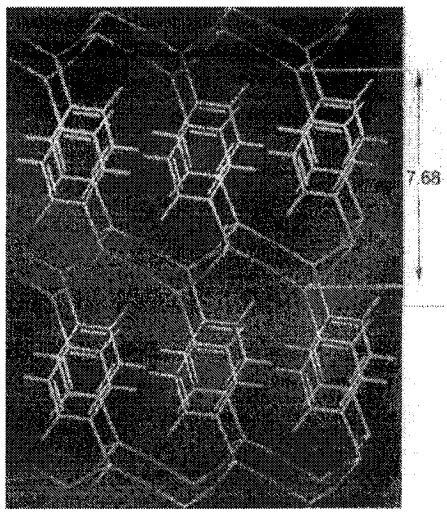

Figure 3.1 Layered arrangement of $O_{1.5}Si\text{-}C_6H_4\text{-}SiO_{1.5}$ units in the walls [59]

Oligomeric surfactants such as nonionic alkyl poly(oxyethylene) surfactants $C_nH_{2n+1}(OCH_2CH_2)_{10}OH$, denoted C_nEO_m, proved to be excellent supramolecular templates for the synthesis of highly ordered mesoporous silicas [10,63] and ethanesilicas [64] under acidic conditions. However, they were not used for the synthesis of other PMOs. The purpose of the current investigation is to apply this synthetic approach to phenylenesilica and to check if the regular stacking of the aromatic rings in the channel walls occurs also under such conditions.

3.2.2 Experimental

Phenylene-bridged mesoporous materials were synthesized using 1,4-bis(triethoxysilyl)benzene (BTEB) as precursor in the presence of oligomeric surfactants Brij 56 ($C_{16}EO_{10}$), Brij 76 ($C_{18}EO_{10}$), Brij 58 ($C_{16}EO_{20}$), and Brij 78

($C_{18}EO_{20}$) under acidic conditions. BTEB was prepared and purified as described in the previous chapter. The alkylethylene oxide oligomeric Brij 56, Brij 58, Brij 76 and Brij 78, concentrated hydrochloric acid and ethanol were purchased from Aldrich. 2M hydrochloric acid was prepared by diluting 83.8 g concentrated hydrochloric acid to a 500 ml solution.

Preparation of phenylene-bridged mesoporous material using Brij 76 (denoted SW3e). 2 g of Brij 76 was dissolved in 10 g of distilled water and 50 g of 2M hydrochloric acid. After 30 minutes of stirring at 50 °C, Brij 76 was dissolved. BTEB (4.225 g) was added to the solution and a white precipitate appeared immediately. The mixture was kept under stirring for 20 h at 50 °C. Then, the mixture was cooled to room temperature. A white precipitate was recovered by filtration, washed thoroughly with water and dried. The surfactant was removed by two consecutive solvent extractions using 150 ml of ethanol and 2 g concentrated HCl for 1 g sample at 50 °C for 5 h. Table 3.1 lists the materials prepared using different amounts of acid.

Table 3.1 Phenylenesilicas prepared in the presence of different amounts of acid

Sample	Amount of acid (ratio to BTEB)
SW1e	6.4
SW2e	4.6
SW3e	7.7
SW37e	9.2

Additional samples (Table 3.2) were prepared using the same procedure, i.e., heating at 50 °C for 20 h while stirring, followed by another heating stage at 50, 70 or 95 °C for 20 h or 48 h under static conditions.

Table 3.2 Conditions of the 2nd preparation stage of phenylenesilicas

Sample	Temperature (°C)	Time (h)
SW38e	50	20
SW41e	70	20
SW42e	50	48
SW43e	95	20
SW44e	95	48

Preparation of phenylene-bridged mesoporous materials using other oligomeric surfactants (Brij 56, Brij 58 and Brij 78). The same procedure as described for Brij 76 was applied using the other oligomeric surfactants. As shown below (Table 3.3), the amount of surfactant was adjusted to keep the surfactant to silsesquioxane molar ratio constant.

Table 3.3 Phenylenesilicas prepared in the presence of different surfactants

Sample	Surfactant used	Amount of surfactant (g)
SW4e	Brij 56	1.96
SW8e	Brij 58	3.16
SW9e	Brij 78	3.24

3.3 Preparation of PMOs using bis(triethoxysilyl)ethylene as precursor

The ethenylene group is very active in organic reactions. Thus, PMOs containing framework ethenylene groups can be used for post-synthesis modifications to generate mesoporous materials with different functionalities. In addition, the only two reports on mesoporous ethenylenesilica [38, 40] described somewhat poor quality materials. Therefore we decided to explore the possibility of preparing highly ordered mesoporous ethenylenesilica and to study the reactivity of the C=C double bond in the obtained materials. The materials were prepared using bis(triethoxysilyl)ethylene as precursor.

3.3.1 Literature review

There are very few reports on periodic mesoporous ethenylene-bridged organosilica. Stein *et al.* [40] synthesized such material under basic conditions using bis(triethoxysilyl)ethylene (BTSEY) precursor in the presence of cetyltrimethylammonium bromide (CTAB) surfactant. The resulting material had disordered structure with narrow pore size distribution. Ozin *et al.* [38] also reported a 2-D hexagonally ordered PMO with ethenylene groups (synthesized under basic conditions using BTSEY in the presence of CTAB surfactant) and a range of ordered materials with a framework composition intermediate between those of pure silica and pure ethenylene PMO (synthesized using mixture of BTSEY and TEOS in the

presence of CTAB surfactant under basic conditions). The materials showed mesoporous systems with hexagonal symmetry throughout the sample with a pore centre-to-centre distance of ~ 4.5 – 5.0 nm. The materials were thermally stable, and exhibited high surface areas. In both studies, the ethenylene groups were found not to be fully accessible for chemical reactions.

As mentioned earlier, oligomeric surfactants have proven to be excellent supramolecular templates for the preparation of highly ordered mesoporous silicas under acidic conditions. The current work aims at extending this synthetic approach to ethenylene-bridged organosilicas. For completeness, preparation of nanoporous ethenylenesilica was also carried out under basic conditions.

Recently, Zhao *et al.* [65] reported that using inorganic salt K_2SO_4, in the presence of triblock copolymer F108 as supramolecular template has a dramatic effect on the structure of the obtained mesophase. They obtained large pore cubic mesoporous single crystal material instead of the usual two dimensional hexagonal SBA-15 silica. Likewise, Flodström *et al.* [66] obtained a cubic ($Ia\bar{3}d$) mesostructured silica upon addition of sodium iodide to the synthesis mixture using P123 as structure directing agent. Another striking example of the effect of additives on the structure of the silica mesophase was provided recently by Ryoo *et al.* [67]. They added butanol to a typical mixture for the synthesis of hexagonal SBA-15 and obtained a highly ordered large mesoporous cubic material. It was thus decided to reproduce the synthesis procedure of Flodström *et al.* [66] and Ryoo *et al.* [67] using bis(triethoxysilyl)ethylene as precursor instead of tetraethyl orthosilicate.

3.3.2 Experimental

Ethenylene-bridged mesoporous materials were synthesized using bis(triethoxysilyl)ethylene (BTSEY) as precursor in the presence of oligomeric surfactants (Brij 56 ($C_{16}EO_{10}$), Brij 58 ($C_{16}EO_{20}$), Brij 76 ($C_{18}EO_{10}$) and Brij 78 ($C_{18}EO_{20}$)) and triblock copolymer Pluronic P123 ($(EO)_{20}(PO)_{70}(EO)_{20}$) under acidic conditions, or alkyltrimethylammonium surfactants under basic conditions. As described earlier, BTSEY was prepared and purified according to the literature [57]. Brij 56, Brij 58, Brij 76, Brij 78, concentrated hydrochloric acid and ethanol were purchased from Aldrich. 2M hydrochloric acid was prepared by diluting 83.8 g concentrated hydrochloric acid to a 500 ml solution.

Preparation of ethenylene-bridged mesoporous material in the presence of alkyl(polyethyleneoxide) surfactants. A typical synthesis was as follows. 2 g of Brij 76 was dissolved in 10 g of distilled water and 50 g of 2M hydrochloric acid. After complete dissolution, BTSEY (3.52 g) was added to the solution and a white precipitate appeared immediately. The mixture was kept stirring for 20 h at 50 °C. Then, it was cooled to room temperature. The white precipitate was recovered by filtration, washed thoroughly with water and dried. The surfactant was removed by two consecutive solvent extractions using 150 ml of ethanol and 2 g concentrated HCl for 1 g sample at 50 °C for 5 h.

Several other ethenylene-bridged mesoporous materials were prepared using other alkyl(polyethyleneoxide) oligomers and the same synthesis method except for the

amount of surfactant (Table 3.4), which was adjusted to keep the overall molar composition of the mixture constant.

Table 3.4 Ethenylenesilicas prepared in the presence of different surfactants

Sample	Surfactant used	Amount of surfactant (g)
SW24e	Brij 76	2.00
SW25e	Brij 56	1.96
SW32e	Brij 58	3.16
SW33e	Brij 78	3.24

Additional ethenylenesilica materials were prepared in the presence of the four oligomeric surfactants (Brij 56, Brij 76, Brij 58 and Brij 78) using the same method, except that the synthesis mixture was kept first under stirring at 50 °C for 20 h, then under static condition for another period of 20 h at 50 °C. The samples were referred to as shown in Table 3.5.

Table 3.5 Ethenylenesilicas prepared in the presence of alkyl(polyethyleneoxide) oligomers using two aging steps

Oligomer used	Sample
Brij 56	SW36e
Brij 76	SW35e
Brij 58	SW55e
Brij 78	SW56e

Preparation of ethenylene-bridged material under basic conditions (SW19e). 1.536 g of C_{16}TMACl was added to a solution of 0.40 g of NaOH in 41.58 g of water. After the surfactant dissolved, 3.52 g BTSEY was added. A precipitate formed at once. The mixture was stirred at 45 °C for 4 days, then cooled to room temperature and filtered. The white solid was dried in ambient air. The surfactant was removed by two consecutive solvent extractions using 150 ml of ethanol and 2 g concentrated HCl for 1 g sample at 55 °C for 6h. Additional materials prepared under different conditions are listed in Table 3.6.

Table 3.6 Different preparation conditions for materials under basic pH

sample	reaction conditions
SW5e	using C_{18}TMACl, stirred at room temperature for 24 h, then aged at 95 °C for 20 h
SW10e	using C_{16}TMABr, aged at 80 °C for 4 days
SW11e	using C_{18}TMACl, stirred at room temperature for 24 h
SW13e	using C_{16}TMACl, stirred at room temperature for 24 h
SW14e	using C_{18}TMACl, stirred at room temperature for 24 h added 0.8 ratio NaOH
SW15e	using C_{18}TMACl, stirred at room temperature for 24 h added 1.5 ratio NaOH
SW16e	using C_{16}TMACl, stirred at room temperature for 48 h
SW17e	using C_{16}TMACl, stirred at 45 °C for 24 h
SW19e	using C_{16}TMACl, stirred at 45 °C for 4 days
SW20e	using C_{16}TMACl, stirred at 55 °C for 4 days

Preparation of ethenylene-bridged mesoporous material using P123 (SW45e). 2 g of P123 was dissolved in 15 g of distilled water and 60 g of 2M hydrochloric acid.

After the mixture was stirred at 35 °C for 1 day, BTSEY (3.6 g) was added to the solution and stirred for 5 minutes. A white precipitate appeared right away. The mixture was kept at 35 °C without stirring for 20 hours, then kept for 2 days in an oven preheated at 90 °C. After cooling to room temperature, a white precipitate was recovered by filtration, washed thoroughly with water and dried. The surfactant was removed by two consecutive solvent extractions using 150 ml of ethanol and 2 g concentrated HCl for 1 g sample at 50 °C for 5 h.

Preparation of ethenylene-bridged mesoporous material using P123 and Butanol (SW51e). 0.986 g of P123 was dissolved in 35.1 g of distilled water, 1.9 g of concentrated hydrochloric acid and 0.932 g butanol at 35 °C. After complete dissolution, BTSEY (1.76 g) was added to the solution and stirred vigorously for 5 minutes. A white precipitate appeared immediately. The mixture was kept stirring slowly at 35 °C for 1 day. It was then put in an oven and kept for 1 day at 100 °C. After cooling to room temperature, the precipitate was recovered, washed, dried and solvent extracted as described above.

Preparation of ethenylene-bridged mesoporous material using P123 and sodium iodide (SW52e). 0.96 g of P123 and 5.62 g sodium iodide was dissolved in 22.5 g of distilled water and 15 g of 4 M hydrochloric acid at room temperature. After P123 and sodium iodide were dissolved, the mixture was moved to 55 °C oven and BTSEY (1.22 g) was added. The solution was stirred vigorously for 1 minute. A white precipitate appeared right after the BTSEY addition. The mixture was kept stirring

slowly at 55 °C for 1 day. Then the mixture was put into 80 °C oven aged for 1 day. After it was cooled to room temperature, the white precipitate was recovered and solvent extracted.

3.3.3 Post –synthesis modification

A potential advantage of having a hybrid framework is that it can be modified further, provided the organic groups are functionalizable and accessible.

3.3.3.1. Literature review

Numerous investigations have been devoted to the modification of terminal organic groups within mesoporous silicas [68]. For instance, the terminal alkane thiols were transformed into sulfonate groups [69]. Although the product was slightly less ordered, the surface area and the pore volume decreased, and most of the pores became micropores, ^{13}C CP MAS NMR data showed that the original thiol disappeared. Stein *et al.* [70] brominated the terminal vinyl groups inside MCM-41, and found that such groups can be brominated completely. Anwander and co-workers [71] utilized vinyl functionalized disilazane reagents to graft vinyl groups to the silica channel walls of preformed mesoporous silica (MCM-41), which was subsequently hydroborated. Ozin *et al.* [72] reported that terminal vinyl groups incorporated directly into mesoporous silica by co-assembling $(EtO)_3SiCH=CH_2$ and TEOS can be hydroborated and subsequently converted into alcohol groups. Only

vinyl groups reacted, but the structure of the material was retained after hydroboration and alcoholysis. The specific surface area, pore volume and PSD also remained largely unchanged. There are however a limited number of investigations dealing with the transformation of organic species directly within the framework of PMOs. For instance, Stein *et al.* [40] and Ozin *et al.* [38] brominated the ethenylene groups incorporated into PMOs obtained by assembling BTSEY with surfactant template. Stein's group found that not all the ethenylene groups in the framework were accessible for bromination because the ethenylene carbon atoms, which resonate at 146 ppm on a ^{13}C CP MAS NMR spectrum did not disappear completely. Ozin's group found that after bromination the structure integrity and order of the material was well maintained. But while some ethenylene groups (~ 10%) were brominated, others reacted with the solvent to form ethane bridges. These results show that ethenylene groups incorporated into the channel walls are partly accessible for chemistry although they can not be brominated completely. Inagaki *et al.* [59] reported the direct sulfonation of phenylene group in the pore walls of mesoporous benzene – silica. Based on these studies, functional organic groups in the framework appeared to be less reactive than terminal groups.

In this work, bromination of ethenylene groups in the framework and terminal vinyl groups was investigated.

3.3.3.2 Experimental

All PMO materials were prepared and characterized as described before. Bromine

and dichloromethane were purchased from Aldrich.

Bromination of ethenylene group in PMOs prepared using BTSEY and Brij 76. 0.05 g mesoporous material (white) was put in a tube connected to a valve. After vacuum treatment, bromine gas was introduced into the tube. The material turned brown. The material was kept in the presence of gaseous bromine for 24 h. It was then washed by dichloromethane until it turned from brown back to white. The final solid was collected by filtration and dried in ambient air.

Bromination of ethenylene group in PMOs prepared using BTSEY and P123. 0.1 g mesoporous material (white) was vacuum treated and contacted with gas. The material, turned brown, was kept in the presence of gaseous bromine for 24 h. It was then washed by dichloromethane until it turned from brown back to white. The white solid was collected by filtration and dried in ambient air.

Bromination of terminal vinyl group in PMOs prepared using TEOS, TEVS and CTAB. The material was prepared by co-condensation of TEOS and TEVS in 1:1 ratio using the method reported by Ozin *et al.* [73]. Bromination of vinyl containing mesoporous silicate was carried out as described above.

Chapter 4

Results and Discussion

4.1 Introduction

All benzene and ethenylene-bridged PMOs were characterized by a number of techniques including XRD, TEM, SEM, nitrogen adsorption, ^{29}Si and ^{13}C NMR, IR, UV-visible, TGA, and elemental analysis. In this work, nitrogen adsorption was used to calculate the surface area, the pore volume and the pore size. XRD helped determine the structure of the mesophases, and provided the d_{100} distances to calculate the unit cell dimensions. In combination with N_2 adsorption data, the d_{100} distance were used to determine the pore wall thickness. TEM allowed to confirm the structure of the materials and their pore sizes. It also provided direct evidence of the order of the pore system or the lack thereof. SEM showed the morphology of the materials. ^{29}Si and ^{13}C NMR was used to prove that the organic groups were located in the framework. The KJS (Kruk-Jaroniec-Sayari) pore diameter [74] was obtained as the value corresponding to the maximum of the pore size distribution. The BET surface area was calculated from $S_a = V_m * N * A_m$, where V_m is the volume of adsorbed monolayer, which is obtained from the BET equation of $P/(V(P_0 - P)) = 1/(V_mC) + (C - 1)/(V_mC) * P/P_0$ (V is the volume adsorbed, P is the adsorbate pressure, and P_0 is the saturation vapor pressure of the adsorbate), N is the Avogadro's number, A_m is the cross-sectional area of the adsorbate molecule, which is 16.2 A^2 for nitrogen. The pore volume was calculated from $V = 0.00156 * V_{(0.95)}$, where $V_{(0.95)}$ is the volume of nitrogen gas (at 0 °C, P = 1 atm) adsorbed at $P/P_0 = 0.95$. The pore wall thickness was calculated using the equation $b = 2d_{100}/(3)^{1/2} - w_{KJS}$. All the data will be presented and discussed in this Chapter.

4.2 Evaluation of bis(triethoxysilyl)benzene containing materials

4.2.1 Results and discussion

Different kinds of oligomeric surfactants were used to prepare phenylene-bridged organosilicates. In addition, different conditions such as the amount of acid, the aging temperature and time were also investigated.

XRD patterns (Figure 4.1) of the surfactant free materials prepared in the presence of Brij 76 revealed a strong peak at 2θ = ca. 1.7 and two minor peaks in the 2θ range of 3 – 3.5°. These features are consistent with the occurrence of two-dimensional hexagonal structure, akin to MCM-41 or SBA-15 mesophases. They correspond to the (100), (110) and (200) reflections. The unit cell dimension (calculated using $a_0 = 2d_{100}/3^{1/2}$, where $d_{100} = 0.15418/(2\sin\theta)$) was 5.83 and 5.13 nm, for samples prepared in the presence of Brij 76 and Brij 56, respectively.

Nitrogen adsorption isotherms for samples prepared in the presence of Brij 56 and Brij 76 (figure 4.2) were typical of periodic mesoporous materials. They exhibited a steep increase in adsorption at P/P_0 = 0.25-0.45 due to capillary condensation of nitrogen in the mesopores. The pore size distributions were narrow, particularly for the sample prepared in the presence of Brij 76. The pore volume, the surface area, the pore size and the pore wall thickness of these two materials are shown in Table 4.1.

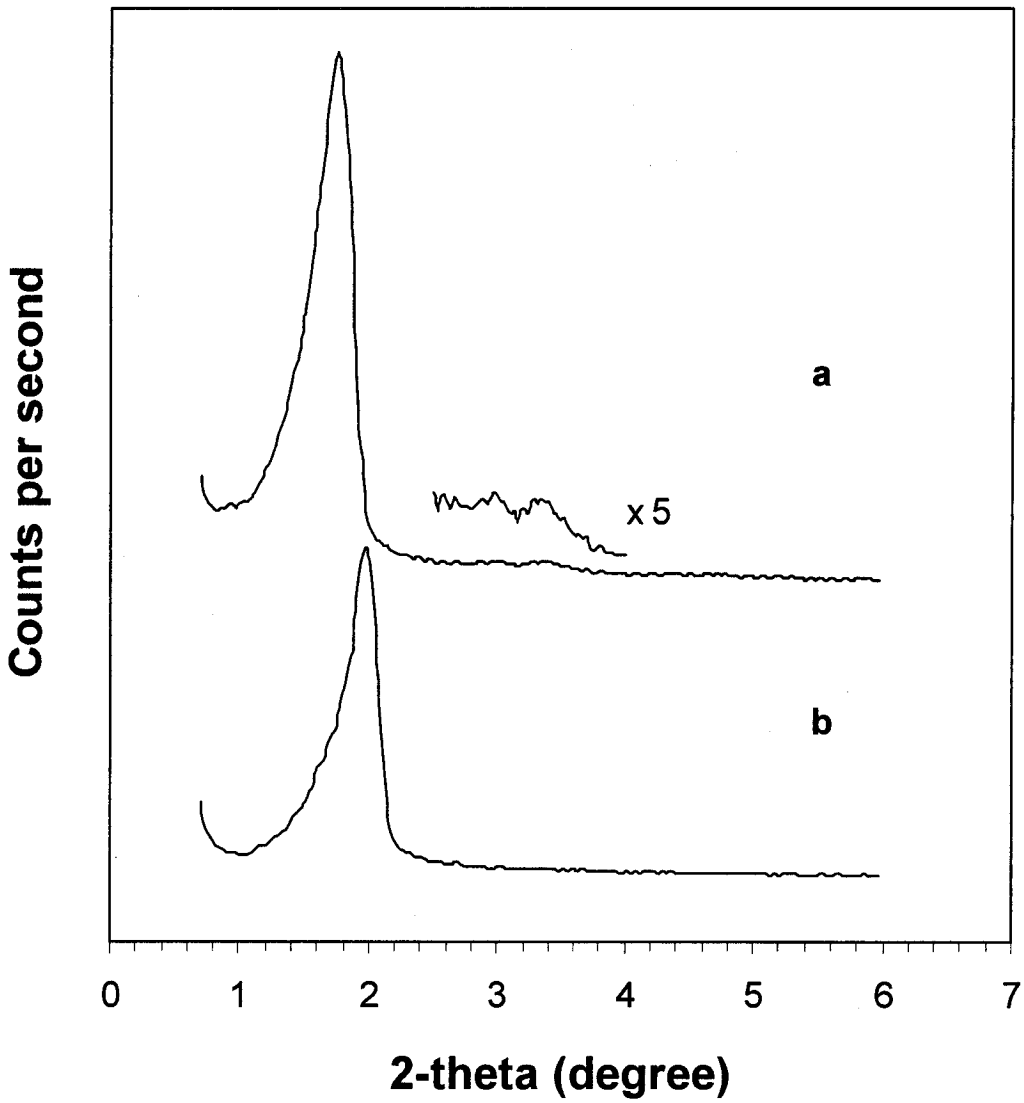

Fig. 4.1 XRD patterns for phenylene-bridged mesoporous organosilicas (after extraction) prepared in the presence of (a) Brij 76, and (b) Brij 56.

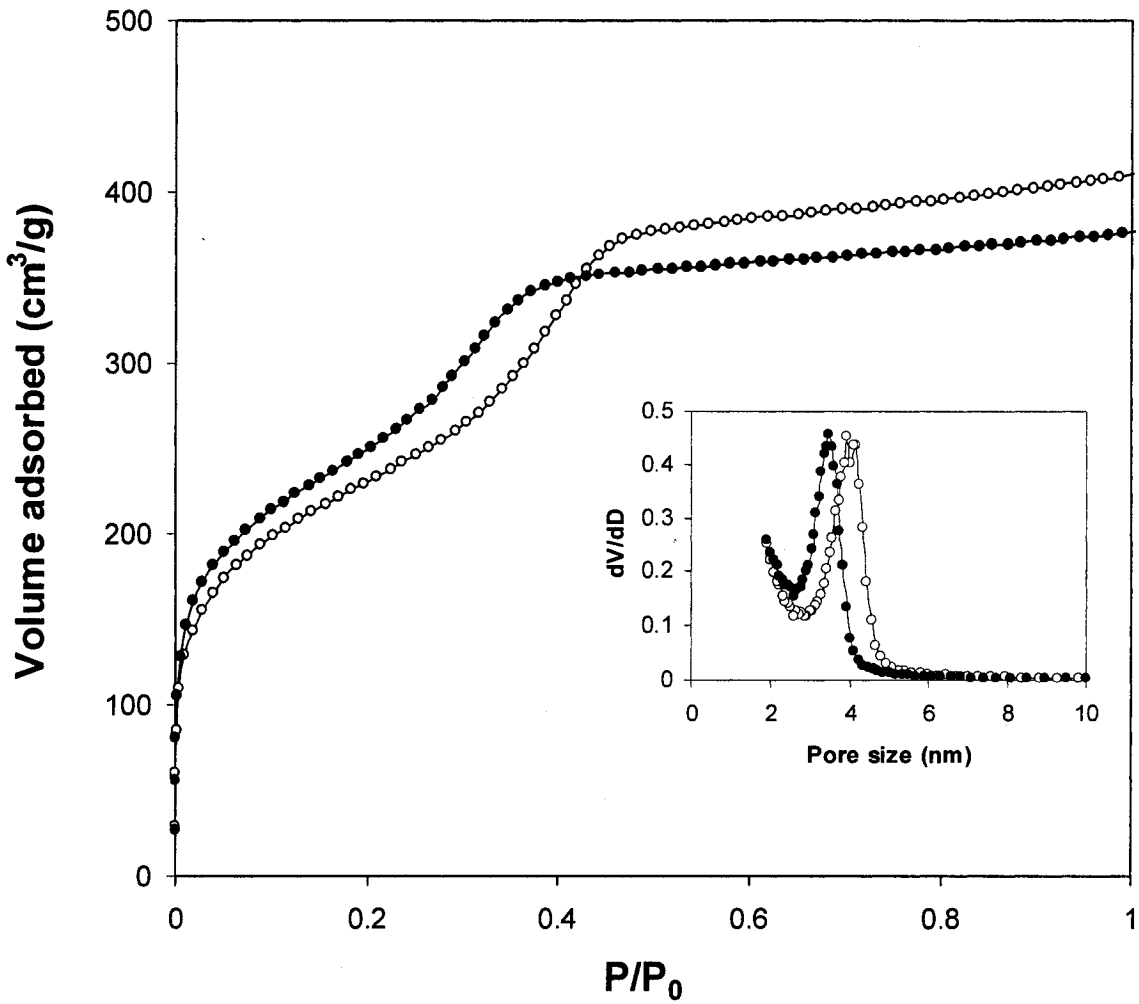

Fig. 4.2 Nitrogen adsorption isotherms for phenylene-bridged mesoporous organosilicas prepared in the presence of Brij 76 (-○-) or Brij 56 (-●-) as structure directing agent

Table 4.1. N_2 Adsorption data for materials prepared in the presence of Brij 56 and Brij 76

Surfactant used	Pore volume cm^3/g	Surface area m^2/g	Pore size nm	Pore wall thickness nm
Brij 76	0.63	840	3.9	1.9
Brij 56	0.58	899	3.5	1.6

A typical ^{29}Si MAS-NMR spectrum for the current phenylene-bridged mesoporous materials is shown in figure 4.3a. It exhibited three main signals at -62.01, -70.35, and -79.21 ppm, assigned to Si species covalently bonded to carbon atoms: T^1 [***Si***C(OH/OEt)$_2$(OSi)], T^2 [***Si***C(OH/OEt)(OSi)$_2$] and T^3 [***Si***C(OSi)$_3$], respectively. These data are consistent with the occurrence of the organic linker within the material framework. Small signals between –90 and –120 ppm attributable to condensed SiO_4 species (Q^n, ***Si***O$_n$, (n = 2-4)) were also present. The overall relative intensity of such signals was below 8%. An additional broad peak appeared at ca. -40 ppm. While this could not be assigned to a particular silicon species, it could be due to a spinning side bands. Unfortunataly, this was not verified.

The ^{13}C NMR spectrum (Fig. 4.3b) was dominated by a peak at 134 ppm, which corresponds to the superposition of unresolved signals from o- and m-carbons in the phenylene ring. This peak exhibited a shoulder attributable to carbon atoms in positions 1 and 4, which are bonded to Si. There were two additional peaks at 16.2 and 58.8 ppm, which were assigned to non-hydrolyzed Si-O-CH_2CH_3 groups. The

^{29}Si and ^{13}C NMR data are consistent with each other, and provide strong evidence for the occurrence of a network composed of $O_{1.5}Si\text{-}C_6H_4\text{-}SiO_{1.5}$ units.

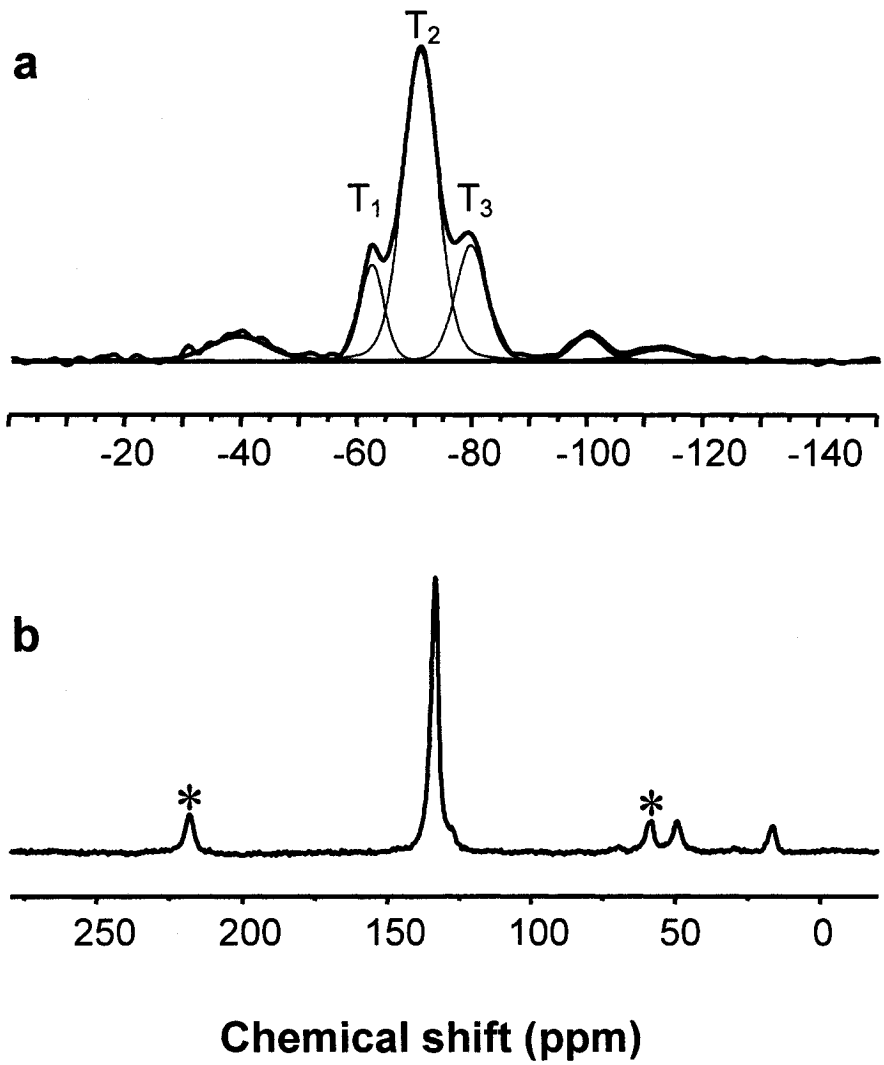

Fig. 4.3 (a) ^{29}Si NMR, and (b) ^{13}C NMR data for the phenylene-bridged mesoporous organosilica prepared in the presence of Brij 76

* refers to spinning side bands.

Transmission electron microscopy (TEM) images of the specimens were obtained on a Jeol JEM-2010 instrument operating at 200 kV. When looking down the pore axis, the hexagonal arrangement of the mesopores was confirmed (Fig. 4.4). The pore centre to pore centre distance was about 5 nm, being consistent with the XRD results. When viewed down the [100] direction, straight lattice fringes were observed with a separation of 4.3 nm, which is the d-spacing of the (010) planes (Fig. 4.5a). In addition, some fine lattice fringes were also visible, although the contrast was very low. In order to study the detailed structure, Fourier transform of the image in Fig. 4.5(a) was performed (Fig. 4.5b). The sharp diffraction spots resulted from the ordering of the mesopores with the d-spacing of 4.3 nm. Two pairs of greatly diffused diffraction disks were also visible, indicating partial ordering in the wall structure in two dimensions. An inverse Fourier transform of Fig. 4.5(b) by removing the background noise enabled us to see the structural details of the framework as shown in Fig. 4.5(c). Wave-like lattice fringes were revealed along two directions. Calculated from both the image and the diffraction pattern, the d-spacings of these fringes were about 1.2 nm and 0.8 nm, respectively. The latter is similar to the d-spacing observed by Inagaki et al. [61], from their crystal-like benzene-silica prepared under basic conditions, and it is believed that the periodicity is related to the separation of the phenylene-bridged molecules. The spacing of 1.2 nm must relate to the length of the molecules, i.e. partial ordering parallel to the molecules. Unlike the observed wall structure of similar materials prepared under basic conditions, the ordering of the bridged molecules is not parallel to the pore axis, but with an angle of about 57°. Furthermore, there was only partial ordering of the

molecules. This is why no sharp diffraction peaks of such ordering were observed in the XRD pattern.

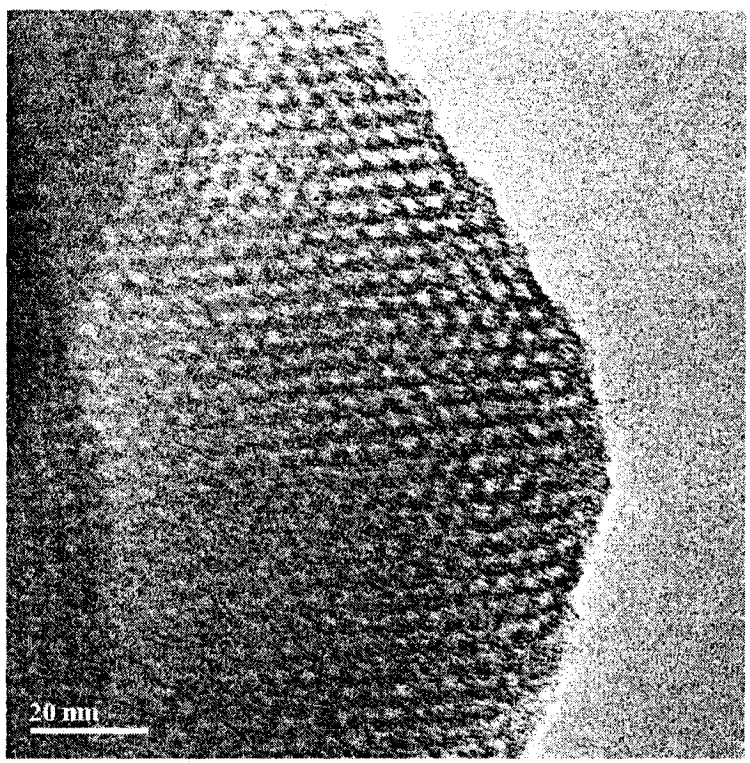

Figure 4.4 TEM image of the phenylene-bridged mesoporous product viewed down the [001] zone axis. The white spots are the direct images of the pores.

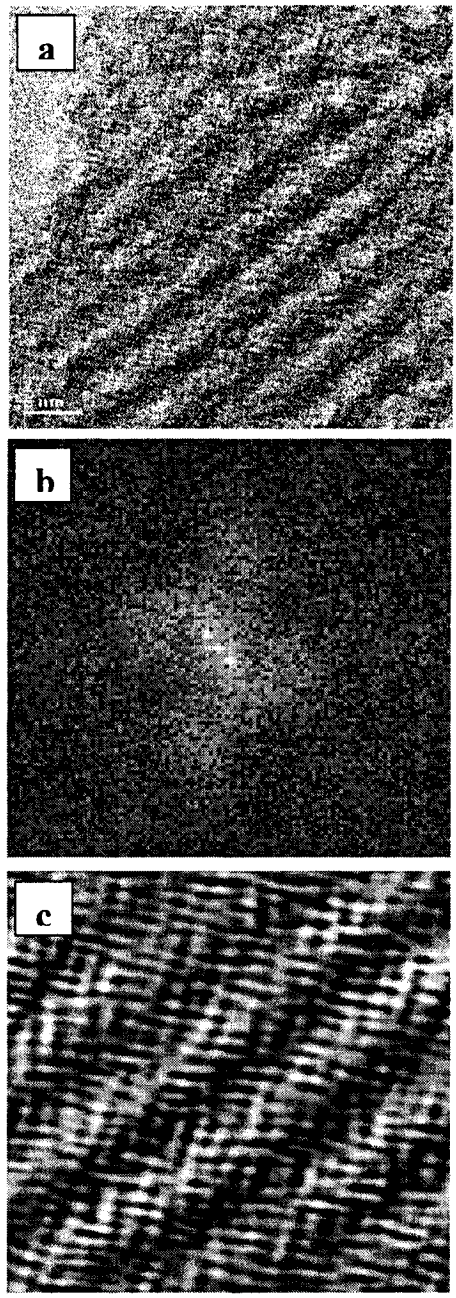

Fig. 4.5 (a) TEM image of the phenylene-bridged mesoporous phase viewed down the [100] zone axis. (b) Diffraction pattern made by Fourier transform of (a). (c) TEM image created by inverse Fourier transform of (b) when the sharp spots and two pairs of diffused spots were considered.

Figure 4.6 shows the pore size distribution of the materials prepared in the presence of Brij 58 (SW8e) and Brij 78 (SW9e) as structure directing agents. This indicates that these two materials had no mesopore with narrow PSD.

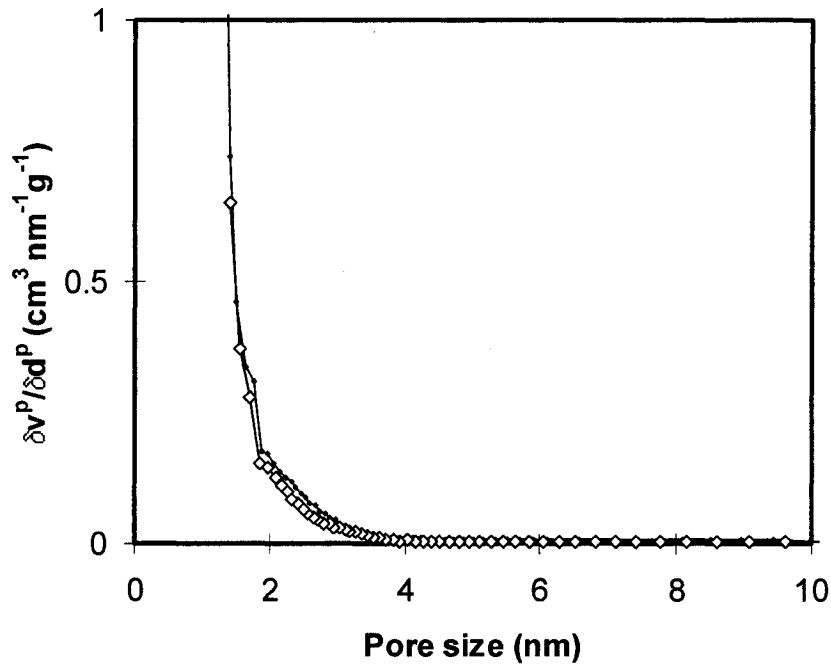

Fig. 4.6 Pore size distribution for phenylene-bridged organosilicas prepared in the presence of Brij 58 (-♦-) and Brij 78 (-◊-)

Nitrogen adsorption and XRD data indicated that although Brij 56 is a suitable template, Brij 76 is the best structure directing agent to prepare high quality mesoporous benzenesilica. TEM observation indicated that in addition to the long range order of the mesopore structure, the material exhibited a novel molecular scale order within the pore walls. Attempts to prepare samples with improved ordering within the pore walls were made by trying different amounts of acid or

procedure described above, another hydrothermal treatment whose duration and temperature were varied from 20 to 48 h and from 50 to 95 °C, respectively. This also included the preparation of samples under the same conditions as described above to check the reproducibility of the molecular order in the pore walls. Table 3.1 shows the details of the preparation conditions.

Figure 4.7 shows the pore size distribution for materials prepared using different amounts of acid. The amounts of acid had relatively little effect on the pore size distribution.

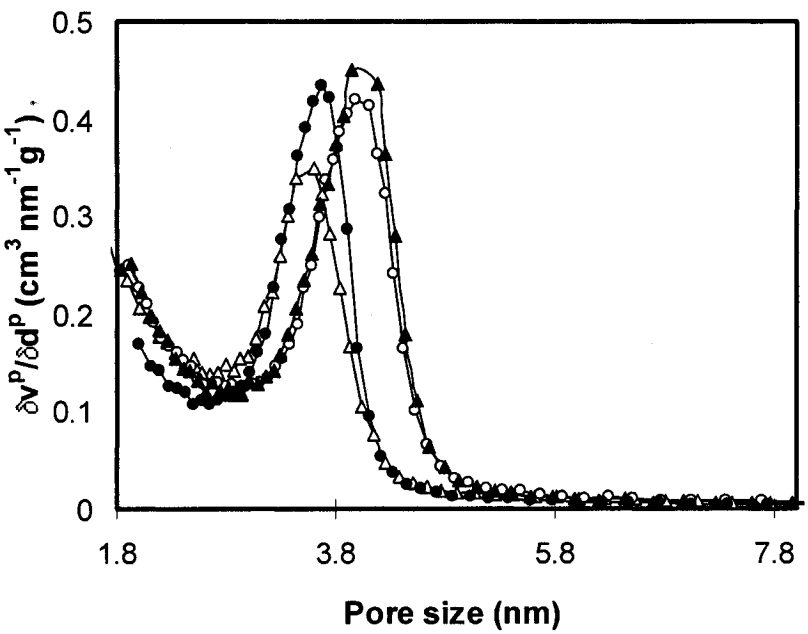

Fig. 4.7 Pore size distribution for phenylene-bridged mesoporous organosilicas prepared in the presence of Brij 76 with the following HCl/BTEB ratios (-●-) 6.4, (-○-) 4.6, (-▲-) 7.7, and (-Δ-) 9.2

Figure 4.8 shows the XRD patterns for samples prepared using an additional hydrothermal stage for 20 h at different temperatures and a single step at 50 °C for 20 h (Fig. 4.8a). This indicates that the long range order of the material improved; however no extra sharp peaks appeared at higher diffraction angles.

Consistently with this observation, the corresponding PSDs (Figure 4.9) showed also a clear improvement as the temperature of the additional synthesis step increased. This indicates that the hydrothermal treatment enhances their long range order, but TEM data showed that these materials exhibited no order within the pore walls.

Figure 4.10 showed PSDs for the materials prepared in the presence of Brij 76 by hydrothermal treatment at 50 °C for 20 h and 48 h. The length of the hydrothermal treatment did not seem to have any significant effect on the PSD.

Nonetheless, the sample prepared under the same condition showed the same ordering in the pore walls as described above, indicating that the synthesis of periodic phenylene-bridged silica with novel ordering in the pore walls is reproducible.

4.2.2 Summary

Among those studied, the best surfactant for the preparation of high quality phenyl-bridged mesoporous organosilica was found to be Brij 76. The best preparation conditions consist of stirring the synthesis mixture at 50 °C for 20 hours, and the best HCl to BTEB ratio is 7.7 to 1. Under these conditions, a partially ordered meoporous material with 3.9 nm pores was obtained. Further hydrothermal treatment did improve the long range order, but as shown by TEM, the materials lost the order within the pore walls.

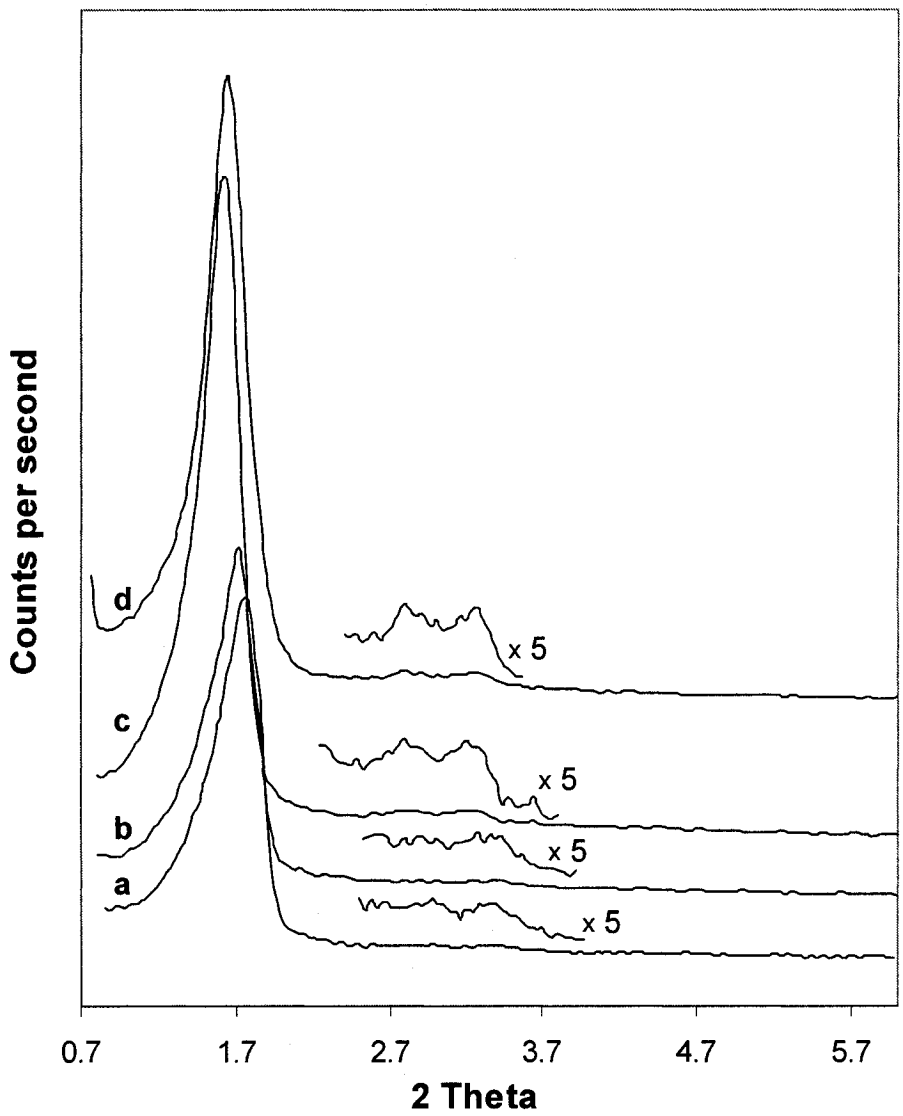

Fig. 4.8 XRD patterns for phenylene-bridged mesoporous organosilicas (after extraction) prepared in the presence of Brij 76 in single step at 50 °C (a), or using a second hydrothermal stage for 20 h at (b) 50 °C, (c) 70 °C, and (d) 95 °C.

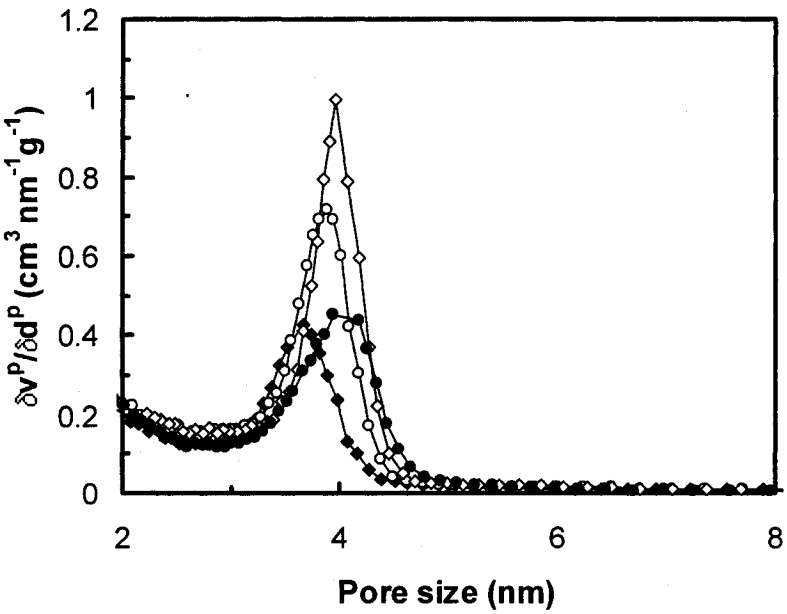

Fig. 4.9 Pore size distribution for phenylene-bridged mesoporous organosilicas prepared in the presence of Brij 76 in single step at 50 °C (-●-), or using a second hydrothermal stage for 20 h at (-♦-) 50 °C, (-○-) 70 °C, and (-◊-) 95 °C.

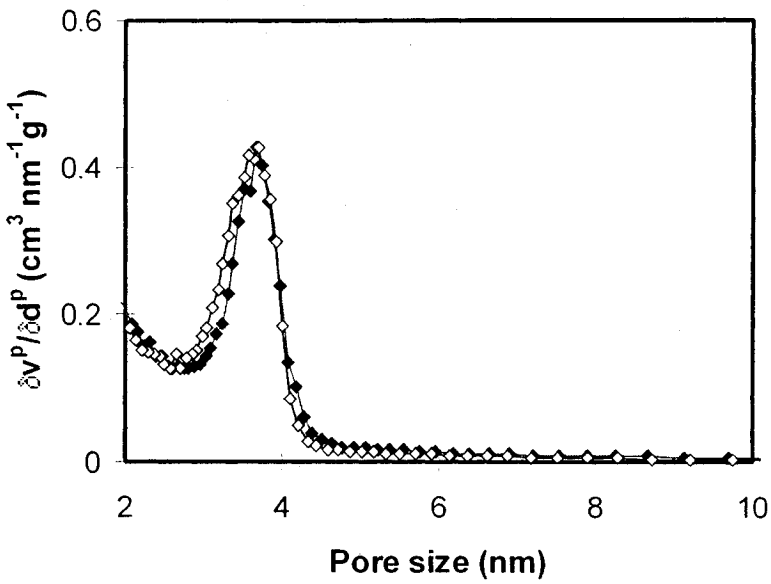

Fig. 4.10 Pore size distribution for phenylene-bridged mesoporous organosilicas prepared in the presence of Brij 76 using a second hydrothermal stage at 50 ºC for (-♦-) 20 h and (-◊-) 48 h

4.3 Evaluation of bis(triethoxysilyl)ethylene containing materials

Different surfactants were used to prepare ethenylene bridged organosilicates, including oligomeric surfactants (Brij 56, Brij 76, Brij 58 and Brij 78), alkyltrimethylammonium surfactants (C_{16}TMACl, C_{18}TMACl and C_{16}TMABr) and triblock copolymer Pluronic P123. Different preparation conditions, such as different hydrothermal treatment temperature and time were also investigated. Nitrogen adsorption, XRD, SEM, NMR and TEM were used to characterize the materials.

4.3.1 Ethenylenesilicas prepared in the presence of oligomeric surfactants

4.3.1.1 Results and discussion

Figure 4.11 shows the pore size distribution for materials prepared using Brij 76 with and without hydrothermal treatment. It shows that after hydrothermal treatment, the average pore size becomes larger and the pore size distribution becomes narrower with higher maximum.

Figure 4.12 shows the XRD pattern for samples prepared in the presence of different oligomeric surfactants. It shows that materials prepared in the presence of Brij 76 and Brij 56 reveal a strong peak at 2θ = ca. 2°, attributable to the (100) diffraction peak from 2D hexagonal unit cells. Moreover, the Brij 76-derived material exhibited

two minor, but well-resolved peaks attributable to (110) and (200) reflections. This assignment is consistent with occurrence of a mesophase with well-ordered hexagonal symmetry (Figure 4.12 a). However, materials prepared in the presence of Brij 58 and Brij 78 (Figure 4.12 c, d) showed the (100) diffraction peak around 2θ = 1.6, but the secondary reflections were not observed.

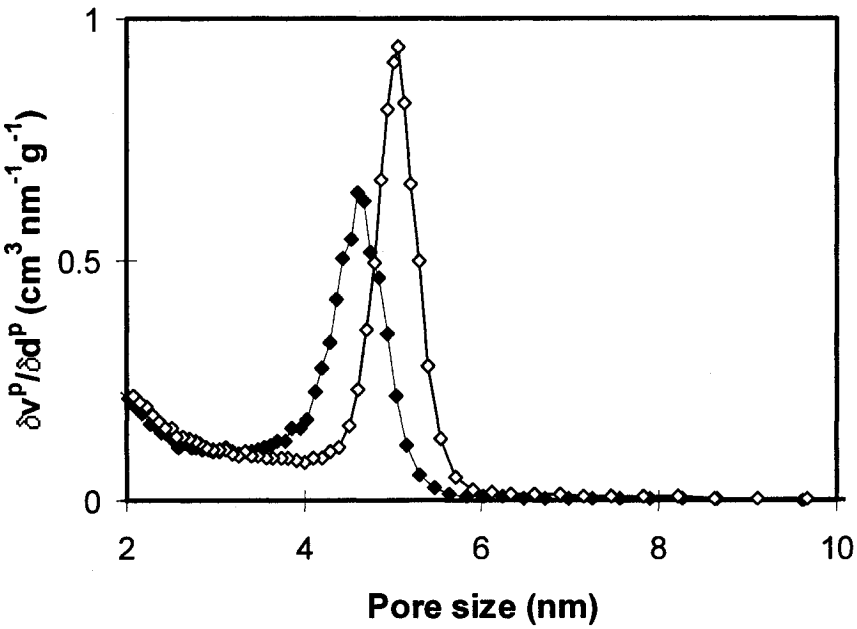

Fig. 4.11 Pore size distribution for ethenylene-bridged mesoporous organosilicas prepared in the presence of Brij 76 in a single step (-♦-) and using a second hydrothermal stage for 20 h at 50 °C (-◊-)

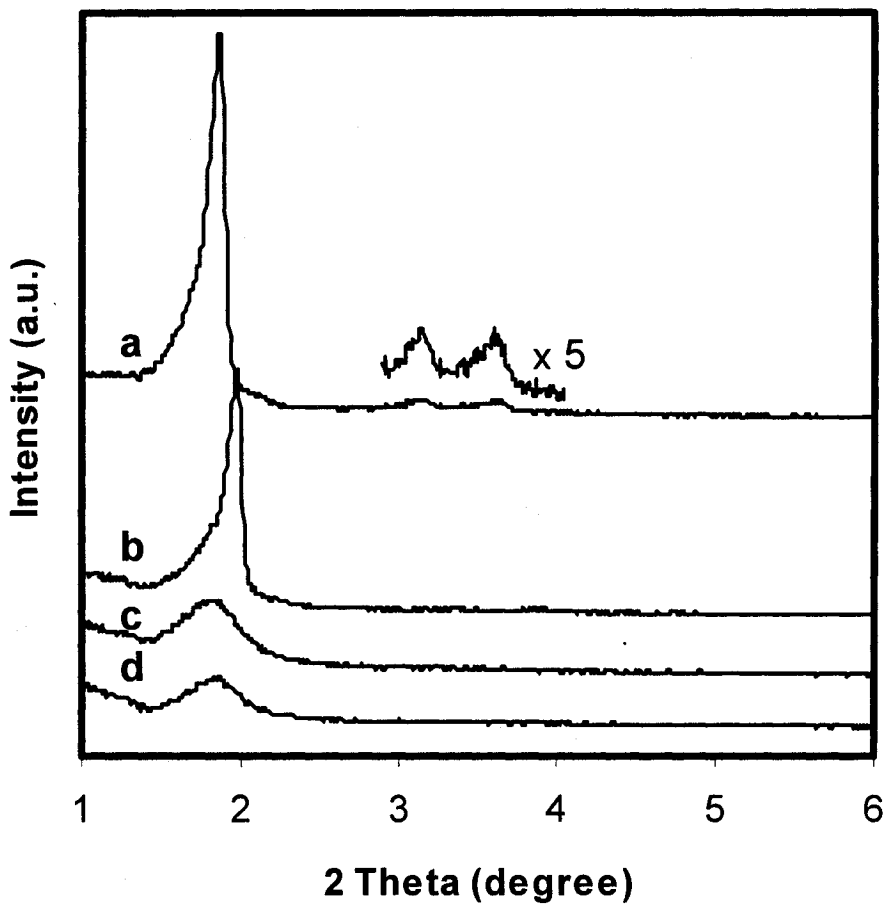

Fig. 4.12 XRD patterns for ethenlyene-bridged mesoporous organosilicas (after extraction) prepared by a second hydrothermal stage for 20 h at 50 °C in the presence of (a) Brij 76, (b) Brij 56, (c) Brij 58, and (d) Brij 78

Nitrogen adsorption - desorption isotherms for ethenlyene-bridged organosilicas prepared under acidic conditions in the presence of different surfactants with hydrothermal treatment at 50 °C are shown in Figure 4.13. The samples prepared in the presence of Brij 76 and Brij 56 exhibited a steep increase due to capillary condensation of nitrogen in the mesopores. Both isotherms also featured a hysteresis loop. The KJS pore diameter, BET surface area and pore volume calculated from the adsorption isotherms are shown in Table 4.2. The pore wall thickness was also included. XRD and nitrogen adsorption data indicated that Brij 76 was the best structure directing agent under acidic conditions for the preparation of ethenlyene-bridged mesoporous organosilica.

Figure 4.14 shows a SEM image for the ethenlyene-bridged organosilica prepared under acidic conditions in the presence of Brij 76 with hydrothermal treatment at 50 °C for 20 h. Most particles consisted of hexagonal rods. The width for the particle was around 0.4 to1 μm and the length varied between 1 and 6 μm.

Table 4.2 Nitrogen adsorption data for samples prepared under acidic condition with hydrothermal treatment at 50 °C for 20 h in the presence of different surfactants

Sample	surfactant	S(m^2/g)	V (cm^3/g)	Pore size (nm)	Pore wall thickness (nm)
Sw35e	Brij76	868	0.83	5.1	1.75
Sw36e	Brij56	894	0.73	4.0	2.18
Sw39e	Brij58	981	0.66	3.5	2.95
Sw40e	Brij78	847	0.63	3.8	2.78

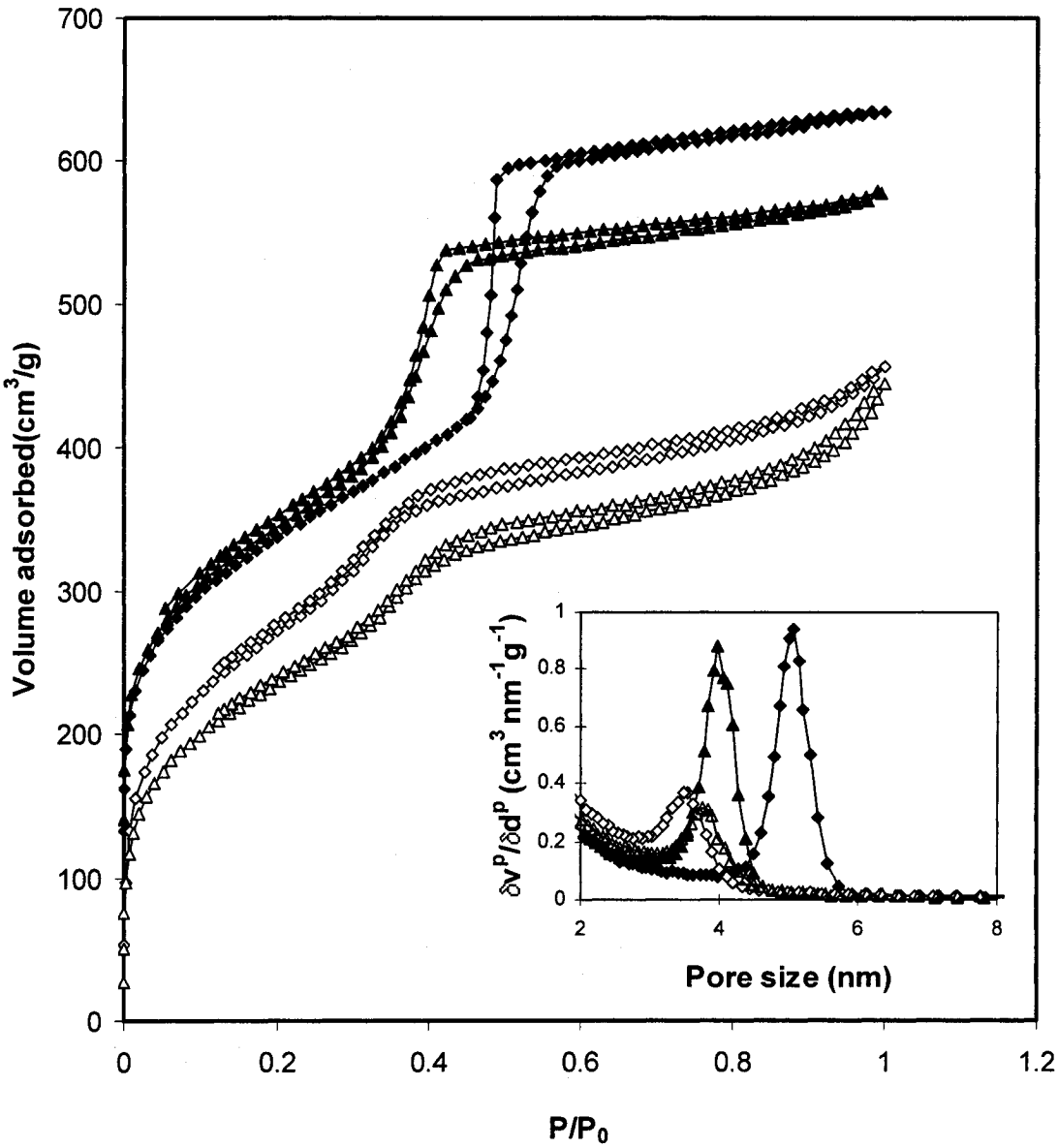

Figure 4.13 Nitrogen adsorption-desorption isotherms for ethenylene-bridged mesoporous organosilicas prepared using a second hydrothermal stage for 20 h at 50 °C in the presence of (-♦-) Brij 76, (-▲-) Brij 56, (-◊-) Brij 58, and (-△-)Brij 78

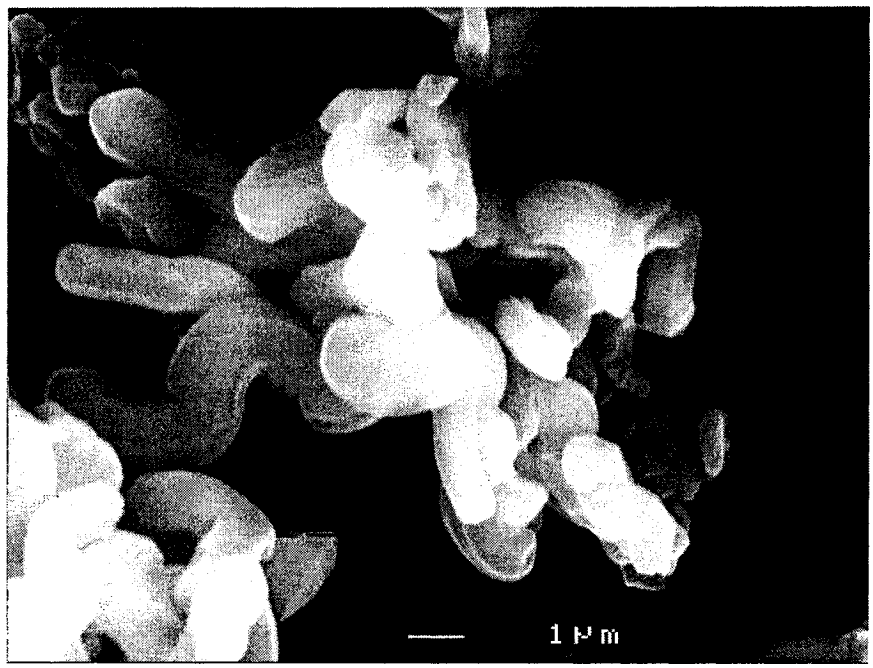

Fig. 4.14 SEM image for ethenylene-bridged organosilica prepared in the presence of Brij 76 using a second hydrothermal stage for 20h at 50°C

The ^{29}Si CPMAS-NMR spectra (Figure 4.15a) for the ethenylene-bridged mesoporous material exhibited only two main signals at -73.14 and -82.63 ppm, assigned to Si species covalently bonded to carbon atoms T^2 [C-***Si***O_2(OH)] and T^3 [C-***Si***O_3], respectively. The absence of SiO_4 species confirms that no carbon-silicon bond cleavage of the BTSEY molecules occurred during synthesis or solvent extraction. The ^{13}C NMR spectra (Figure 4.15b) had a single strong peak at 145.86 ppm, which corresponds to the ethenylene carbon atoms. There were also two additional peaks at 16.07 and 58.17 ppm, which were assigned to non-hydrolyzed Si-O-CH_2CH_3 groups. The ^{29}Si and ^{13}C NMR data are consistent with each other, and provide strong evidence for the occurrence of a network composed of $O_{1.5}$Si-CH=CH-$SiO_{1.5}$ units.

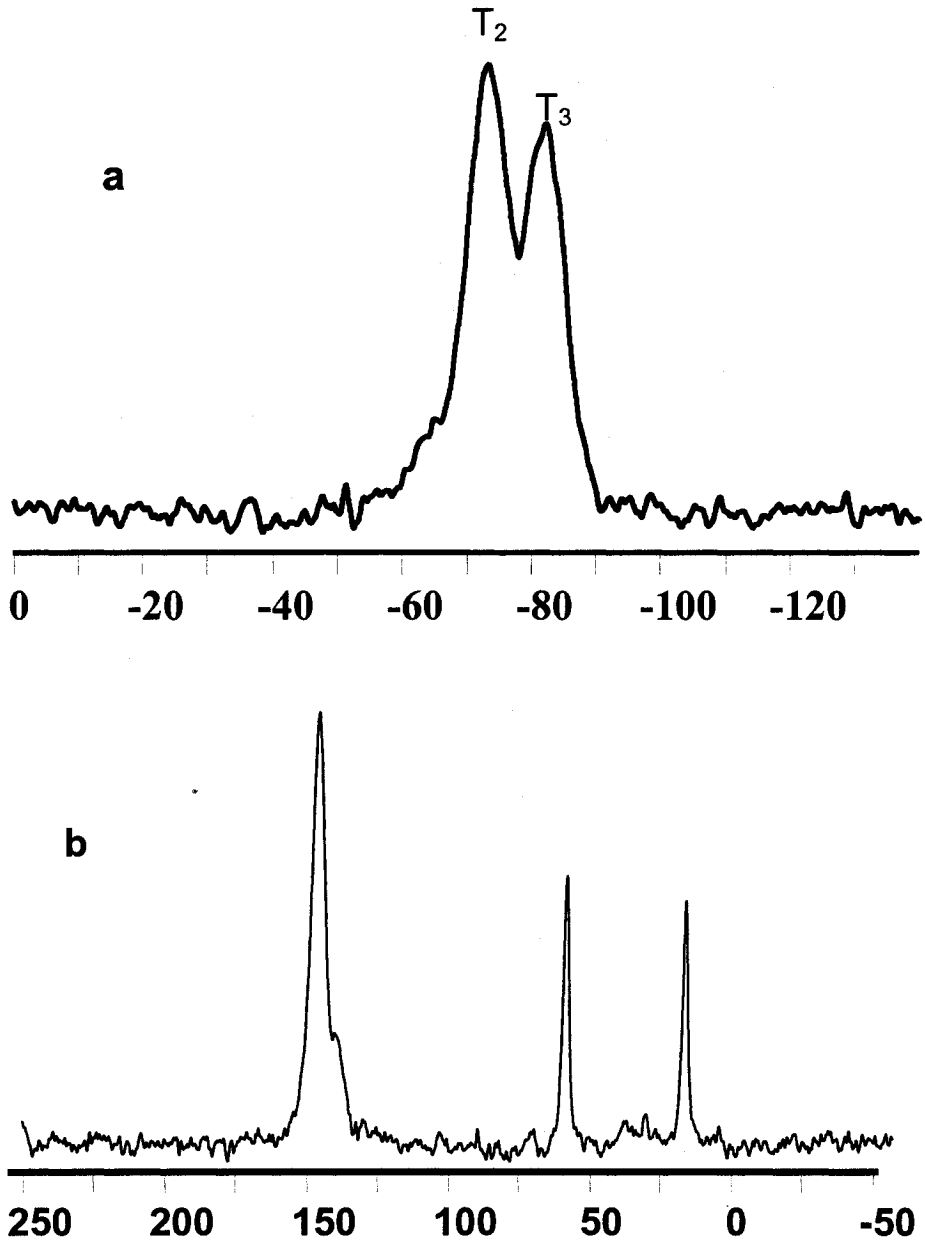

Fig. 4.15 (a) ^{29}Si NMR, and (b) ^{13}C NMR data for the ethenylene-bridged mesoporous organosilica prepared using a second hydro-thermal stage for 20 h at 50 °C in the presence of Brij 76

Figure 4.16 shows TEM images for the ethenylene-bridged mesoporous organosilicas prepared under acidic conditions in the presence of Brij 76 (Fig. 4.16a) and Brij 56 (Fig. 4.16b) with hydrothermal treatment at 50 °C for 20 h. This showed that both materials had hexagonal pore structure and the pore sizes were 5.4 nm and 4.6 nm, respectively, which are comparable to data obtained by XRD and nitrogen adsorption.

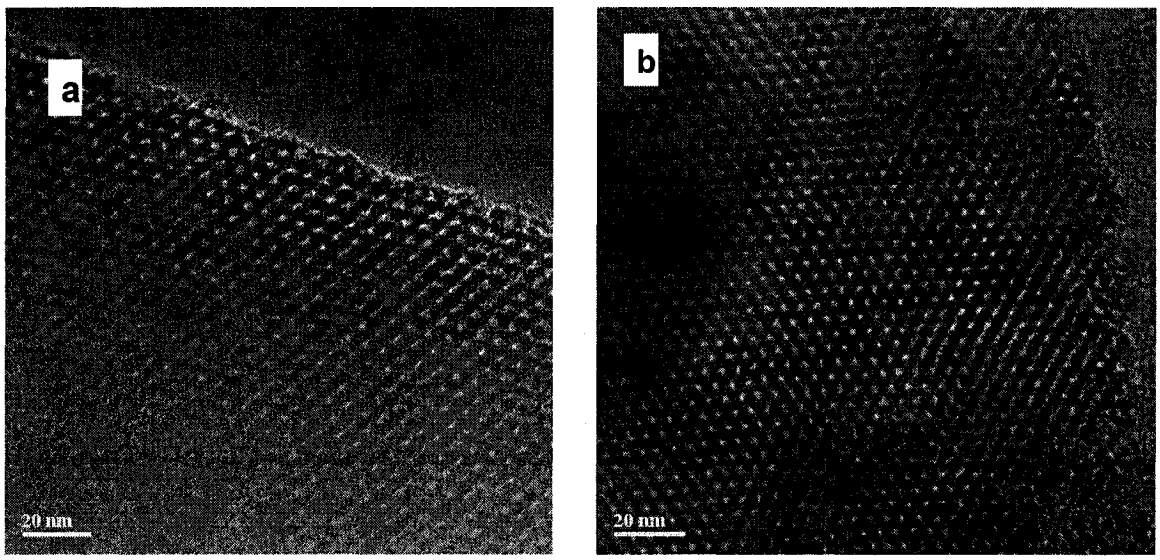

Figure 4.16 TEM images for ethenylene-bridged mesoporpous organosilicas prepared with hydrothermal treatment at 50 °C for 20 h in the presence of (a) Brij 76 and (b) Brij 56

4.3.1.2 Summary

Using ethenylene-silicon precursor and Brij 76, a highly ordered mesoporous material with two-dimensional hexagonal structure was prepared. Its pore size was 5.1 nm, and its particles consisted of hexagonal rods. ^{29}Si and ^{13}C NMR data provide directly evidence for the occurrence of a network composed of $O_{1.5}Si$-CH=CH-$SiO_{1.5}$ units. Likewise Brij 56 gave rise to a good quality material with 4.0 nm pores. Oligomers with large headgroup, namely Brij 58 and Brij 78 gave materials with somewhat broader pore size distribution.

4.3.2 Ethenylenesilica prepared in the presence of triblock copolymer P123

4.3.2.1 Results and discussion

The powder X-ray diffraction pattern for the solvent-extracted sample is shown in Figure 4.17. It reveals a strong peak at 2θ = 0.95 and a small broad peak at ca. 1.8. These features are consistent with the occurrence of two-dimensional hexagonal structure. The unit cell dimension was 10.74 nm.

Figure 4.18 shows the nitrogen adsorption isotherm for the material obtained in the presence of P123 as suporamolecular template. It exhibits a very steep increase in adsorption at P/P_0 = 0.72-0.77 due to capillary condensation of nitrogen in the

mesopores. It also featured a hysteresis loop. The KJS pore diameter was 8.6 nm, the BET surface area was 676 m^2/g and the pore volume was 0.91 cm^3/g.

The ^{29}Si CPMAS-NMR spectrum (Figure 4.19a) for the ethenylene-bridged mesoporous material exhibited only two main signals at -73.14 and -82.10 ppm, assigned to Si species covalently bonded to carbon atoms T^2 [C-$\boldsymbol{Si}O_2$(OH)] and T^3 [C-$\boldsymbol{Si}O_3$], respectively. The absence of SiO_4 species confirms that no carbon-silicon bond cleavage of the BTSEY molecules occurred during synthesis. The ^{13}C NMR spectrum (Figure 4.19b) had a strong single peak at 146.21 ppm, which corresponds to the ethenylene carbon atoms. The ^{29}Si and ^{13}C NMR data are consistent with each other, and provide strong evidence for the occurrence of a network composed of $O_{1.5}$Si-CH=CH-Si$O_{1.5}$ units.

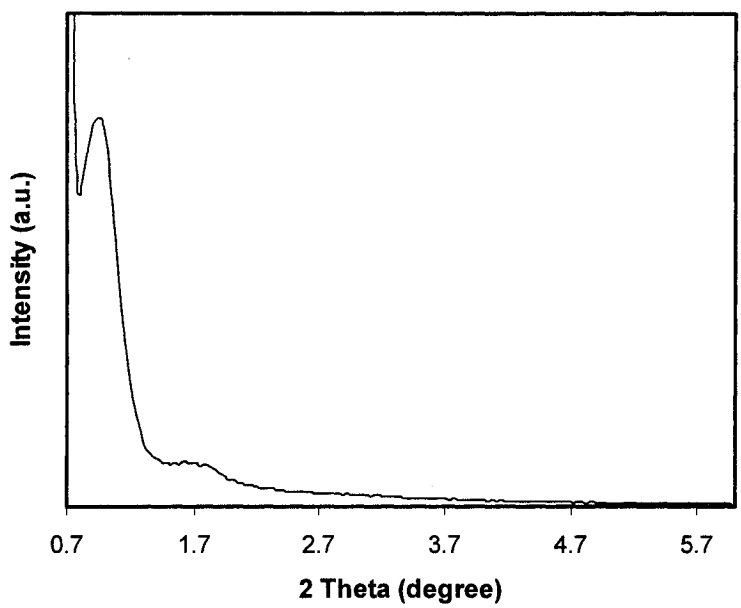

Fig. 4.17 XRD pattern for ethenylene-bridged mesoporous organosilica (after extraction) prepared in the presence of triblock copolymer P123

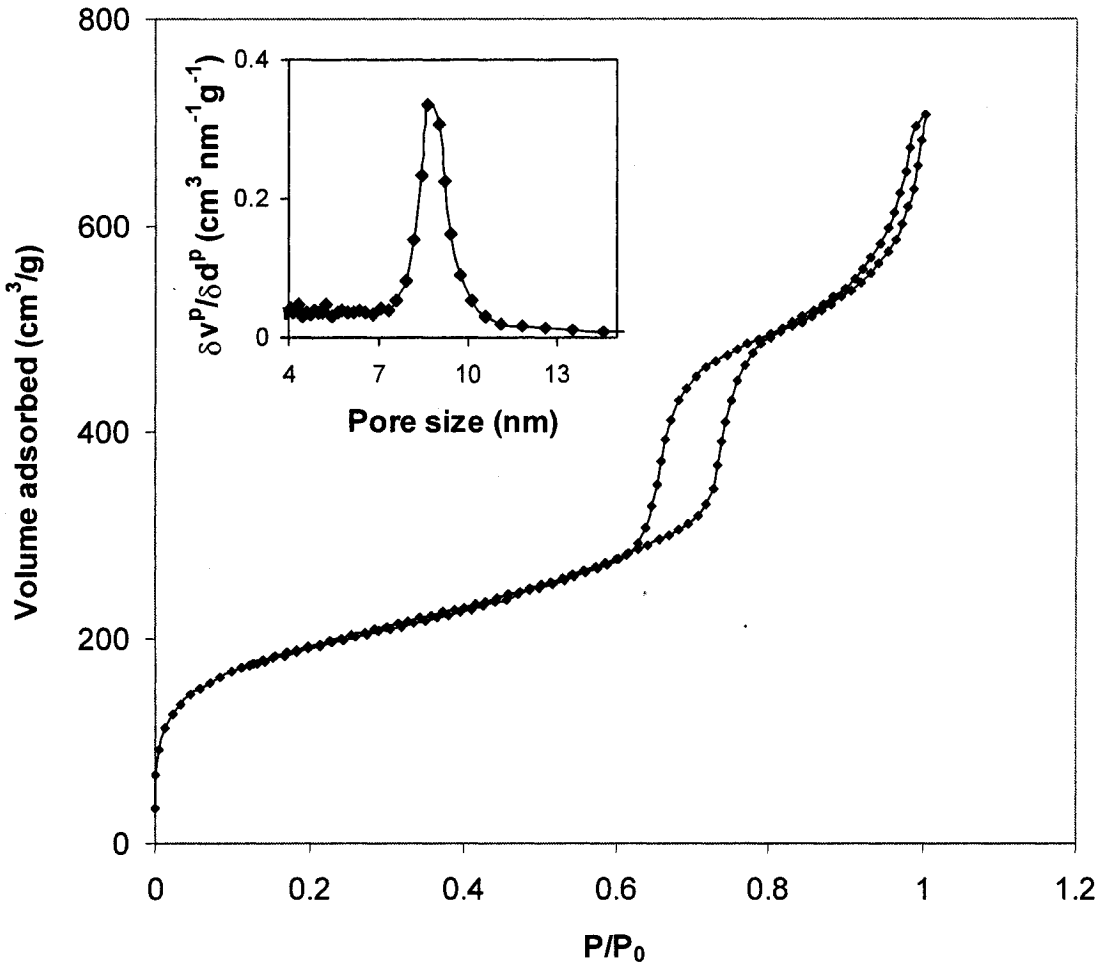

Fig. 4.18 Nitrogen adsorption-desorption isotherm for ethenylene-bridged mesoporous organosilica prepared in the presence of triblock copolymer P123

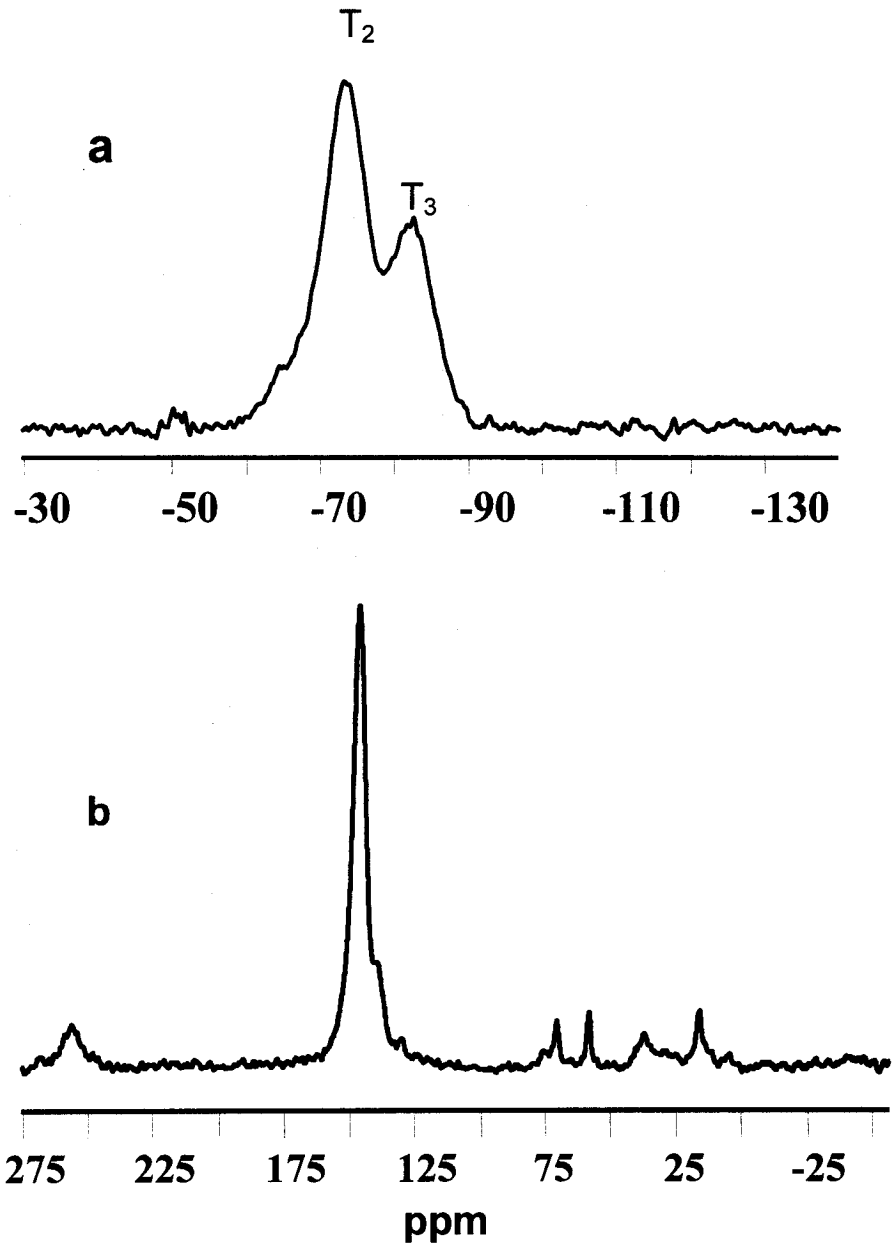

Fig. 4.19 (a) ^{29}Si NMR, and (b) ^{13}C NMR data for the ethenylene-bridged mesoporous organosilica prepared in the presence of triblock copolymer P123

Recent literature data indicated that addition of butanol [68] or NaI [67] to the synthesis mixture of mesoporous silica in the presence of P123 generated cubic mesophases. We found it interesting to investigate whether this dramatic effect occurs when ethenylenesilicon is used as precursor.

Figure 4.20 shows the XRD patterns for solvent-free materials obtained using P123 in the presence of butanol and NaI additives along with the sample prepared with no additives (described earlier). Both samples exhibited a strong sharp peak at low diffraction angles. The material which was prepared using butanol had two additional small peaks, whereas the other material had a single broad peak. These data indicate that all materials exhibit two-dimensional hexagonal structure.

Figure 4.21 shows the pore size distribution for materials obtained using ethenylene containing precursor, P123, and butanol or NaI. Adding butanol had a dramatic effect on the pore-size distribution, which becomes much narrower, indicating the occurrence of much better ordered porous system. However, addition of NaI had a slightly negative effect as the pore size distribution became somewhat broader.

Figure 4.22 shows the nitrogen adsorption-desorption isotherms for materials obtained using the ethenylene-containing precursor, P123, and butanol or NaI as additives. In the presence of butanol, the adsorption step became steeper which is consistent with the narrower pore size distribution. Table 4.3 lists pore system information for these materials.

Figure 4.23 shows TEM images for the material obtained using the ethenylene-containing precursor, P123, and butanol as additives. This showed that the material

had hexagonal pore structure and the pore sizes were 8.2nm, which is comparable to data obtained by XRD and nitrogen adsorption.

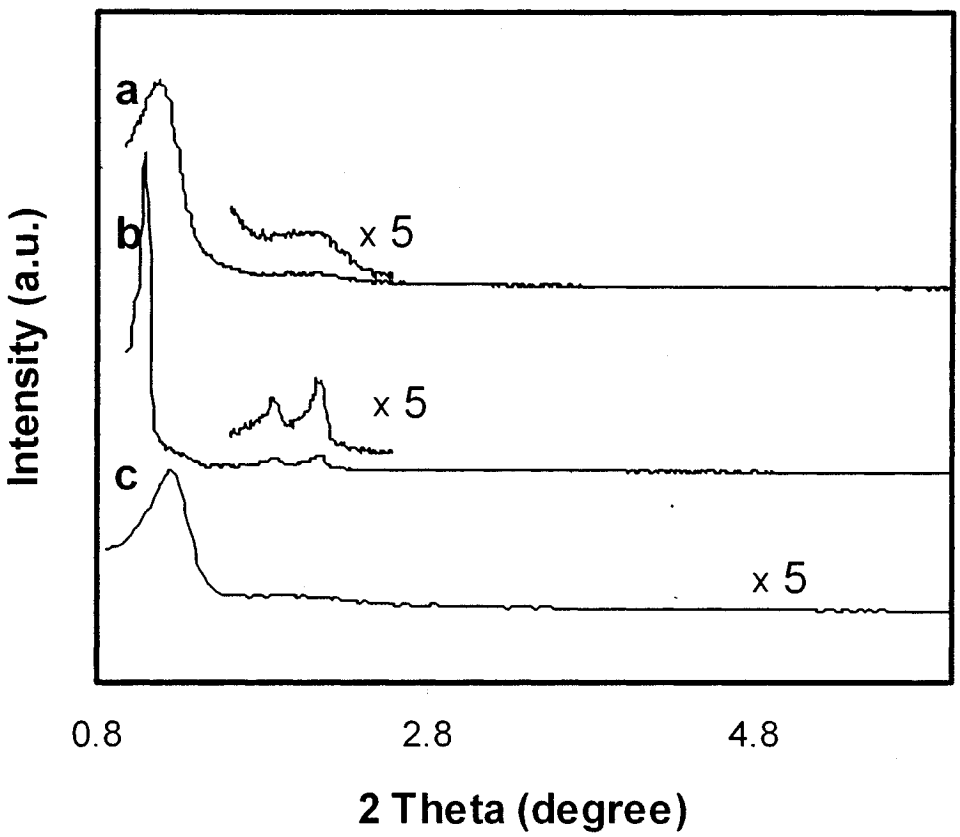

Fig. 4.20 XRD patterns for ethenylene-bridged mesoporous organosilica (after extraction) prepared in the presence of (a) P123, (b) P123 + butanol, and (c) P123 + sodium iodide

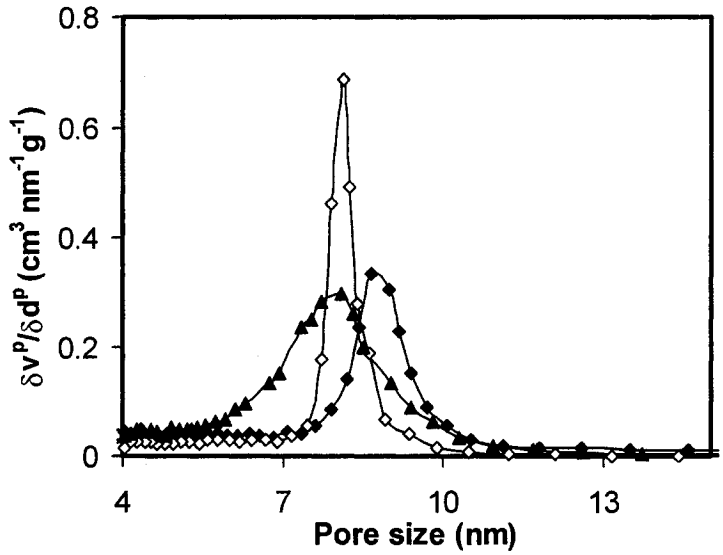

Fig. 4.21 pore size distribution for ethenylene-bridged mesoporous organosilicas prepared in the presence of triblock copolymer P123 only (-♦-), P123 + butanol (-◊-), and P123 + sodium iodide (-▲-)

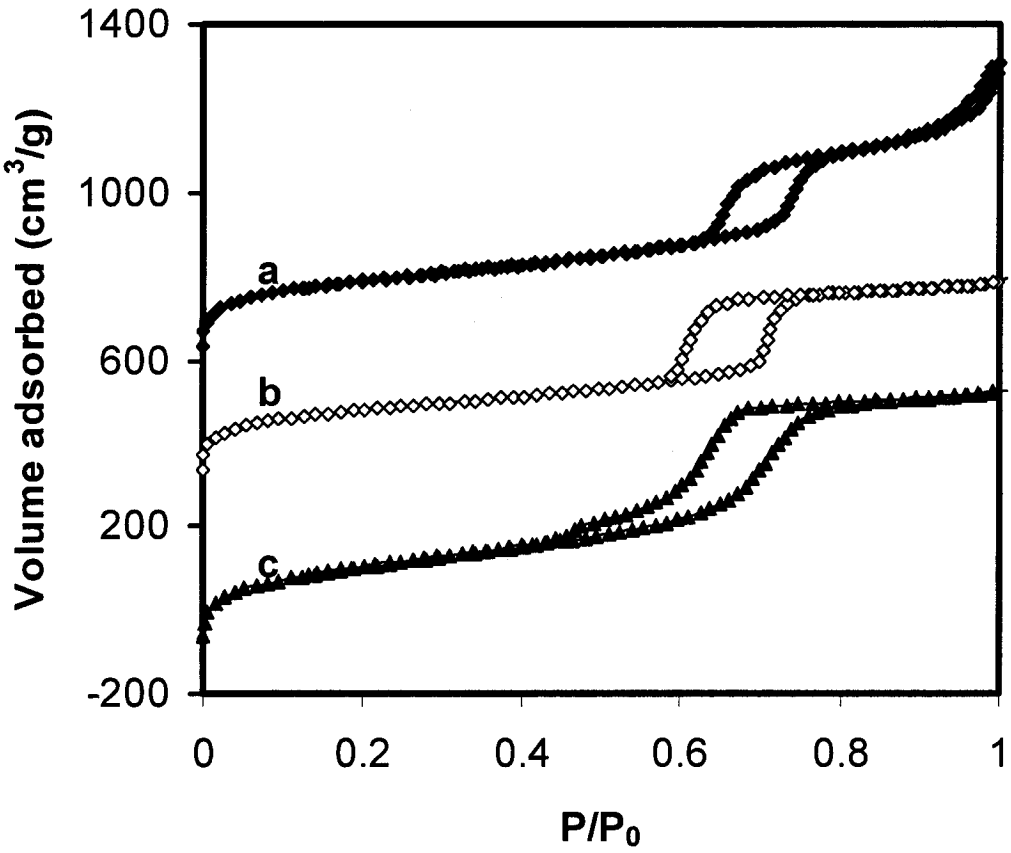

Fig. 4.22 Nitrogen adsorption-desorption isotherms for ethenlyene-bridged mesoporous organosilicas in the presence of triblock copolymer P123 only (-♦-) (+600), P123 + butanol (-◊-) (+200), and P123 + sodium iodide (-▲-) (-200)

Table 4.3 Pore system data for materials prepared in the presence of P123 (SW45e), P123 + butanol (SW51e) and P123 + NaI (SW52e)

Sample	d_{100} nm	Surface area m^2/g	Pore Size nm	Pore volume cm^3/g	Pore wall thickness nm
SW45e	8.58	676	8.65	0.924	1.26
SW51e	9.40	624	8.01	0.744	2.84
SW52e	7.07	718	7.90	0.953	0.26

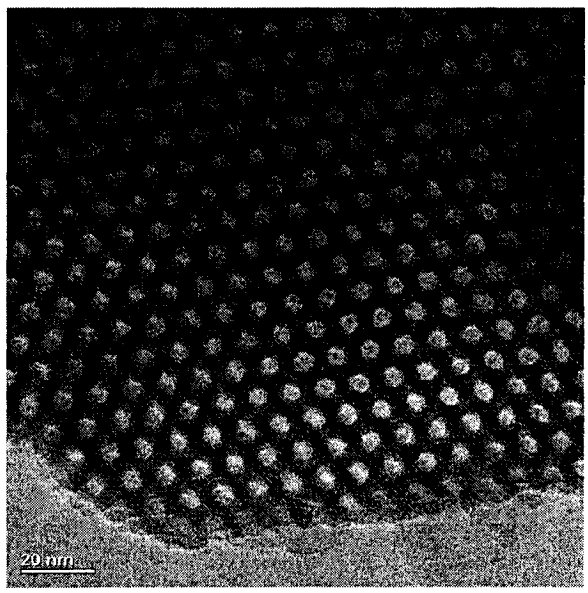

Figure 4.23 TEM Image of ethenylene-bridged mesoporous organosilicas prepared in the presence of triblock copolymer P123 + butanol viewed down [001] zone axis.

4.3.2.2 Summary

Using bis(triethoxysilyl)ethylene and P123, a large pore (8.6 nm) mesoporous material with 2D-hexagonal structure was prepared. The ^{29}Si and ^{13}C NMR data provided strong evidence that the framework is comprised of $O_{1.5}Si\text{-}CH{=}CH\text{-}SiO_{1.5}$. When butanol was added, the pore size distribution became narrower and the structure more ordered. However, contrary to pure silica, no cubic mesophase was obtained.

4.3.3 Ethenylenesilica prepared in the presence of alkyltrimethylammonium

4.3.3.1 Results and discussion

Table 4.4 lists the pore volume, surface area and pore size distribution (calculated from the nitrogen adsorption branch) for materials obtained using bis(triethoxysilyl)ethylene precursor in the presence of alkyltrimethylammonium surfactant under different conditions (preparation conditions listed in Table 3.3). It showed that SW19e is the best material.

Figure 4.24 shows the powder X-ray diffraction pattern for solvent-extracted SW19e sample. It revealed only a single peak at $2\theta = 2.25^{\circ}$.

Figure 4.25 shows the nitrogen adsorption isotherm for sample SW19e. It exhibits an increase in adsorption at P/P_0 = 0.32-0.42 due to capillary condensation of nitrogen in the mesopores. The KJS pore diameter was 3.6 nm, the BET surface area was 1271 m^2/g and pore volume was 0.91 cm^3/g.

Table 4.4 N_2 adsorption data for materials prepared under different Conditions

sample	pore volume cm^3/g	surface area m^2/g	pore size nm
SW10e	0.194	234	3.5
SW11e	0.362	723	3.33 + <2
SW13e	0.557	1053	2.48 + <2
SW14e	0.332	680	2.27 + <2
SW15e	0.471	957	2.53 + <2
SW16e	0.655	1178	3.07
SW17e	0.550	951	3.50
SW19e	0.914	1270.6	3.62
SW20e	0.601	894.31	3.94

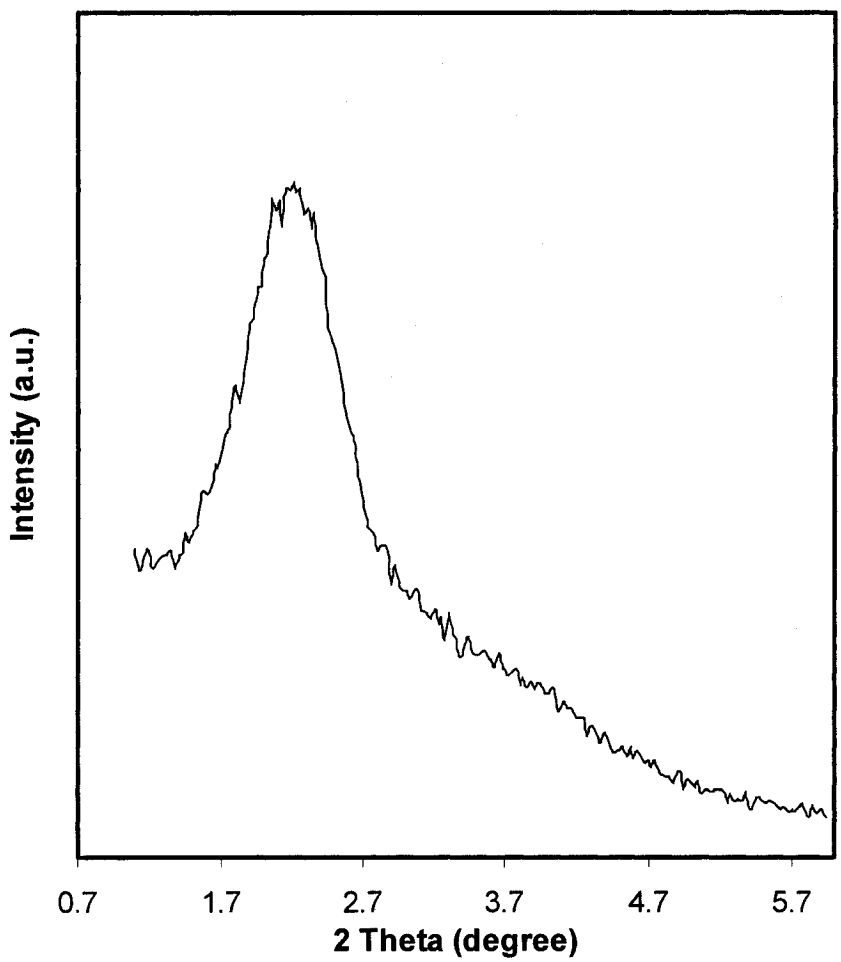

Fig. 4.24 XRD patterns for ethenylene-bridged mesoporous organosilica (after extraction) prepared in the presence of C_{16}TMACl

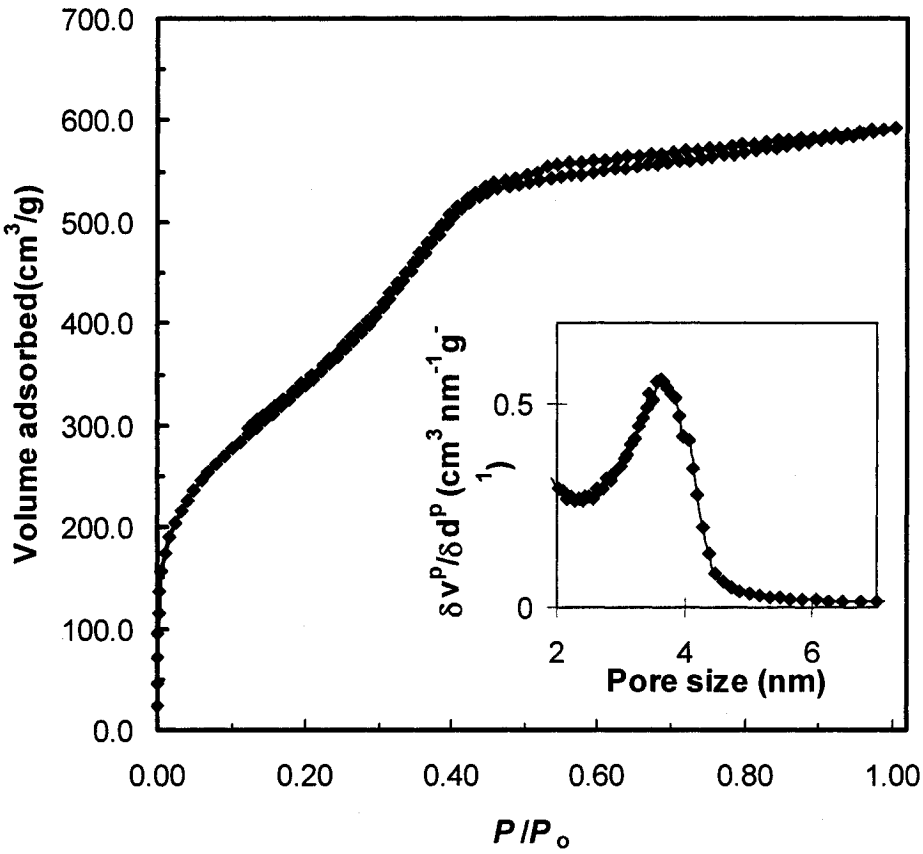

Figure 4.25 Nitrogen adsorption-desorption isotherms for ethenylene-bridged mesoporous organosilica prepared in the presence of C_{16}TMACl

The ^{29}Si MAS-NMR spectrum (Fig. 4.26a) of sample SW19e exhibited two main signals at -73.66 and -83,03 ppm, assigned to Si species covalently bonded to carbon atoms: T^2 [C-***Si***O_2(OH)] and T^3 [C-***Si***O_3], respectively. A small signal at -64.31ppm was assigned to T^1 [C-***Si***$O(OH)_2$]. The signal at -109.8 ppm attributable to condensed SiO_4 species was also present. The relative intensity of this signal was below 8%. The ^{13}C NMR spectrum (Fig. 4.26 b) showed a single strong peak at 146.3 ppm, which corresponds to the ethenylene carbon atoms. The ^{29}Si and ^{13}C NMR data are consistent with each other, and provide strong evidence for the occurrence of a network composed of $O_{1.5}$Si-CH=CH-$SiO_{1.5}$ units.

4.3.3.2 Summary

Using bis(triethoxysilyl)ethylene precursor and C_{16}TMACl surfactant, a high quality mesoporous organosilica was prepared. The material had very large surface area (1270 m^2/g) and 3.6 nm pores. The ^{29}Si and ^{13}C NMR data showed that the framework was comprised mostly of $O_{1.5}$Si-CH=CH-$SiO_{1.5}$ units.

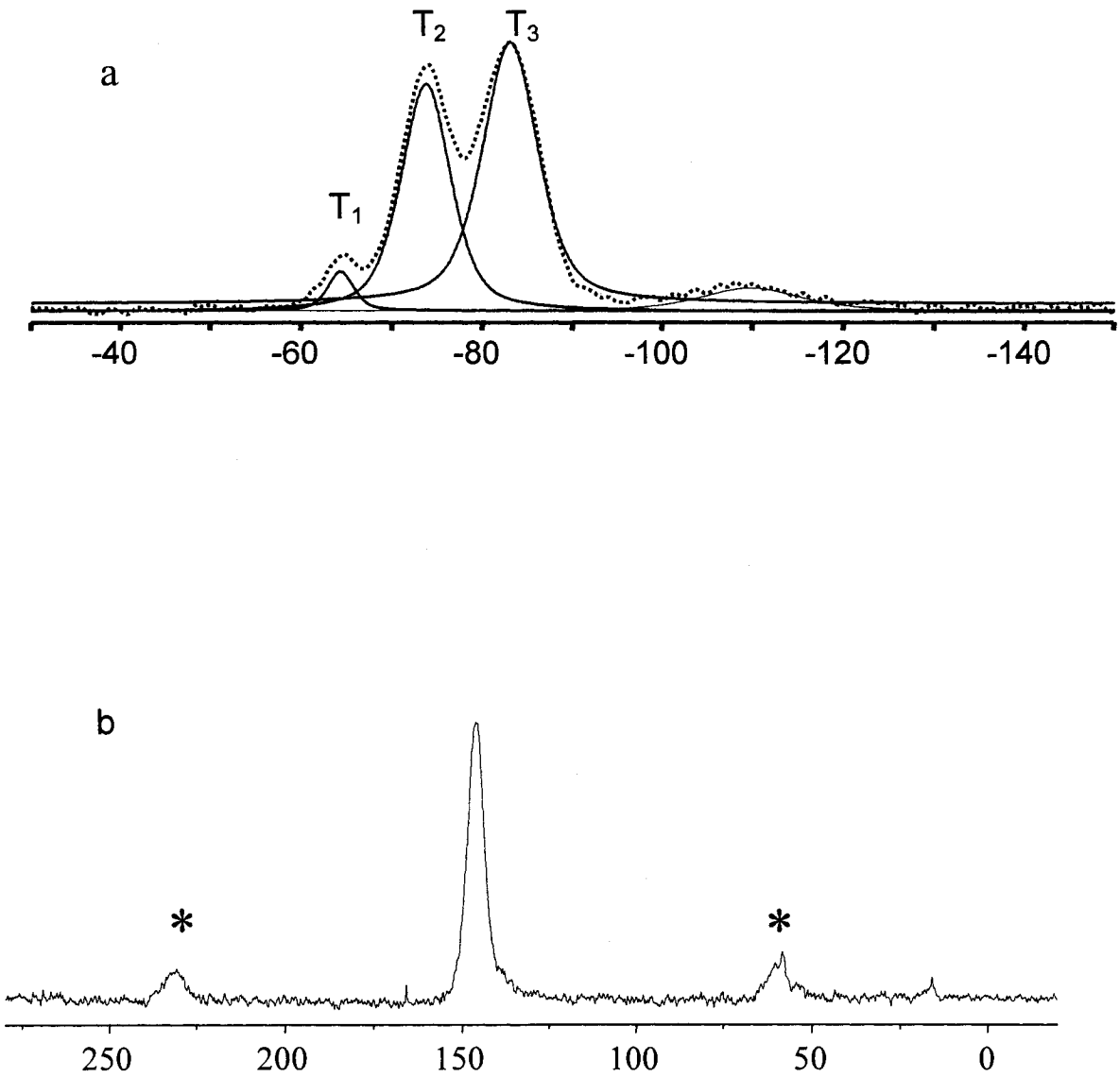

Fig. 4.26 (a) ^{29}Si NMR, and (b) ^{13}C NMR data for the ethenylene-bridged mesoporous organosilica prepared in the presence of C_{16}TMACl

4.4 Evaluation of post-synthesis reactions

4.4.1 Results and disscussion

Bromination was investigated for materials containing C=C double bonds. After bromination, nitrogen adsorption, XRD and ^{13}C NMR were used to characterize the obtained materials. Nitrogen adsorption and XRD were used to investigate the effect of bromination on the pore structure of the material. ^{13}C NMR was used to indicate that the bromination did take place by detecting carbon atoms bonded to bromine.

Figure 4.27 shows XRD patterns for mesoporous ethenylenesilica (SW35e) obtained in the presence of Brij 76 before and after bromination. Both spectra exhibited one strong and two small peaks. This indicates that the pore structure did not change through bromination.

Figure 4.28 shows nitrogen adsorption isotherms for the same material before and after bromination. After bromination, the pore size decreased from 5.1 to 4.4 nm, the BET surface decreased from 868 to 489 m^2/g and the pore volume decreased from 0.83 to 0.46 cm^3/g.

After bromination, ^{13}C NMR data show the appearance of a new peak at 33.9 ppm (Figure 4.29). It was assigned to C-Br, indicating that bromine did add to the double bond. However, the peak at 146.29 ppm assigned which to C=C did not disappear completely indicating that not all the double bonds reacted.

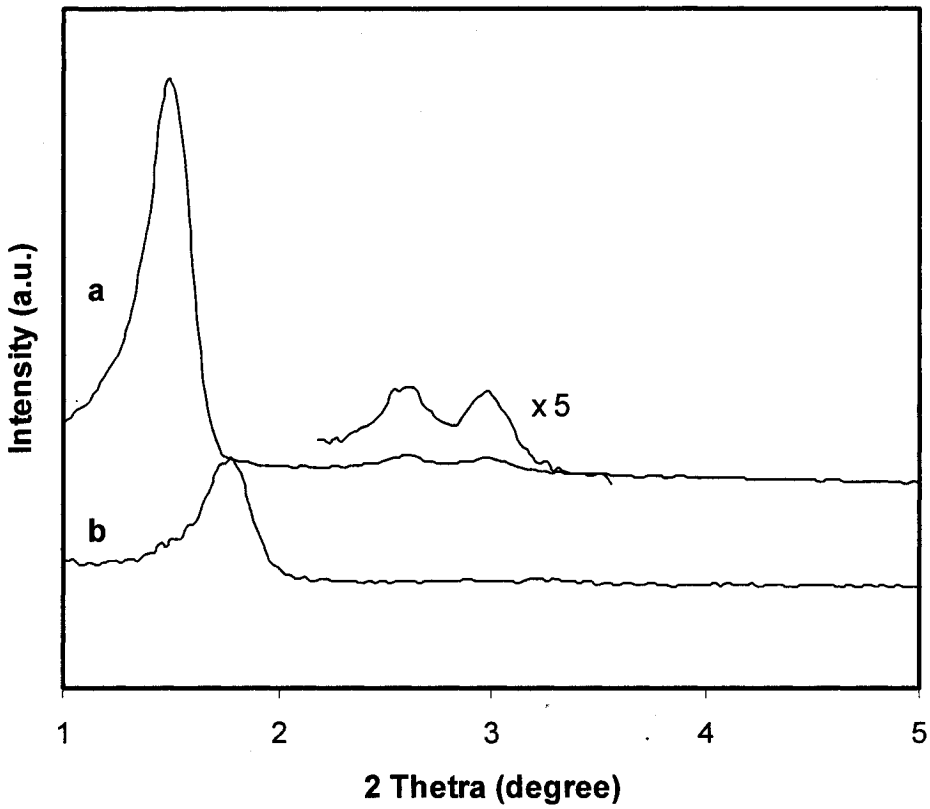

Figure 4.27 XRD patterns for ethenylene-bridged mesoporous organosilicas prepared in the presence of Brij 76 using a second hydrothermal stage for 20 h at 50 ºC (a) before, and (b) after bromination

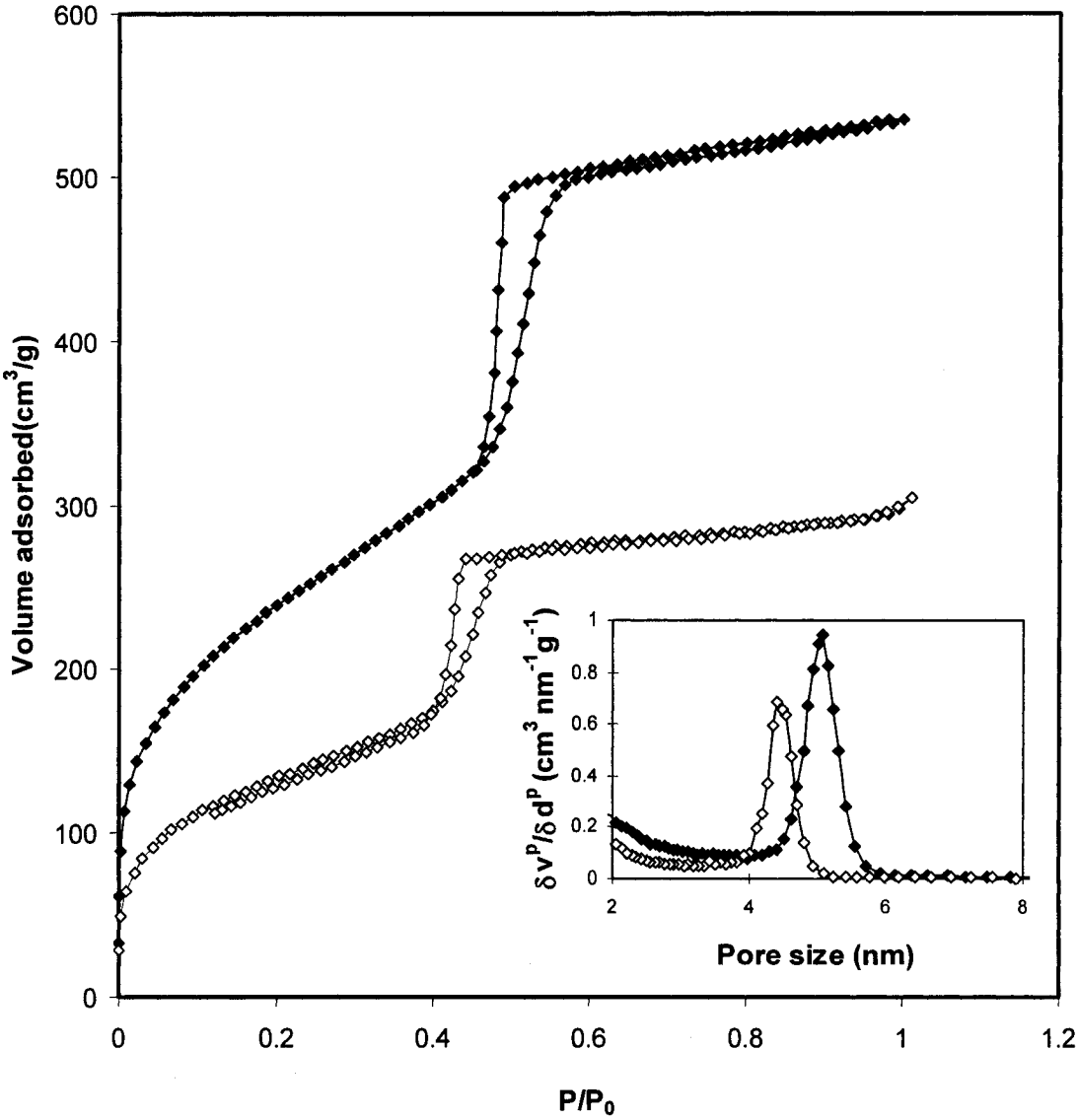

Fig. 4. 28 Nitrogen adsorption-desorption isotherms for ethenylene-bridged mesoporous organosilicas prepared in the presence of Brij 76 using a second hydrothermal stage for 20 h at 50 °C (-♦-) before, and (-◊-) after bromination

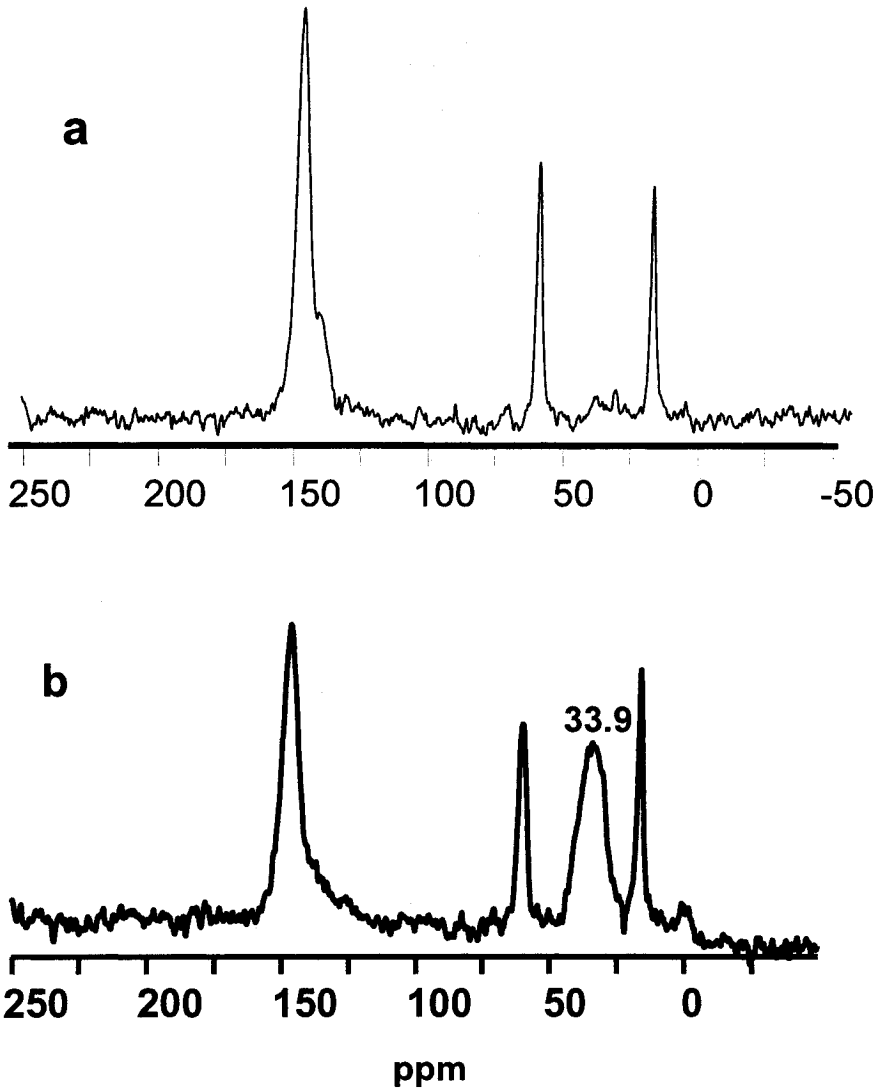

Fig. 4.29 ^{13}C NMR for ethenylene-bridged mesoporous organosilicas prepared in the presence of Brij 76 using a second hydrothermal stage for 20 h at 50 °C (a) before, and (b) after bromination

Figure 4.30 is XRD patterns for mesoporous ethenylenesilica (SW45e) obtained in the presence of P123 before and after bromination. Only the intensity of the main peak decreased after bromination indicating that the pore structure was mostly preserved.

Figure 4.31 shows nitrogen adsorption isotherms for the same material before and after bromination. After bromination, the pore size decreased from 8.64 to 8.53 nm. The BET surface area and pore volume also decreased from 676 to 338 m^2/g and from 0.91 to 0.59 cm^3/g, respectively.

After bromination, a ^{13}C NMR peak, assigned to C-Br, appeared at 32.87 ppm indicating that the bromine did add to the double bond (Figure 4.32). However, the peak at 146.41 ppm attributable to C=C persisted indicating that not all the double bonds were accessible to bromine.

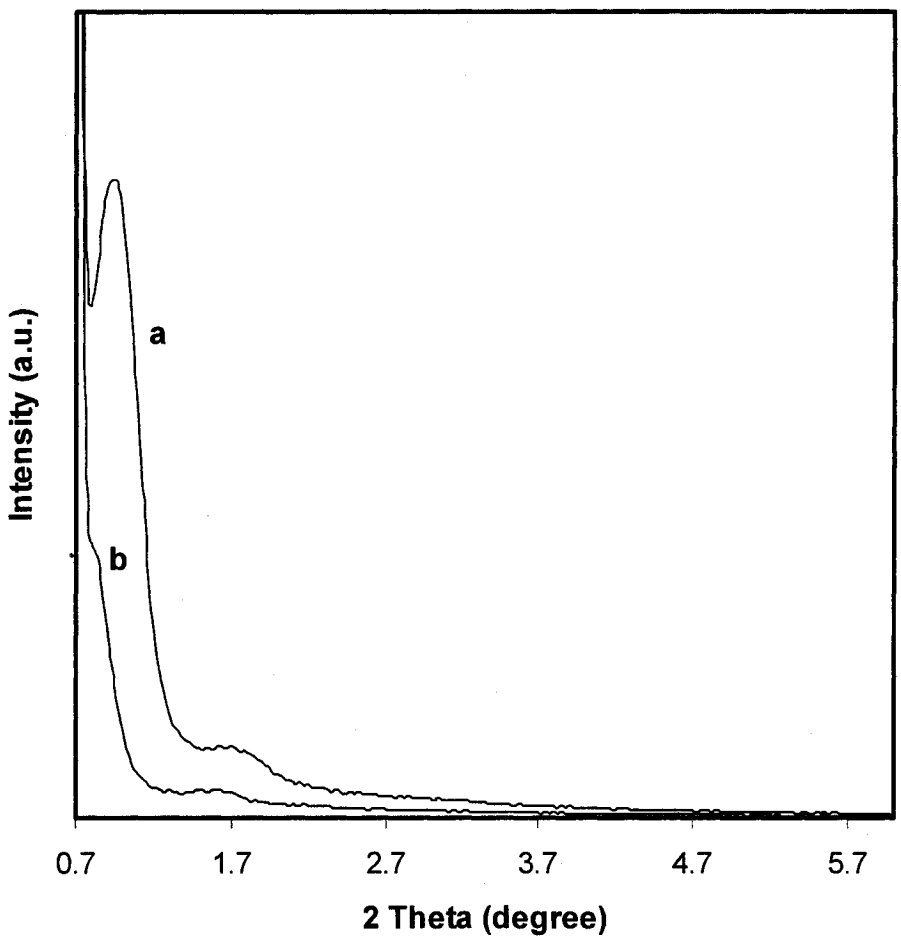

Figure 4.30 XRD patterns for ethenylene-bridged mesoporous organosilicas prepared in the presence of triblock copolymer P123 (a) before, and (b) after bromination

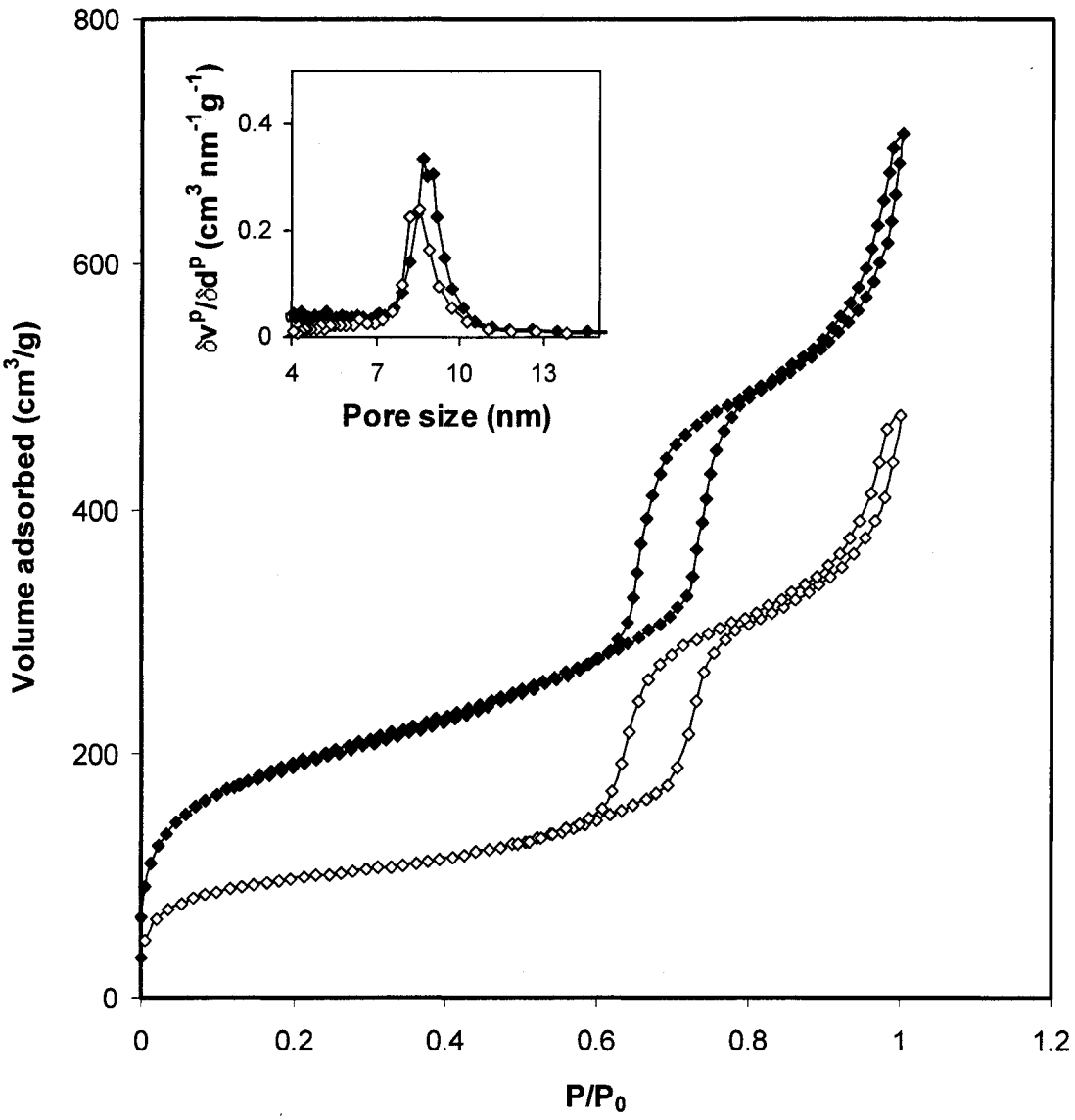

Fig. 4.31 Nitrogen adsorption-desorption isotherms for ethenylene-bridged mesoporous organosilicas prepared in the presence of triblock copolymer P123 (-♦-) before, and (-◊-) after bromination

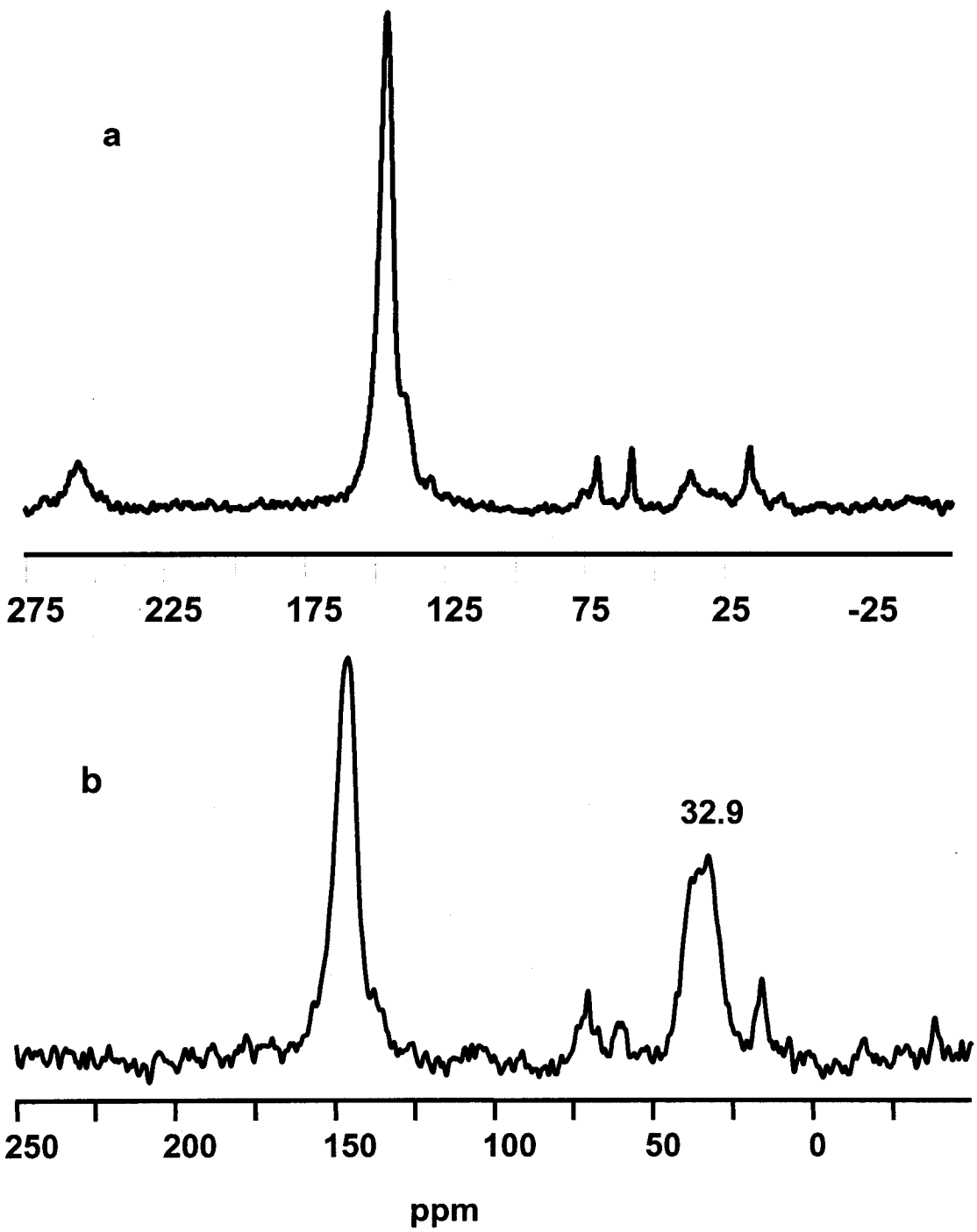

Fig. 4.32 ^{13}C NMR for ethenylene-bridged mesoporous organosilicas prepared in the presence of triblock copolymer P123 (a) before, and (b) after bromination

Figure 4.33 shows the nitrogen adsorption isotherms for materials obtained by co-condensation of TEOS and TEVS in the presence of CTAB, before and after bromination. After bromination, the pore size decreased from 2.4 to under 2 nm, the BET surface area decreased from 1133 to 532 m^2/g and the pore volume from 0.57 to 0.23 cm^3/g.

Figure 4.34 shows that upon bromination, a ^{13}C NMR peak assigned to C-Br appeared at 35.55 ppm. This indicates that bromine did add to the C=C double bond. In addition, the two peaks at 129.4 and 134 which belonged to the vinyl group disappeared completely, indicating that the vinyl group reacted fully with bromine.

4.4.2 Summary

Ethenylene-bridged mesoporous materials prepared in the presence of Brij 76 or triblock copolymer P123 were submitted to bromination. ^{13}C NMR data showed that only a fraction of the C=C double bonds inside the wall reacted with bromine, the remaining ethylene groups were not accessible. One possible reason maybe the bromine molecule is too big. Thus, not enough bromine can diffuse inside the pore system to react with the C=C double bond. Another possible reason is that part of C=C species are hidden within the pore wall. Material containing vinyl groups was also tested for bromination. The ^{13}C NMR experiment indicated that all the terminal C=C double bonds were available for reaction.

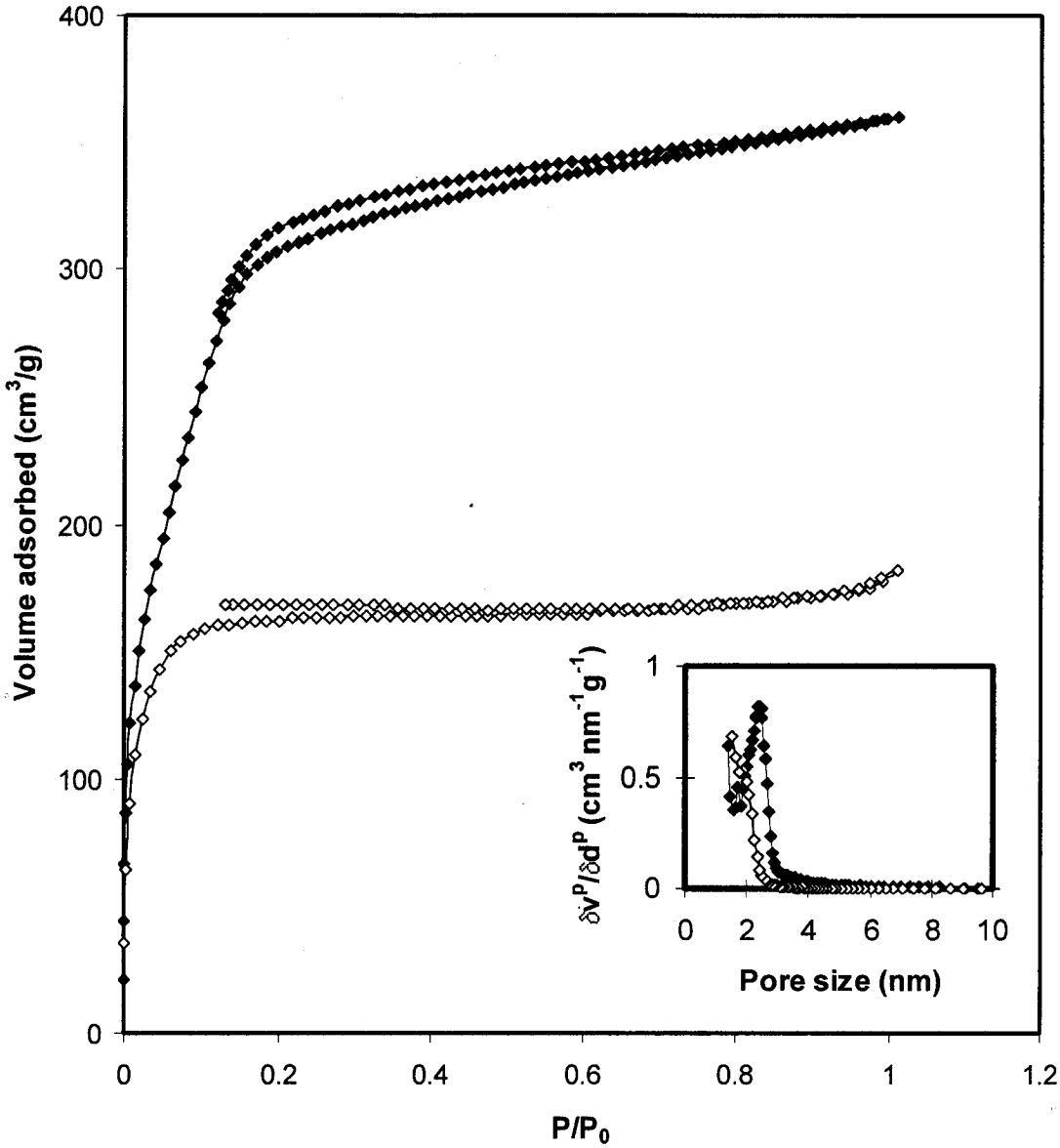

Fig. 4.33 Nitrogen adsorption-desorption isotherms for vinyl and ethenylene containing mesoporous organosilicas prepared in the presence of CTAB (-♦-) before, and (-■-) after bromination

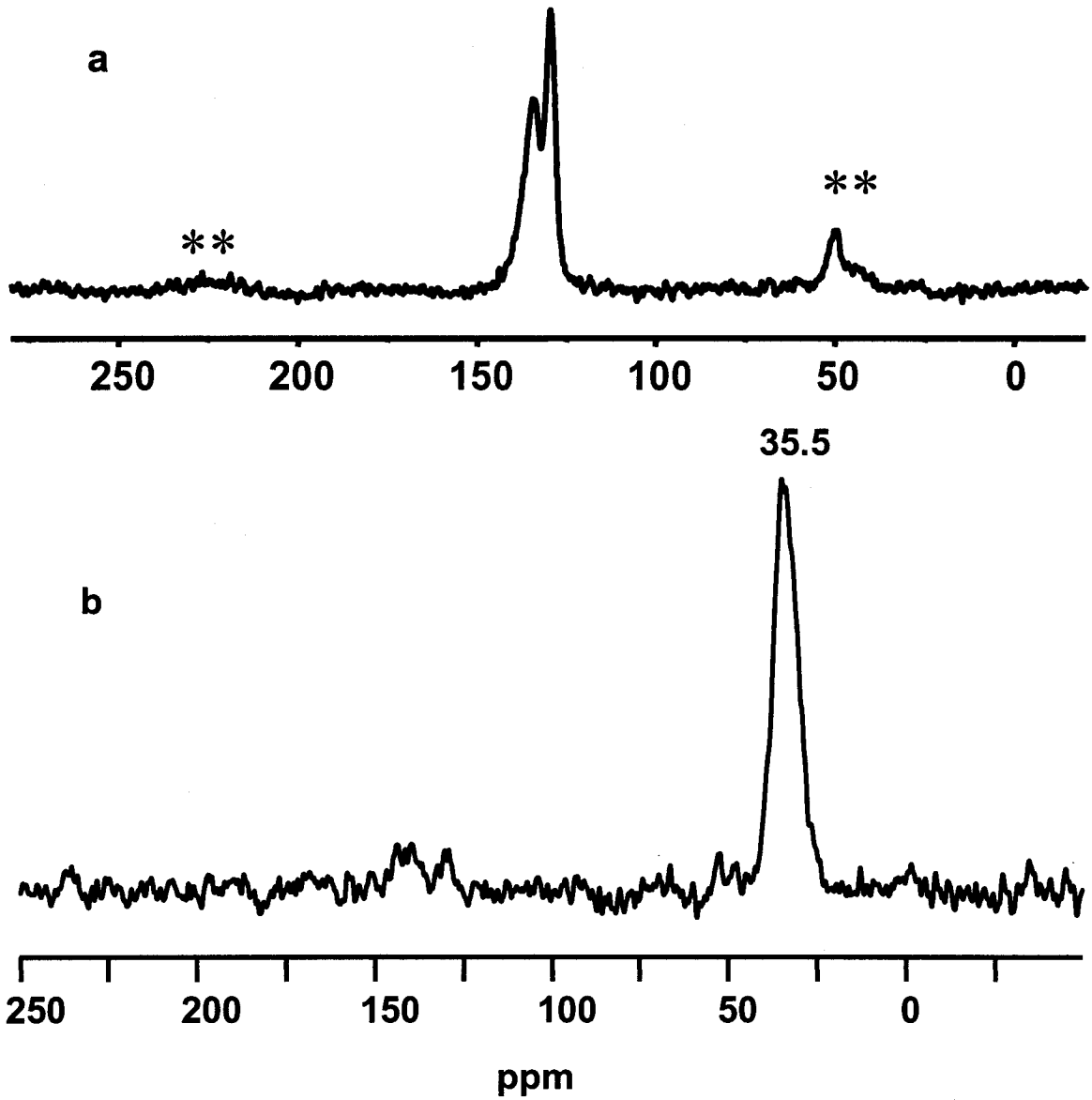

Fig. 4.34 ^{13}C NMR for vinyl and ethenylene containing mesoporous organosilicas prepared in the presence of CTAB (a) before, and (b) after bromination

Chapter 5

Conclusion

Organosilicon precursors, bis(triethoxysilyl)benzene and bis(triethoxysilyl)ethylene have been prepared in good yields. ^{1}H, ^{13}C NMR and mass spectrometry techniques were used to characterize them unambiguously.

Using bis(triethoxysilyl)benzene precursor and Brij 76, excellent quality mesoporous organosilicas were prepared under acid conditions. XRD showed that this material has a two-dimensional hexagonal structure. Nitrogen adsorption showed that the pore size was 3.9 nm, the surface area was 840 m^2/g, and the pore volume was 0.634 cm^3/g. ^{29}Si and ^{13}C NMR provided direct evidence that $O_{1.5}Si\text{-}C_6H_4\text{-}SiO_{1.5}$ did build in the wall of the channel. Detailed TEM studies showed this material has partial molecular order in the pore walls.

Likewise, bis(triethoxysilyl)ethylene and Brij 76 gave rise to a high quality mesoporous material under acid conditions. XRD indicated that it is two-dimensional hexagonal structure. This mesophase has 5.1 nm pore diameter, 868 m^2/g surface area, and 0.83 cm^3/g pore volume. SEM showed that its particles consisted of hexagonal rods. The ^{29}Si and ^{13}C NMR indicated that the $O_{1.5}Si\text{-}CH{=}CH\text{-}SiO_{1.5}$ units are located in the framework.

The use of bis(triethoxysilyl)ethylene in the presence of triblock copolymer P123 also afforded a ordered mesoporous material which has 8.6 nm pore dores. XRD data were consistent with the occurrence of a two-dimensional hexagonal structure. The ^{29}Si and ^{13}C NMR provided direct evidence that the framework consisted mainly of $O_{1.5}Si\text{-}CH{=}CH\text{-}SiO_{1.5}$ units. Addition of butanol did improve the pore size distribution. However, no cubic structure was obtained.

Using bis(triethoxysilyl)ethylene under basic conditions in the presence of C_{16}TMACl gave rise to a mesoporous material with very large surface area (1271 m^2/g) and pore volume (0.91 cm^3/g).

Bromination of materials with framework ethylene showed that the C=C double bonds were reactive, but not fully accessible. However, bromination for the material containing vinyl groups indicated that all terminal double bonds reacted with bromine.

The Phenylene-bridged mesoporous organosilicas can also be further modified because of the high reactivity of the phenyl ring. Future work may be focused on the reactions at the phenyl ring to generate PMOs with special properties. The phenylene-bridged mesoporous organosilica obtained under acidic conditions in the presence of Brij 76 has partial molecular order in the pore wall. Further investigations to get higher molecular order in the pore walls should be undertaken.

The C=C double bonds inside ethenylene-bridged mesoporous organosilicas were partially accessible. Many chemical reactions such as amination could be achieved in the future.

The preparation of ethenylenesilica mesophases with different symmetry than MCM-41 is worthwhile pursuing. Synthetic strategies leading to cubic mesoporous silicas such as the use of additives and typical surfactant, e.g. Pluronic F127, divalent ammobnium-based surfactant, maybe systematically investigated using BTSEY as precursor.

References

1. Yanagisawa, T.; Shimizu, T.; Kuroda, K.; Kato, C. *Bull. Chem. Soc. Jpn.* **1990**, 63, 988.
2. Inagaki, S.; Fukushima, Y.; Kuroda, K. *J. Chem. Soc., Chem. Commun.* **1993**, 680.
3. Di Renzo, F.; Cambo, H.; Dutartre, R. *Microporous Mesoporous Mater.* **1997**, 10, 283.
4. Sayari, A.; Jaroniec, M.; eds. "Nanoporous Materials III", *Elsevier, Amsterdam* **2002**.
5. Kresge, C. T.; Leonowicz, M. E.; Roth, W. J.; Vartuli, J. C.; Beck, J. C. *Nature* **1992**, 359, 710.
6. Beck, J. S.; Vartuli, J. C.; Roth, W. J.; Leonowicz, M. E.; Kresge, C. T.; Schmitt, K. D.; Chu, C.T-W.; Olson, D. H.; Sheppard, E. W.; McCullen, S. B.; Higgins, J. B.; Schlenker, J. L. *J. Am. Chem. Soc.* **1992**, 114, 10834.
7. Huo, Q.; Margolese, D. I.; Ciesla, U.; Demuth, D. G.; Feng, P.; Gier, T. E.; Sieger, P.; Firouzi, A.; Chmelka, B. F.; Schüth, F.; Stucky, G. D. *Chem. Mater.* **1994**, 6, 1176.
8. Sakamoto, Y.; Kaneda, M.; Terasaki, O.; Zhao, D. Y.; Kim, J. M.; Stucky, G. D.; Shin, H. J.; Ryoo, R. *Nature* **2000**, 408, 449.
9. Huo, Q.; Leon, R.; Petroff, P. M.; Stucky, G. D. *Science* **1995**, 268, 1324.
10. Zhao, D. Y.; Huo, Q.; Feng, J.; Chmelka, B. F.; Stucky, G. D. *J. Am. Chem. Soc.* **1998**, 120, 6024.

11. Zhao, D. Y.; Huo, Q.; Feng, J.; Kim, J.; Han, Y.; Stucky, G. D. *Chem. Mater.* **1999**, 11, 2668.

12. Yu, C.; Yu, Y.; Zhao, D.; *Chem. Commun.* **2000**, 575.

13. Asefa, T. ; MacLachlan, M. J. ; Grondey, H. ; Coombs, N. ; Ozin, G. A. *Angew. Chem. Int. Ed.* **2000**, 39, 1808.

14. Bagshaw, S. A. ; Prouzet, E. ; Pinnavaia, T. J. *Science* **1995**, 269, 1242.

15. Kim, S. S. ; Zheng, W. ; Pinnavaia, T. J. *Science* **1998**, 282, 1302.

16. Tanev, P. T. ; Pinnavaia, T. J. *Science* **1996**, 271, 1267.

17. Sayari, A.; Yang, Y.; Kruk, M.; Jaroniec, M. *J. Phys. Chem. B* **1999**, 103, 3651.

18. Sayari, A.; Hamoudi, S.; Yang, Y.; Moudrakovski, I. L. ; Ripmeester, J. R. *Chem. Mater.* **2000**, 12, 3857.

19. Chenite, A.; Le Page, Y.; Karra, V.R. ; Sayari, A. *J. Chem. Soc., Chem. Commun.* **1996**, 413.

20. Liu, P.; Moudrakovski, I. L.; Liu, J. ; Sayari, A. *Chem. Mater.* **1997**, 9, 2513.

21. Yang, H. ; Coombs, N. ; Ozin, G. A. *Nature* **1997**, 386, 692.

22. Zhao, D.; Sun, J.; Li, Q.; Stucky, G. D. *Chem. Mater.* **2000**, 12, 275.

23. Yada, M.; Hiyoshi, H.; Ohe, K.; Machida, M.; Kijima, T. *Inorg. Chem.* **1997**, 36, 5565.

24. Lin, H. P.; Mou, C. Y. *Science* **1996**, 273, 765.

25. Firouzi, A.; Monnier, A.; Bull, L. M.; Besier, T.; Sieger, P.; Huo, Q.; Walker, S. A.; Zasadzinski, J. A.; Glinka, C.; Nicol, J.; Margolese, D.; Stucky, G. D.; Chmelka, B. F. *Science* **1995**, 267, 1138.

26. Firouzi, A.; Atef, F.; Oertli, A. G.; Stucky, G. D.; Chmelka, B. F. *J. Am. Chem. Soc.* **1997**, 119, 3596.

27. Huo, Q.; Margolese, D. I.; Ciesla, U.; Demuth, D. G.; Feng, P.; Gier, T. E.; Sieger, P.; Firouzi, A.; Chmelka, B. F.; Schüth, F.; Stucky, G.D. *Chem. Mater.* **1994**, 6, 1176.

28. Tanev, P. T.; Pinnavaia, T. J. *Science* **1995**, 267, 865.

29. Antonelli, D. M.; Ying, J. Y. *Angew. Chem. Int. Ed. Engl.* **1996**, 35, 426.

30. (a) Ozin, G. A.; Chomski, E.; Khushalani, D.; MacLachan, M. J. *Curr. Opin. Colloid Interface Sci.* **1998**, 3, 181. (b) Moller, K.; Bein, T.; Fischer, R. X. *Chem. Mater.* **1998**, 10, 1841. (c) Wu, J.; Gross, A. F.; Tolbert, S. H. *J. Phys. Chem. B* **1999**, 103, 2374.

31. (a) Vartuli, J. C.; Shih, S. S.; Kresge, C. T.; Beck, J.S. *Stud. Surf. Sci. Catal.* **1998**, 117, 13. (b) Wang, L. Z.; Shi, J. L.; Yu, J.; Yan, D. S. *J. Inorg. Mater.* **1999**, 14, 333.

32. (a) Hata, H.; Saeki, S.; Kimura, T.; Sugahara, Y.; Kuroda, K. *Chem. Mater.* **1999**, 11, 1110. (b) Kemner, K. M.; Feng, X.; Liu, J.; Fryxell, G. E.; Wang, L.; Kim, A. Y.; Gong, M.; Mattigod, S. *J. Synchrotron Radiat.* **1999**, 6, 633. (c) Zhao, D. Y.; Yang, P. D.; Huo, Q. S.; Chmelka, B. F.; Stucky, G. D. *Curr. Opin. Solid State Mater. Sci.* **1998**, 3, 111.

33. Keefe, M. H.; Slone, R. V.; Hupp, J. T.; Czaplewski, K. F.; Snurr, R. Q.; Stern, C. L. *Langmuir* **2000**, 16, 3964.

34. (a) Pater, J. P. G.; Jacobs, P. A.; Martens, J. A. *J. Catal.* **1999**, 184, 262. (b) Morey, M. S. ; Davidson, A. ; Stucky, G. D. *J. Porous Mater.* **1998**, 5, 195.

35. Asefa, T.; Yoshina-Ishii, C.; MacLachlan, M. J.; Ozin, G. A.; *J. Mater. Chem.* **2000**, 10, 1751.

36. Inagaki, S.; Guan, S.; Fukushima, Y.; Ohsuna, T.; Terasaki, O. *J. Am. Chem. Soc.* **1999**, 121, 9611.

37. Guan, S.; Inagaki, S.; Ohsuna, T.; Terasaki, O. *J. Am. Chem. Soc.* **2000**, 122, 5660.

38. Asefa, T.; MacLachlan, M. J.; Coombs, N.; Ozin, G. A. *Nature* **1999**, 402, 867.

39. Fan, H.; Lu, Y.; Stump, A.; Reed, S. T.; Baer, T.; Schunk, R.; Perez-Luna, V.; Lopez, G. P.; Brinker, C. J. *Nature* **2000**, 405, 56.

40. Melde, B. J.; Holland, B. T.; Blanford, C. F.; Stein, A. *Chem. Mater.* **1999**, 11, 3302.

41. Ozin, G. A. *Chem. Commun.* **2000**, 419.

42. MacLachlan, M. J.; Asefa, T.; Ozin, G. A. *Chem. Eur. J.* **2000**, 6, 2507.

43. Lu, Y.; Fan, H.; Doke, N.; Loy, D. A.; Assink, R. A.; LaVan, D. A.; Brinker, C. J. *J. Am. Chem. Soc.* **2000**, 122, 5258.

44. Inagaki, S.; Guan, S.; Fukushima, Y.; Ohsuna, T.; Terasaki, O. *Stud. Surf. Sci. Catal.* **2000**, 129, 155.

45. Yoshina-Ishii, C.; Asefa, T.; Coombs, N.; MacLachlan, M. J.; Ozin, G. A. *Chem. Commun.* **1999**, 2539.

46. Brunauer, S.; Deming, L. S.; Deming, W. S. ; Teller, E. *J. Am. Chem. Soc.* **1940**, 62, 1723.

47. Kruk, M.; Jaroniec, M.; Guan, S.; Inagaki, S.; *J. Phys. Chem. B* **2001**, 105, 681.

48. Shea, K. J.; Loy, D. A.; Webster, O. W. *J. Am. Chem. Soc.* **1992**, 114, 6700.

49. Small, J. H.; Shea, K. J.; Loy, D. A. *J. Non-Cryst. Solids* **1993**, 160, 234.

50. Corriu, R. J. P.; Moreau, J. J. E. ; Thepot, P. ; Man, M. W. C. *Chem. Mater.* **1992**, 2, 1217.

51. Corriu, R. J. P.; Moreau, J. J. E. ; Thepot, P. ; Man, M. W. C.; Chorro, C.; Lere-Porte, J. –L.; Sauvajol, J. –L. *Chem. Mater.* **1994**, 6, 640.

52. Corriu, R. J. P.; Granier, M.; Lanneau, G. F. *J. Organomet. Chem.* **1998**, 562, 79.

53. (a) Oviatt, H. W. , Jr.; Shea, K. J.; Small, J. H. *Chem. Mater.* **1993**, 5, 943. (b) Loy, D. A.; Jamison, G. M.; Baugher, B. M.; Russick, E. M.; Assink, R. A.; Prabaker, S.; Shea, K. J. J. *Non-Cryst. Solids* **1995**, 186, 44.

54. (a) Loy, D. A.; Baugher, B. M.; Prabaker, S.; Assink, R. A.; Shea, K. J. *Mater. Res. Soc. Symp. Proc. (Adv. Porous Mater.)* **1995**, 371, 229. (b) Baugher, B. M.; Loy, D. A.; Prabaker, S.; Assink, R. A.; Shea, K. J.; Oviatt, H. *Mater. Res. Soc. Symp. Proc. (Adv. Porous Mater.)* **1995**, 371, 253.

55. Marciniec, B.; Gulinski, J.; Urbaniak, W. *Pol. J. Chem.* **1982**, 56, 287.

56. Marciniec, B.; Gulinski, J.; *J. Organomet. Chem.* **1983**, 253, 349.

57. (a) Marciniec, B.; Maciejewski, H.; Gulinski, J.; Rzejak *J. Organomet. Chem.* **1989**, 362, 273. (b) Loy, D. A. ; Carpenter, J. P. ; Yamanaka, S. A.; McClain, M. D.; Greaves, J.; Hobson, S.; Shea, K. J. *Chem. Mater.* **1998**, 10, 4129.

58. Marciniec, B.; Gulinski, J.; *J. Organomet. Chem.* **1984**, 266, C19.

59. Inagaki, S.; Guan, T.; Ohsuna, T.; Terasaki, O. *Nature* **2002**, 416, 304.

60. Yang, Q.; Kapoor, M. P.; Inagaki, S. *J. Am. Chem. Soc.,* **2002**, 124, 9694.

61. Goto, Y.; Inagaki, S. *Chem. Commun.* **2002**, 2410.

62. Temtsin, G.; Asefa, T.; Bittner, S.; Ozin, G. A. *J. Mater. Chem.* **2001**, 11, 3202.

63. Kim, J. M.; Sakamoto, Y.; Hwang, Y. K.; Kwon, Y. -U.; Terasaki, O.; Park, S. -E.; Stucky, G. D. *J. Phys. Chem. B* **2002**, 106, 2552.

64. Sayari, A.; Yang, Y. *Chem. Commun.* **2002**, 2582.

65. Yu, C.; Tian, B.; Fan, J.; Stucky, G. D.; Zhao, D. *J. Am. Chem. Soc.* **2002**, 124, 4556.

66. Flodström, K.; Alfredsson, V.; Källrot, N. *J. Am. Chem. Soc.* **2003**, 125, 4402.

67. Kleitz, F.; Chio, S. H.; Ryoo, R. *Chem. Commun.* **2003**, 2136.

68. Sayari, A. Hamoudi, S. *Chem. Mater.* **2001**, 13, 3151.

69. (a) Lim, M. H.; Blanford, C. F.; Stein, A. *Chem. Mater.* **1998**, 10, 467. (b) Margolese, D.; Melero, J. A.; Christiansen, S. C.; Chmelka, B. F.; Stucky, G. D. *Chem. Mater.* **2000**, 12, 2448. (c) Van Rhijn, W. M.; De Vos, D. E. ; Sels, B. F. ; Bossaert, W. D. ; Jacobs, P.A. *Chem. Commun.* **1998**, 317.

70. Lim, M. H. ; Blanford, C. F. ; Stein, *A. J. Am. Chem. Soc.* **1997**, 119, 4090.

71. (a) Anwander, R.; Palm, C.; Stelzer, J.; Groeger, O.; Engelhardt, G. *Stud. Surf. Sci. Catal.* **1998**, 117, 135. (b) Anwander, R.; Nagl, I.; Widenmeyer, M.; Engelhardt, G.; Groeger, O.; Palm, C.; Röser, T. *J. Phys. Chem. B.* **2000**, 104, 3532.

72. Asefa, T.; Kruk, M.; MacLachlan, M. J.; Coombs, N.; Grondey, H.; Jaroniec, M.; Ozin, G. A. *J. Am. Chem. Soc.* **2001**, 123, 8520.

73. Kruk, M.; Asefa, T.; Jaroniec, M.; Ozin, G.A. *J. Am. Chem. Soc.* **2002**, 124, 6383.

74. Kruk, M.; Jaroniec, M.; Sayari, A. *Langmuir* **1997**, 13, 6267.